General Disclaimer

One or more of the Following Statements may affect this Document

- This document has been reproduced from the best copy furnished by the organizational source. It is being released in the interest of making available as much information as possible.

- This document may contain data, which exceeds the sheet parameters. It was furnished in this condition by the organizational source and is the best copy available.

- This document may contain tone-on-tone or color graphs, charts and/or pictures, which have been reproduced in black and white.

- This document is paginated as submitted by the original source.

- Portions of this document are not fully legible due to the historical nature of some of the material. However, it is the best reproduction available from the original submission.

DOPPLER MEASUREMENTS OF THE IONOSPHERE ON THE OCCASION OF THE APOLLO-SOYUZ TEST PROJECT

Part I

MARIO D. GROSSI and RAY H. GAY

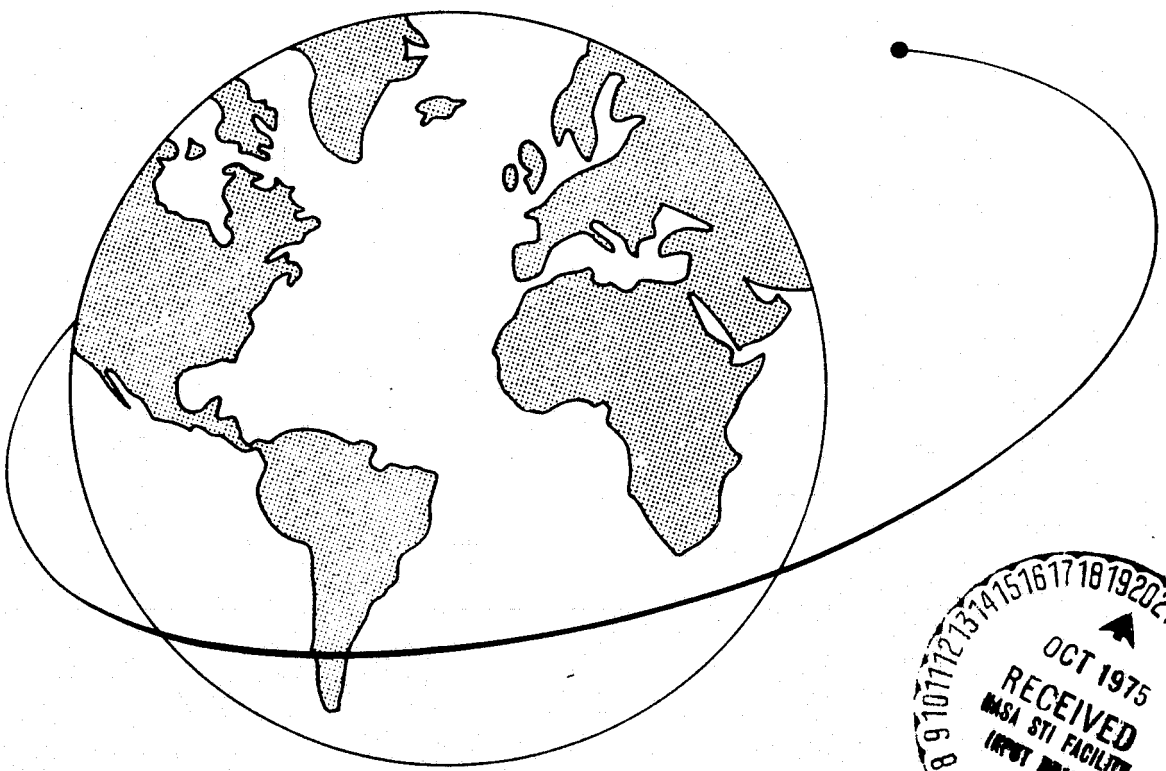

Smithsonian Astrophysical Observatory
SPECIAL REPORT 366

TABLE OF CONTENTS

ILLUSTRATIONS

TABLES

ABSTRACT

A computer simulation of the ionospheric experiment of the Apollo-Soyuz Test Project (ASTP) has been performed. ASTP is the first example of USA/USSR cooperation in space and is scheduled for summer 1975. The experiment consists of performing dual-frequency doppler measurements (at 162 and 324 MHz) between the Apollo Command Service Module (CSM) and the ASTP Docking Module (DM), both orbiting at 221-km height and at a relative distance of 300 km. A network of ground stations will also operate and will collect differential and rotating doppler data in DM-to-ground radio paths. The computer simulation has shown that, with the doppler measurement resolution of approximately 3 mHz provided by the instrumentation (in 10-sec integration time), ionospheric-induced doppler shifts will be measurable accurately at all times, with some rare exceptions occurring when the radio path crosses regions of minimum ionospheric density. The computer simulation has evaluated the ability of the experiment to measure changes of columnar electron content between CSM and DM (from which horizontal gradients of electron density at 221-km height can be obtained) and to measure variations in DM-to-ground columnar content (from which an averaged columnar content and the electron density at the DM can be deduced, under some simplifying assumptions). The simulation has confirmed the expectation that simultaneous measurements of horizontal gradients and space-to-ground columnar content substantially increase the accuracy of data inversion.

DOPPLER MEASUREMENTS OF THE IONOSPHERE ON THE OCCASION OF THE APOLLO-SOYUZ TEST PROJECT

Part I: Computer Simulation of Ionospheric-Induced Doppler Shift*

Mario D. Grossi and Ray H. Gay

1. INTRODUCTION

A spacecraft-to-spacecraft doppler-tracking experiment will be performed by the Smithsonian Astrophysical Observatory on occasion of the forthcoming Apollo-Soyuz Test Project (ASTP). The ASTP mission, scheduled for summer 1975, is the first example of USA/USSR cooperation in space. The primary goal of the doppler-tracking experiment is to refine the anomalies of the earth's gravity field.

The experiment consists of measuring, with a doppler-tracking radio link, the relative velocity between the ASTP docking module (DM) and the Apollo command service module (CSM). The DM and CSM will both orbit at 221-km height and will stay at a relative distance of 300 km for approximately 24 hours (the duration of data taking). From doppler signals in a dual-frequency VHF link from the DM to the CSM, the relative-velocity data will be inverted into anomalies of the earth's gravity field with a threshold sensitivity of the order of 10 mgal. The integration time for the doppler measurements will be 10 sec.

---

*This report covers the computer simulation of the ionospheric-induced doppler shifts (Part I). Part II (SAO Special Report No. 367) covers the inversion of differential and rotating doppler shifts.

This research was supported by NASA under contract NAS 9-13837 to the Smithsonian Astrophysical Observatory.

This experiment, known by the code name ASTP/MA-089, is the first attempt at testing the so-called "low–low" satellite-to-satellite doppler-tracking approach for gathering data on medium-wavelength features (horizontal wavelength from about 300 to approximately 1000 km) of the earth's gravity field. The method, called low–low to emphasize the low height of the two orbiting terminals of the doppler-tracking link, has been described in the literature by Wolf (1969), Comfort (1973), and Schwartz (1970). Its comparative merits with respect to the so-called low–high satellite-to-satellite doppler-tracking scheme [described in the literature by Von Bun (1972) and named this way because one terminal is in a high orbit and the second in a low orbit] are still a subject of debate.

The Apollo-Soyuz Test Project will give us the first opportunity to compare the two approaches. In fact, in addition to the low–low method tested with the MA-089 experiment, Goddard Space Flight Center will be conducting an on-board ASTP low–high experiment, known under the code name of MA-128.

In the MA-089 experiment, the doppler error induced in the measurements by the ionosphere will be corrected by a dual-frequency method (Guier and Weiffenbach, 1960). The spacecraft-to-spacecraft doppler-tracking link will, in fact, operate at two coherent, harmonically related frequencies, 162 and 324 MHz, and the effect of the ionosphere will be quantitatively determined by exploiting the phenomenon of ionospheric frequency dispersion. These frequency values have been chosen because instrumentation has already been developed and is available and ground stations tuned at 162 and 324 MHz have already been deployed.

By means of a transmitter installed on board the DM as a dual-frequency beacon, an ionospheric experiment (Grossi, 1974) will also be performed (see Figure 1), in which differential doppler data will be collected in DM-to-CSM paths and differential and rotating doppler data will be collected in DM-to-earth paths. The doppler measurement resolution will be of the order of 3 mHz, with a 10- to 100-sec integration time.

The use of the DM as a terminal of the MA-089 doppler-tracking link was initially suggested by NASA Astronaut Commander Eugene Cernan.

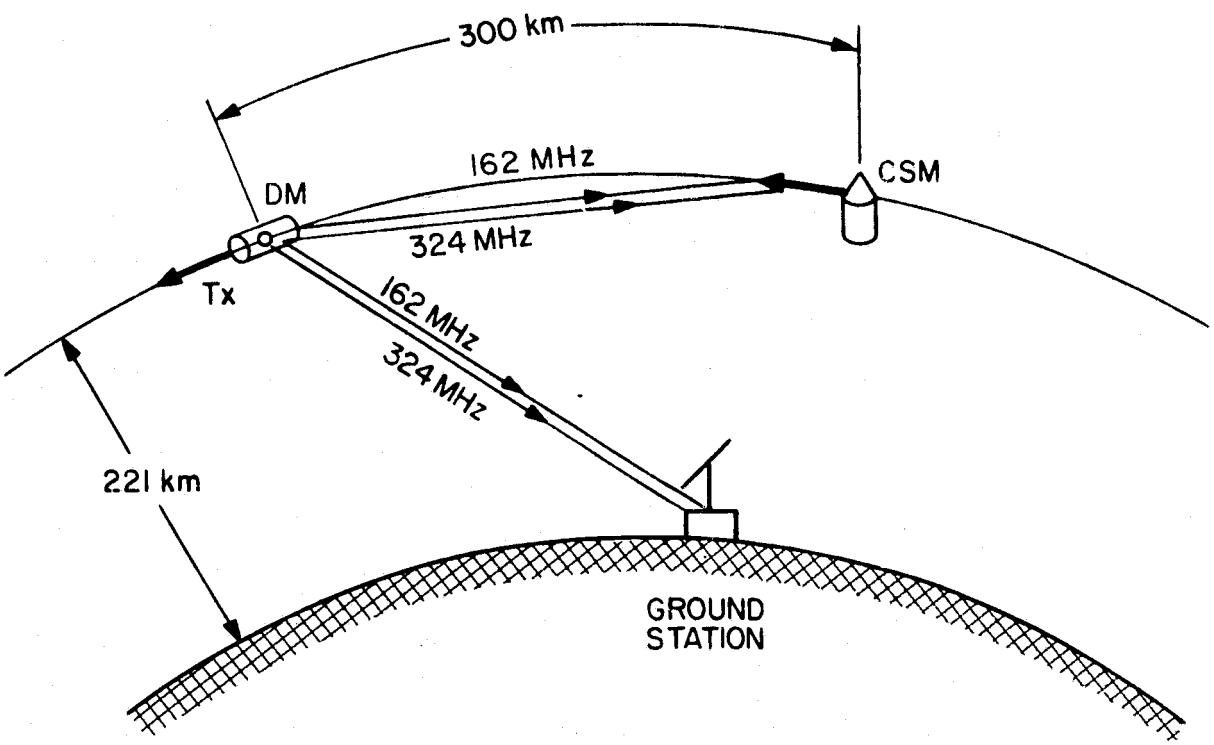

Figure 1. Measurement links of the ASTP doppler-tracking experiment.

Although these ionospheric measurements are secondary to the gravity-field measurements of the MA-089 experiment, chronologically they were proposed to the National Aeronautics and Space Administration earlier (Grossi, 1972), when the ASTP mission was known as the International Rendezvous and Docking Mission 1975 (IRDM 1975).

2. SCIENTIFIC GOALS

The MA-089 ionospheric experiment represents an extension of well-known methods (differential doppler and rotating doppler) of measuring the integrated electron concentration and other properties of the ionosphere along a radio path between a terminal moving in the ionosphere or above it and a station on the ground. Even before artificial-satellite flights, these techniques were in use in suborbital rocket flights (Seddon, 1953; Jackson and Seddon, 1958) performed to measure ionospheric parameters. Since 1957, a wealth of literature has appeared, based on the use of multifrequency doppler links between satellites (orbiting inside the ionosphere and above it) and ground stations (Al'pert, 1958, 1965; Garriott, 1960a, b; de Mendoza, 1963; Misyura et al., 1964). Recent additions to the literature include papers by Al'pert (1973, 1974) and Tyagy (1974).

The fundamental problem that users of space-to-ground doppler links must face is the fact that the differential doppler shift observed when receiving two coherent, harmonically related frequencies is directly connected to the time derivative of the columnar electron content and not to the columnar content itself. This difficulty can be removed if simultaneous measurements of the Faraday rotation (also called rotating doppler shift) affecting the link are carried out. When the rotating doppler shift is not observed, the problem is underdetermined, and the accuracy obtainable from inverting the differential doppler data into columnar content strongly depends on the presence of horizontal gradients in that region of the ionosphere that is swept through by the space-to-ground radio path while the space-borne terminal is in motion.

The MA-089 experiment introduces a new measurement feature, which is connected to the problem of horizontal gradients: namely, the measurement of their values at a height of 221 km (the common orbital height of both the DM and the CSM) in the orbital plane of the DM/CSM pair. These measurements are performed simultaneously with space-to-ground differential doppler measurements, by using the DM as a dual-frequency beacon.

As will be shown in Part II of this report, a significant increase in accuracy in the inversion of differential doppler data into columnar content is achievable.

In summary, the MA-089 experiment will yield the following:

A. Changes of the columnar electron content between the two spacecraft, from which the horizontal gradient of the electron density at a height of 221 km (along the orbital path of the DM/CSM pair) will be obtained.

B. Variations in the ground-to-spacecraft columnar content, from which an averaged columnar content and the electron density at the DM location can be deduced under some simplifying assumptions.

In addition, it will be possible to try to probe traveling ionospheric disturbances (TID) with both the space-to-ground link and the DM-to-CSM link. This will enable us to measure the TID electron-density fluctuations with respect to the surrounding background, to sample the TID wave structure, and to monitor the motion of the TID.

Finally, the experiment will attempt to detect the boundaries of turbulent regions of the ionosphere, such as the aurora oval and the equatorial sporadic E belt.

3. MEASUREMENT APPROACH

3.1 Description of the Method

Let us consider first a simple case: the vertical ascent in the ionosphere of a spacecraft that carries the transmitter (with pulsation ω_1) of a doppler-tracking link. The receiving terminal is on the ground. When the spacecraft is at a height r(t), the link's phase-path length is

$$\Phi_1(t) = \frac{\omega_1}{c} \int_0^{r(t)} n_1(r)\, dr \quad , \tag{1}$$

and its time derivative is

$$\dot{\Phi}_1(t) = \frac{\omega_1}{c} \frac{d}{dt} \int_0^{r(t)} n_1(r)\, dr \quad , \tag{2}$$

where c is the velocity of light in free space and n(r) is the index of refraction at height r. The change of phase path with time is due in part to the spacecraft motion and in part to temporal changes of the index of refraction along the vertical between the spacecraft and the ground. If there are no temporal changes along the path, then by assuming the spacecraft to be at height r_0 at time t_0, we have

$$\dot{\Phi}_1(t_0) = \frac{\omega_1}{c}\, \dot{r}(t_0)\, n_1(r_0) \quad . \tag{3}$$

If there are temporal changes, equation (2) becomes

$$\dot{\Phi}_1(t_0) = \frac{\omega_1}{c} \left[\dot{r}(t_0)\, n_1(r_0) + \int_0^{r(t)} \frac{\partial n_1(r)}{\partial t}\, dr \right] \quad , \tag{4}$$

where the term $\int_0^{r(t)} [\partial n_1(r)/\partial t]\, dr$ represents the temporal variation of the columnar refractivity in the entire vertical path between the spacecraft and the ground. The problem is underdetermined, and unless this variation is otherwise measured or becomes negligibly small, the inferring of $n_1(r_0)$ from $\dot{\Phi}_1(t_0)$ is affected by error.

When the effects of the earth's magnetic field and the collision frequency on the index of refraction are disregarded, equation (3) can be rewritten as follows:

$$\dot{\Phi}_1(t_0) = \frac{\omega_1}{c}\, \dot{r}(t_0) \left(1 - \frac{2\pi e^2 N}{m\omega_1^2}\right) , \tag{5}$$

where N is the electron density and e and m are the charge and the mass of the electron, respectively; $2\pi e^2/m = 1587.6$, when N is in electrons m^{-3} and ω_1 is in rad sec^{-1}. From equation (3), we can determine the local index of refraction (and, hence, the electron density) at the spacecraft height by monitoring the received doppler shift and by knowing, independently, the ascension velocity of the spacecraft and the frequency radiated. When operating with a single frequency, it is necessary to know these two parameters very accurately. Since the ionospheric-generated doppler shift is a few millihertz, we must know the spacecraft velocity with an accuracy better than a fraction of a millimeter per second (when the link operates with a wavelength of, say, 1 m) and the frequency of the link within a fraction of a millihertz (with integration times of the order of 10 to 100 sec, the duration of the ionospheric crossing). However, by adding a second frequency, ω_2, that is phase coherent and harmonically related to ω_1, the equation of the differential doppler shift in the spacecraft-to-ground link, when temporal changes of the columnar refractivity between the spacecraft and the ground are neglected, becomes

$$\delta\dot{\Phi} = \dot{\Phi}_1(t) - \frac{\omega_1}{\omega_2}\, \dot{\Phi}_2(t) = \frac{\omega_1}{c}\, \frac{d}{dt} \int_0^{r(t)} [n_1(r) - n_2(r)]\, dr = \frac{\omega_1}{c}\, \dot{r}(t_0)\, [n_1(r_0) - n_2(r_0)] \quad . \tag{6}$$

If we disregard the refractive effects of the earth's magnetic field and the collision frequency, we get

$$\delta\dot{\Phi} = \frac{\omega_1}{c}\,\dot{r}(t_0)\,\frac{2\pi e^2 N}{m}\left(\frac{\omega_1^2 - \omega_2^2}{\omega_1^2\,\omega_2^2}\right) \quad . \tag{7}$$

From equation (7), we can now deduce that the contribution to the measurement error, arising from an error in estimating the link's frequencies, is virtually eliminated.

We see from equation (5) that an error in frequency contributes directly to the error of $\dot{\Phi}_1(t_0)$. However, from equation (7), we find that the error in frequency must now be multiplied by the quantity $(n^2 - 1)\omega_1^{-2}$, which is usually very small. For instance, if $\omega_1/\omega_2 = n = 2$ and $\omega_1 = 2\pi \times 300 \times 10^6$ rad sec^{-1}, we have $(n^2 - 1)\omega_1^{-2} = 8.6 \times 10^{-19}$, and therefore the influence of the frequency error in the overall error of $\dot{\Phi}_1(t_0)$ is eliminated.

When the spacecraft trajectory is no longer vertical, other analytical expressions will have to be employed. Alternative formulas have already been developed by several authors and are available from the literature. For the case in which horizontal gradients of the electron content are negligible, we can write (following Al'pert, 1973):

$$\delta\dot{\Phi}(t) = a_0\left[-\frac{\dot{z}_s}{\cos\phi_s}\,N_s + \left(\dot{r}_s + \frac{\dot{z}_s}{\cos\phi_s}\right)\overline{N}\right] \quad , \tag{8}$$

where the velocity components correspond to the height z_s of the transmitter, N_s is the local value of the electron concentration at that height,

$$\overline{N} = \frac{1}{z_s}\int_0^{z_s} N\,dz \tag{9}$$

is the mean value of the integrated electron concentration in a column of 1-cm^2 cross section, and the coefficient a_0 is

$$a_0 = \frac{2\pi e^2}{m} \frac{\omega_1}{c} \left(\frac{1}{\omega_1^2} - \frac{1}{\omega_2^2} \right) \quad . \tag{10}$$

In equation (8), $r(t)$ denotes the time-dependent radius vector joining the point of observation to the moving source, which is assumed to be approaching the observer and located at height $z(t)$. Moreover, the radial, horizontal, and vertical velocity components of the source are denoted, respectively, by $\dot{r}(t)$ (along the line of sight), $\dot{x}(t)$, $\dot{y}(t)$, and $\dot{z}(t)$.

In the general case, we can write for the electron concentration

$$N = N(R, \theta, \chi, t) = N(z, x, y, t) \quad , \tag{11}$$

where (see Figure 2)

$$R = R_0 + z \quad , \quad x = R_0\theta \quad , \quad y = R_0\chi \quad , \tag{12}$$

and (z, θ, χ) is a variable coordinate in a spherical orthogonal coordinate system along the wave-propagation trajectory joining the point of observation (0, 0, 0) and the point (z_s, θ_s, χ_s) where the transmitter is located at time t. The difference in the doppler frequency shifts for the two coherent radio waves can then be written in the form

$$\delta\dot{\Phi}(t) = a_0 \frac{d}{dt} \int_{R_0}^{R_s(t)} N(x, y, z, t) \frac{dz}{\cos \phi(t)} \quad . \tag{13}$$

If certain conditions are satisfied, as happens in the case of the MA-089 experiment, we obtain (Al'pert, 1973)

$$\delta\dot{\Phi} = a_0 \left[- N_s \frac{\dot{z}_s}{\cos \phi_s} + \overline{N}_x \left(\dot{r}_s + \frac{\dot{z}_s}{\cos \phi_s} \right) - \overline{N}_y \dot{y}_s - N_t \right] \quad . \tag{14}$$

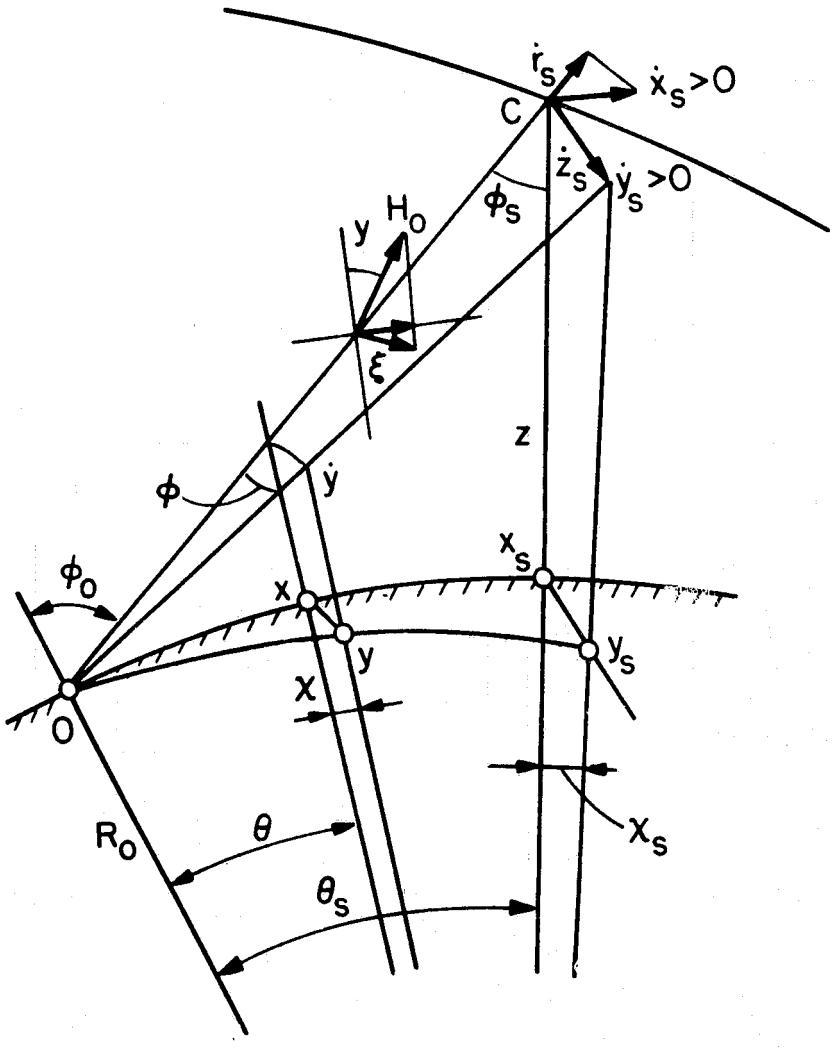

Figure 2. Nomenclature used in equations (11) through (15).

When the further simplifying assumption is made that the medium is plane parallel (i.e., the earth's sphericity is neglected), the various parameters of equation (14) are defined as follows (Al'pert, 1973):

$$\overline{N}_x = \frac{1}{z_s} \int_0^{z_s} N \, dz + \frac{1}{z_s \sin \phi_0 \cos \phi_0} \int_0^{z_s} \frac{\partial N}{\partial x} \, z \, dz \quad ,$$

$$\overline{N}_y = \frac{1}{z_s \cos \phi_0} \int_0^{z_s} \frac{\partial N}{\partial y} \, z \, dz \quad ,$$

$$N_t = \frac{1}{\cos \phi_0} \int \frac{\partial N}{\partial t} \, dz \quad . \tag{15}$$

Even in the planar approximation, the problem is underdetermined. This difficulty is, in part, alleviated in the MA-089 experiment by the fact that the DM-to-CSM dual-frequency link measures the quantity $\partial N/\partial x$ (the horizontal gradient in the orbital plane) at the ASTP orbital height:

$$\delta\dot{\Phi} = \dot{\Phi}_1(t) - \frac{\omega_1}{\omega_2} \dot{\Phi}_2 = \frac{\omega_1}{c} \frac{\partial}{\partial t} \left[\int_{DM}^{CSM} n_1(x) \, dx - \int_{DM}^{CSM} n_2(x) \, dx \right] \quad . \tag{16}$$

Assuming the two spacecraft remain at a constant separation (relative velocity = 0), we obtain

$$\delta\dot{\Phi} = \frac{\omega_1}{c} \int_{DM}^{CSM} \frac{\partial}{\partial x} [n_1(x) - n_2(x)] \frac{\partial x}{\partial t} \, dx \quad . \tag{17}$$

By neglecting the refractive effects of the earth's magnetic field and the collision frequency, we can rewrite equation (17) as follows:

$$\delta\dot{\Phi} = \frac{\omega_1}{c} \frac{2\pi e^2}{m} \left(\frac{\omega_1^2 - \omega_2^2}{\omega_1^2 \omega_2^2} \right) \int_{DM}^{CSM} \frac{\partial N}{\partial x} \frac{\partial x}{\partial t} \, dx \quad , \tag{18}$$

where $\partial x/\partial t$ is known from orbital-mechanics considerations and $\partial N/\partial x$ can therefore be obtained from the measured values of $\delta\dot{\Phi}$ in the DM-to-CSM path. Before it can be used in equation (15), however, $\partial N/\partial x$ must be known all along the vertical z. In fact, what is needed is the function $\int_0^z (\partial N/\partial x)(z)\, dz$ (and not just $\partial N/\partial x$ at the ASTP orbital height of 221 km). We must therefore construct a model of $\partial N/\partial x$ (z) in the lower ionosphere, with the constraint of satisfying both the value measured at 221 km by the DM-to-CSM link and a value equal to zero at the ionosphere's bottom. A linear variation of the gradient between these two values thus seems to be an acceptable assumption.

In the DM-to-CSM link, the transmitting antenna is linearly polarized and the receiving antenna is circularly polarized. Therefore, we cannot observe the Faraday rotation (rotating doppler) phenomenon. In the DM-to-ground link, though, we plan to adopt on the ground a receiving antenna that is linearly polarized and expect to be able to monitor the amplitude of the received signal. If these expectations materialize, we can observe the quantity $\delta\dot{\Phi}_H$, which, for quasi-longitudinal propagation (Tzedilina, 1962; Al'pert, 1965), can be expressed

$$\delta\dot{\Phi}_H = \frac{2\pi e^2}{m\omega^2} \frac{d}{dt} \int_0^z \omega_H \, (\cos\theta)\, N \frac{dz}{\cos\phi} \quad , \tag{19}$$

where $\delta\dot{\Phi}_H$ is the frequency at which the amplitude of the received signal changes. In the absence of horizontal gradients in the electron-density profile, equation (19) reduces to

$$\delta\dot{\Phi}_H = \frac{2\pi e^3 H_0}{m^2 \omega^2 c^2} H_0 \left\{ - \frac{\cos\theta_s \dot{z}_s}{\cos\phi_s} N_s + \sin\gamma_s \left[\left(\dot{r}_s + \frac{\dot{z}_s}{\cos\phi_s} \right) \mp \sin\xi_0 \dot{y}_s \right] N \right\} \quad , \tag{20}$$

where γ is the angle between H_0 and the vertical z, ξ is the angle between the projection of H_0 along the y axis in the yz plane and the xz plane, and

$$\cos\theta = \cos\phi\cos\gamma + \sin\phi\sin\gamma\cos\xi \quad .$$

We can now obtain N_s and $\overline{N}$ at any given point by means of equations (14) and (20). If we no longer assume the absence of horizontal gradients in the electron-density profile, we must go back to the general formula (19).

3.2 Evaluation of the Measurement Error

3.2.1 Instrumentation contribution

The instrumentation error in the MA-089 experiment is dominated by the following two sources of inaccuracy:

A. Oscillator instabilities. The frequency-stability curve in Figure 3 indicates that each oscillator has a stability of approximately 1.5 parts in 10^{12} (for 10- to 100-sec integration time). Because each link of the doppler-tracking system uses two oscillators, we have, at 324 MHz, an error

$$\Delta f = 324\times 10^6 \times 1.5\times 10^{-12}\sqrt{2} = 0.687 \text{ mHz}.$$

At 162 MHz, $\Delta f = 0.3435$ mHz.

B. Phase-locked-loop tracking error. The signal-to-noise ratios (SNR) expected to be available in the doppler-tracking link are

~32 db at 162 MHz ,

~26 db at 324 MHz .

The tracking-error variance in the phase-locked loop, therefore, will be

$$\sigma_p^2 = 6.3\times 10^{-4} \text{ rad}^2 \text{ at 162 MHz} \quad ,$$

$$\sigma_p^2 = 2.5\times 10^{-3} \text{ rad}^2 \text{ at 324 MHz} \quad .$$

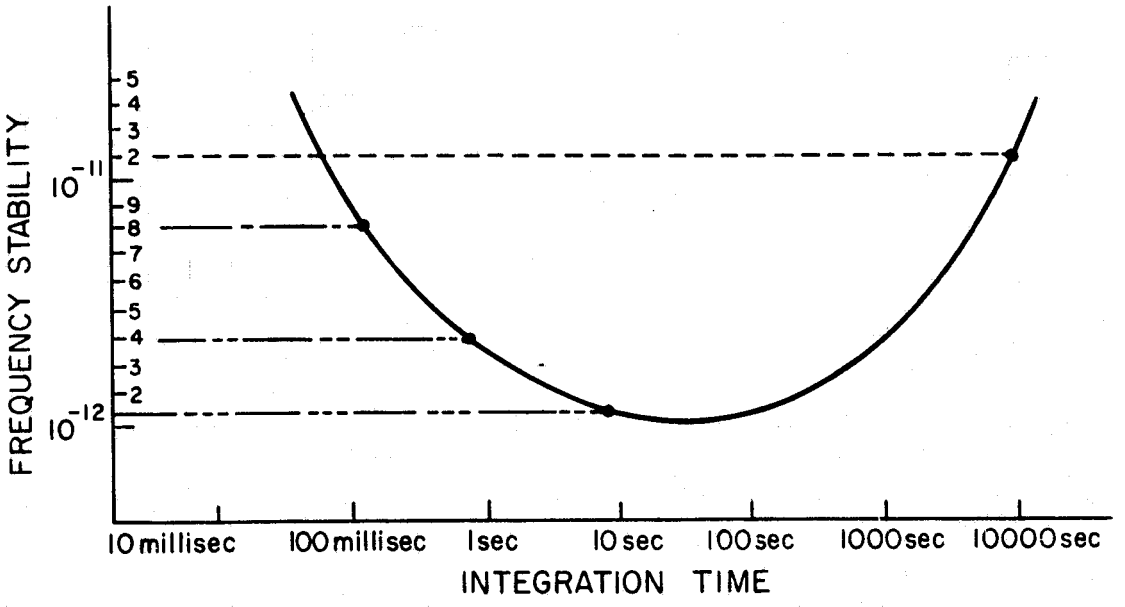

Figure 3. Curve of the stability of the oscillators used in the ASTP doppler-tracking experiment.

Since the lower frequency is doubled before it is sent to the doppler processor, the phase-error variances for the two channels are identical; and since the loop bandwidths are both 5 Hz, the phase errors observed at time intervals $T_i = 10$ sec are independent. The total root-mean-square error, therefore, is

$$\sigma_f = \sigma_p \frac{\sqrt{2}}{2\pi T_i} = \frac{\sqrt{2} \times 10^{-2} \times 2.5}{2\pi \times 10} = 0.565 \text{ mHz} \quad .$$

The total instrument error in taking raw doppler data at 324 MHz is thus approximately 0.8 mHz.

We performed laboratory tests on the ASTP doppler-tracking instrumentation with the transmitting and receiving terminals connected back to back by means of an attenuator that simulates path losses. The following errors were typically measured:

2.04 mHz at 162 MHz ,

1.89 mHz at 324 MHz ,

1.25 mHz for the differential doppler shift .

The increase in error above the expected value is attributed to the inability of the oscillators to perform as well as they could in principle. This is not, however, the sole reason for downgrading our measuring-accuracy ambitions. As we show in Section 3.2.2, even with oscillators performing as expected, multipath propagation effects would cause the doppler error vastly to exceed the value of 0.8 mHz, initially estimated to be the overall error for the instrumentation.

3.2.2 Multipath propagation effects

Because the antennas used at the two terminals of the doppler-tracking link have low directivity (the transmitting antenna on the DM has an average gain of -5 db, and the receiving antenna on the CSM, a gain of +6 db), reflections from the earth's surface, as well as the DM-to-CSM direct ray, will reach the CSM antenna. This is a well-known multipath phenomenon.

A simplified analysis of this effect can be carried out by assuming that the multipath structure contains only two rays (Figure 4) and that reflection on the earth's surface takes place at the midpoint R.

Because the electric vector of the transmitted signal is perpendicular to the orbital plane of the spacecraft, the direct wave and the wave incident on the earth's surface are horizontally polarized. If the electric field at the CSM (see Figure 4) arriving from the DM along the direct path ℓ_{12} is E_0, the reflected electric field at CSM arriving along the indirect path is

$$E_r = \frac{\ell_{12}}{s} DR_h E_0 e^{j(\phi_h - \theta)} \quad ,$$

where D, the defocusing factor due to the earth's curvature, is given by

$$D = \left[\left(1 + \frac{s}{2r \sin \psi}\right) \left(1 + \frac{s}{2r}\right)\right]^{-1/2} \quad ;$$

R_h and ϕ_h are the magnitude and phase of the Fresnel reflection coefficient for horizontal polarization; and θ is the phase-path difference, given by

$$\theta = \frac{2\pi}{\lambda} (s - \ell_{12}) \quad .$$

The total field at the CSM is

$$E_{tot} = E_0 + \frac{\ell_{12}}{s} DR_h E_0 e^{j(\phi_h - \theta)} \quad ,$$

from which it follows that

$$\frac{|E_{tot}|^2}{|E_0|^2} = 1 + \left(\frac{\ell_{12}}{s} DR_h\right)^2 + 2 \frac{\ell_{12}}{s} DR_h \cos (\phi_h - \theta) \quad ,$$

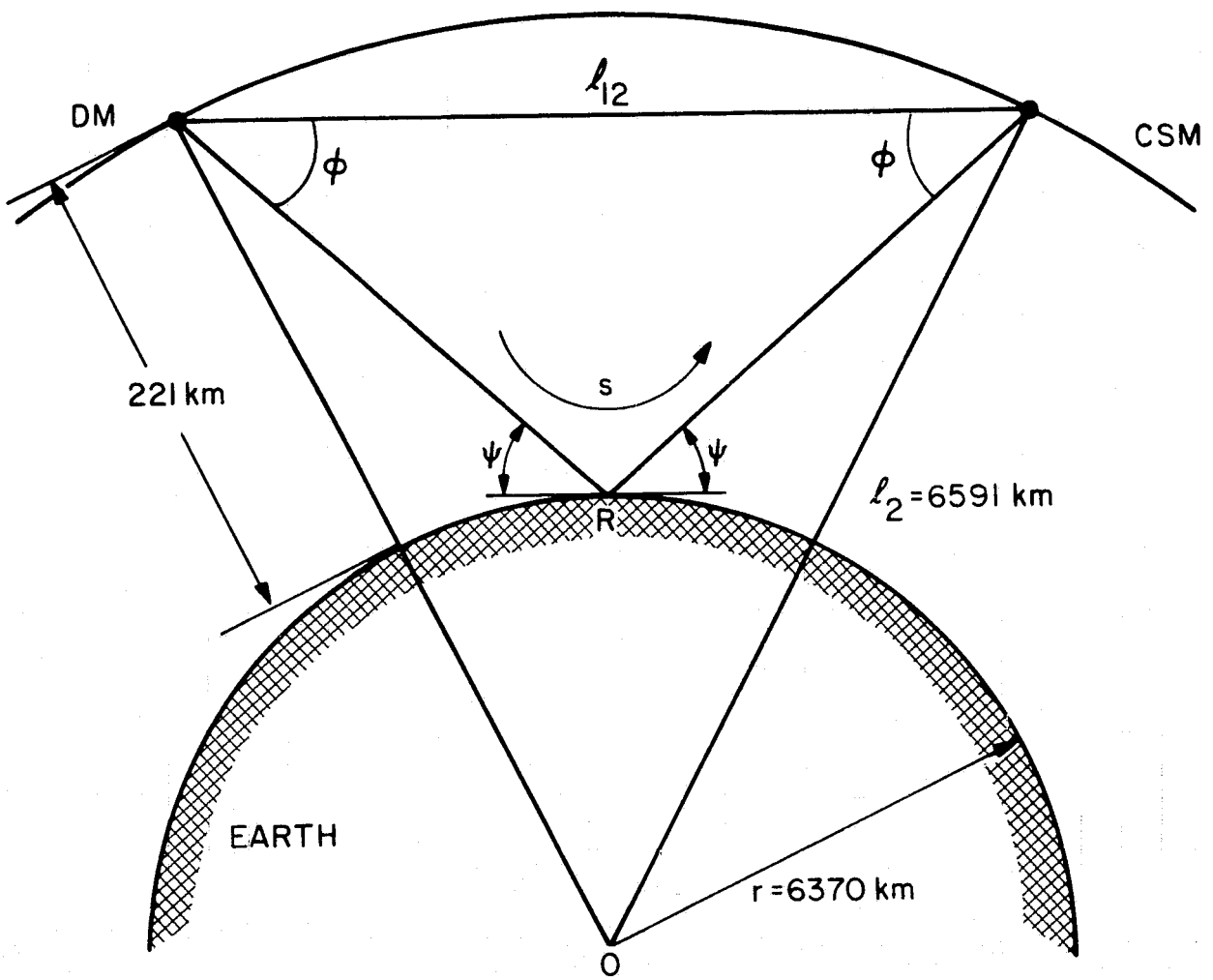

Figure 4. Multipath configuration.

where

$$s = 2\left\{\ell_2^2 + r^2 - 2\ell_2 r\left[1 - \left(\frac{\ell_{12}}{2\ell_2}\right)^2\right]^{1/2}\right\}^{1/2} .$$

Assuming isotropic antennas at both ends of the link, we have plotted $|E_{tot}|^2/|E_0|^2$ in Figures 5 through 8 for desert and sea water, for two frequencies. Values of $|E_{tot}|/|E_0|$ are also given in column 4 of Tables 1 through 4. It follows from the above equations that the normalized reflected field at the CSM is

$$\frac{|E_r|}{|E_0|} = \frac{\ell_{12}}{s} DR_h .$$

Column 5 of Tables 1 through 4 lists some values of $|E_r|/|E_0|$. The tables and graphs indicate that the worst situations occur when reflection takes place on sea water. It can be shown that the worst-case SNR degradations (see Figures 7 and 8 for the case of 300-km range and 56° grazing angle) are

-8 db at 324 MHz ,

-6 db at 162 MHz .

The multipath problem can be alleviated by tilting the CSM in such a way that, in the direction from which the ray reflected from the ground is received, the antenna has a substantially smaller gain than in the DM/CSM line of sight. Figures 9 through 12 indicate that when the CSM antenna has a 10-db gain difference in the two directions, the degradation due to sea-water reflection is less than 1 db at 162 and 324 MHz. For a 15-db gain difference, the multipath effect on the link's SNR becomes totally negligible.

The problems created by the multipath phenomenon are not, however, limited solely to the deterioration of the SNR, which is largely limited and therefore inconsequential. Unfortunately, the multipath problem also unfavorably affects the behavior of the phase-locked loops. According to an analysis performed by Stiffler et al. (1975), the error due to this last effect can be evaluated as 2.7 mHz (in 10-sec integration time)

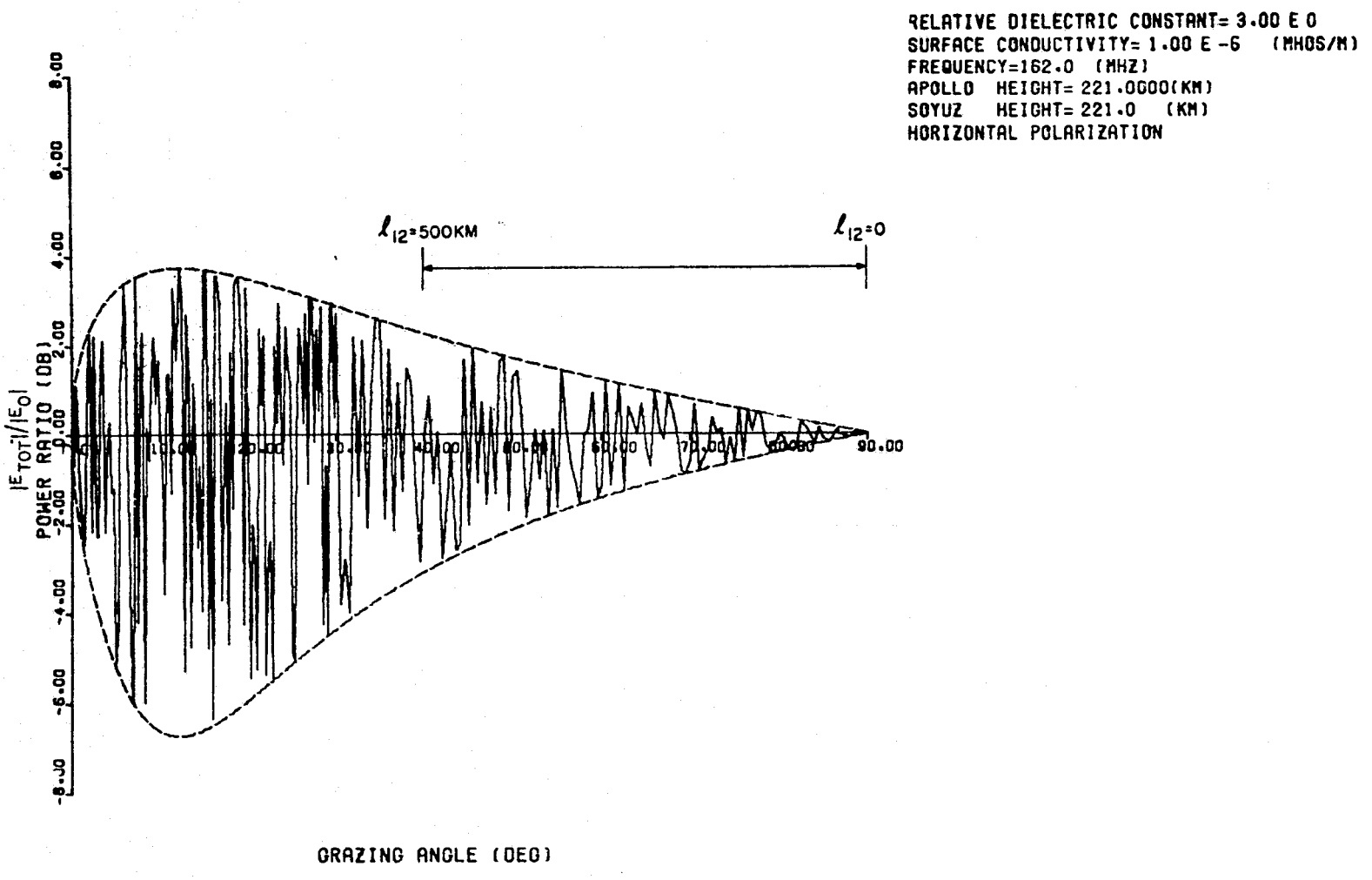

Figure 5. Signal fluctuations at the receiver terminal (162 MHz, DM-to-CSM link above desert).

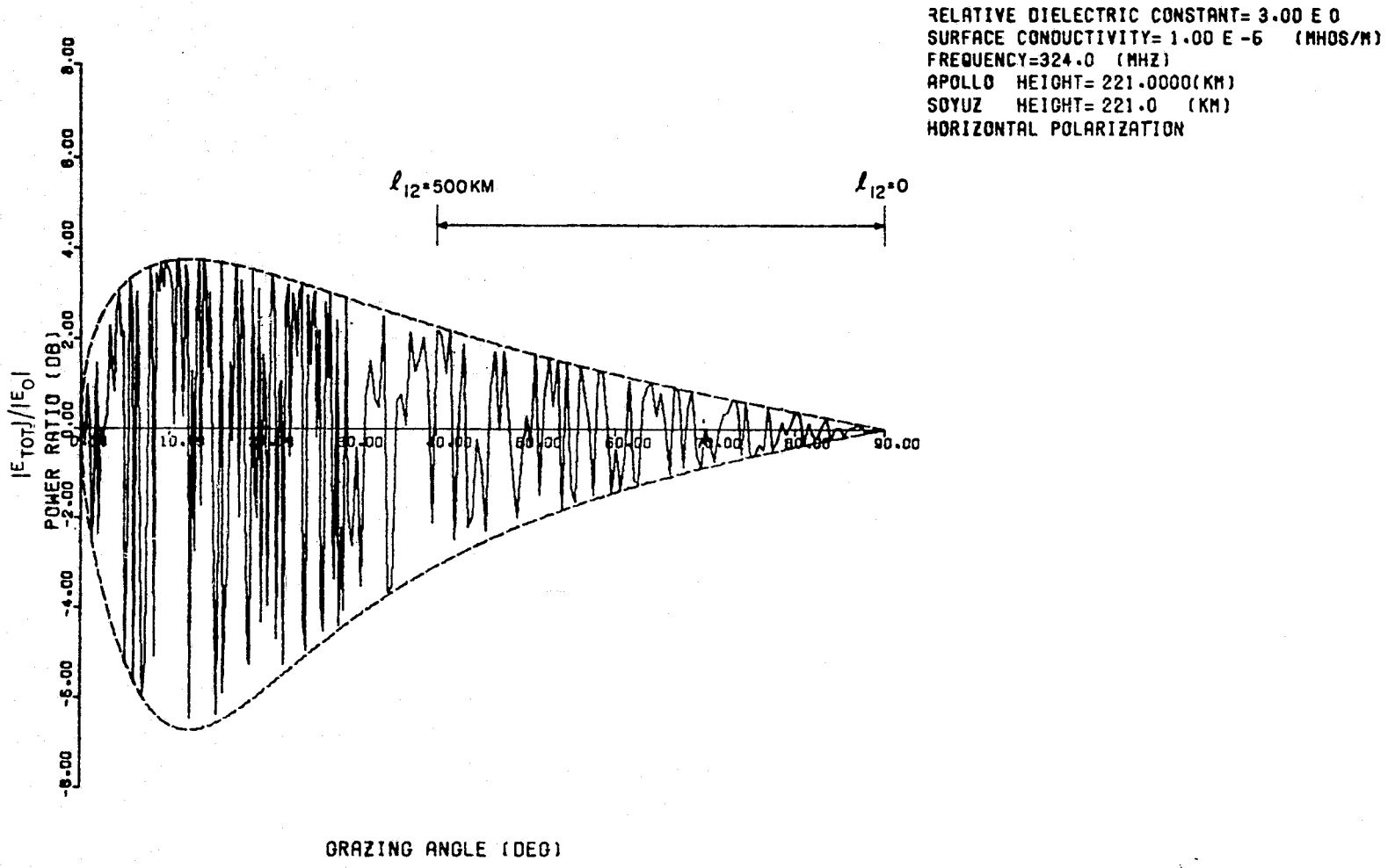

Figure 6. Signal fluctuations at the receiver terminal (324 MHz, DM-to-CSM link above desert).

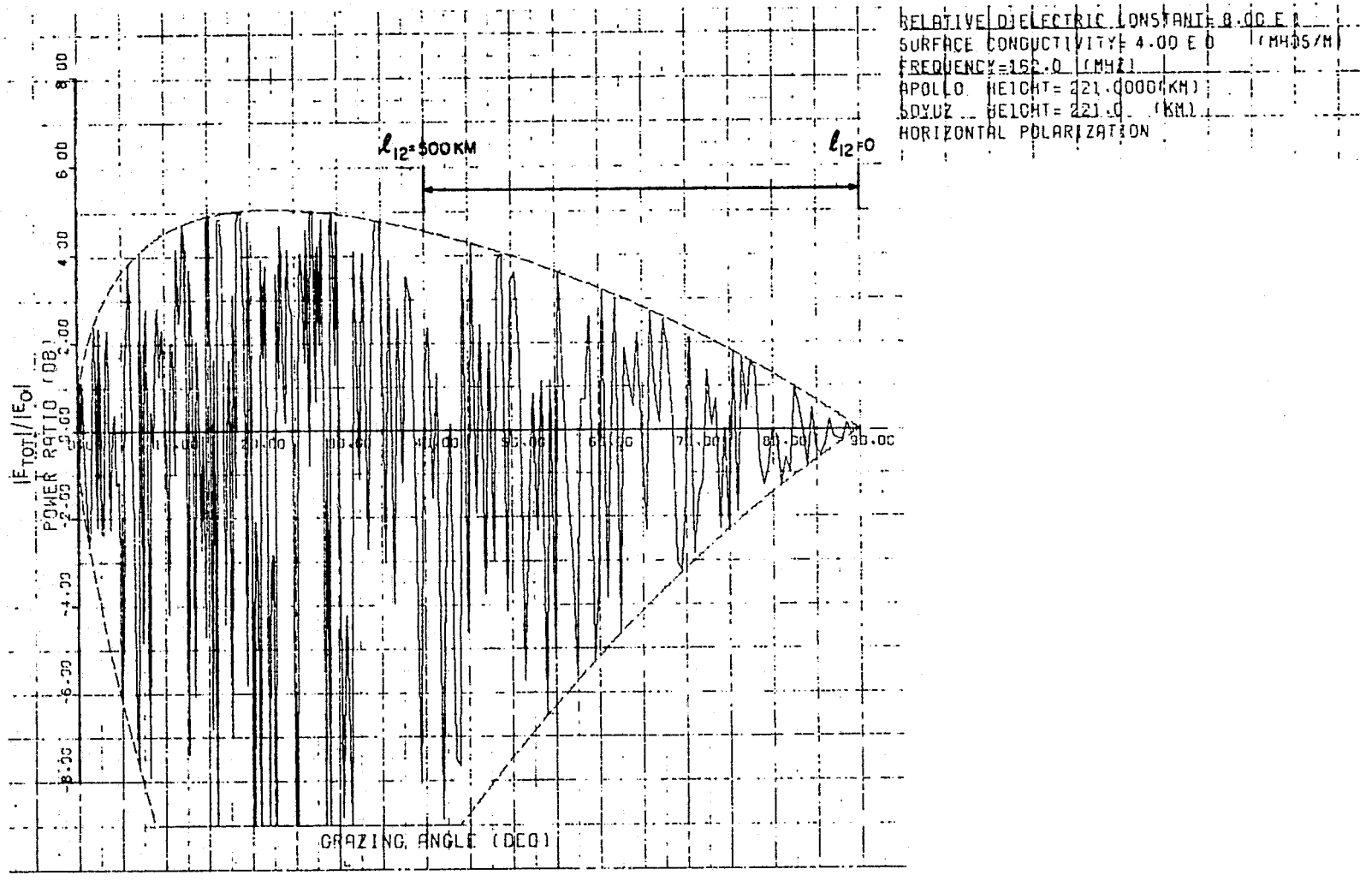

Figure 7. Signal fluctuations at the receiver terminal (162 MHz, DM-to-CSM link above sea water).

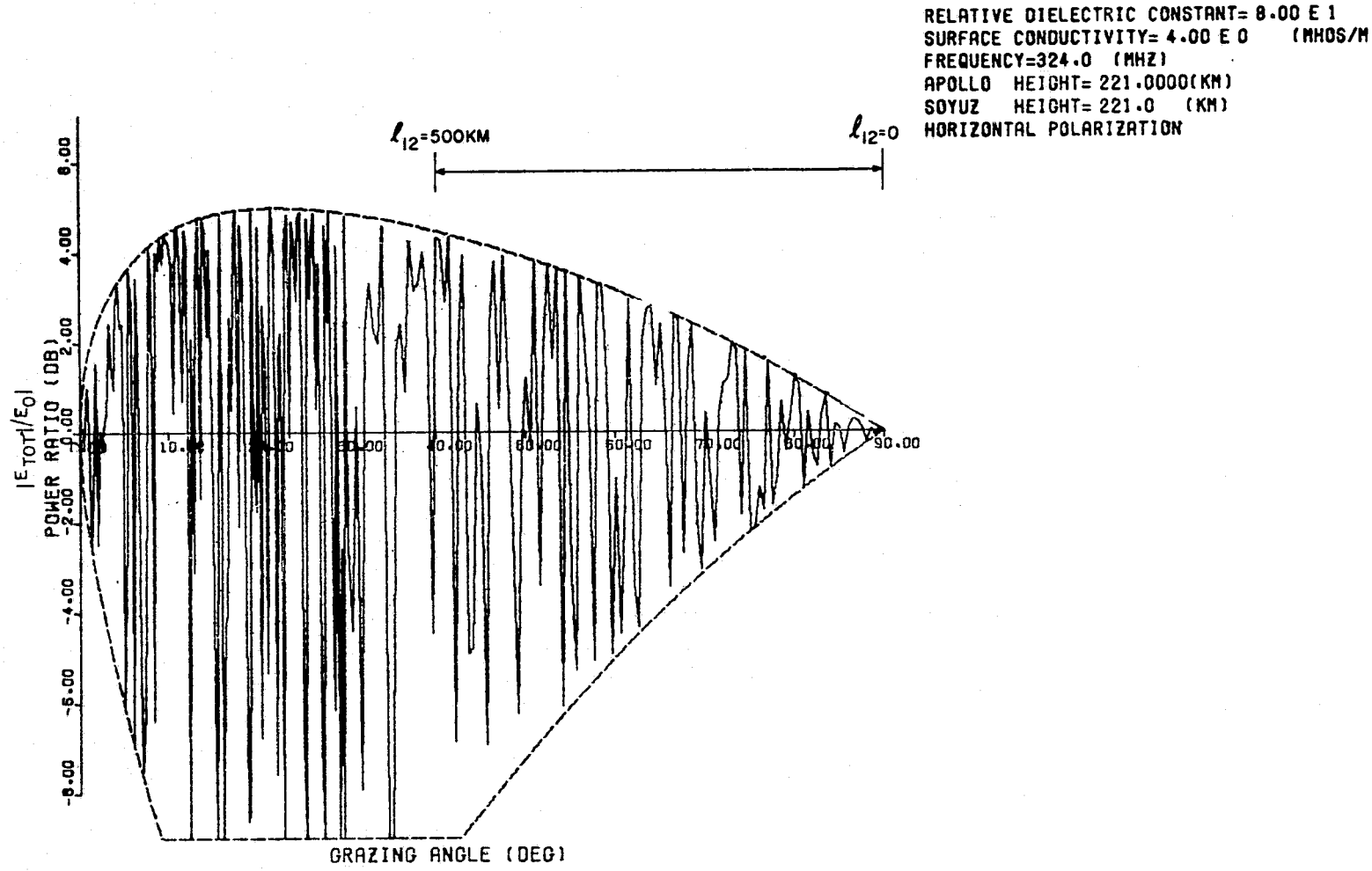

Figure 8. Signal fluctuations at the receiver terminal (324 MHz, DM-to-CSM link above sea water).

Table 1. Multipath characterization (162-MHz link above desert).

Surface dielectric constant = 3
Surface conductivity = 10^{-5} mhos m^{-1}
Frequency = 162 MHz
Height of both spacecraft = 221 km
Radius of earth = 6370 km
Maximum separation of spacecraft = 500 km

Grazing angle	Direct path length (km)	Indirect path length (km)	$\frac{\lvert E_{tot}\rvert}{\lvert E_0\rvert}$ (db)	$\frac{\lvert E_r\rvert}{\lvert E_0\rvert}$ (db)
83°.50	50.35	444.76	-0.02	-30.60
77.00	101.95	453.22	0.07	-24.45
71.00	151.89	466.54	-0.80	-20.96
65.50	200.73	484.06	-0.72	-18.51
60.50	248.74	505.14	1.19	-16.63
55.50	301.41	532.14	1.42	-14.95
51.50	347.93	558.91	-1.87	-13.72
47.50	399.47	591.29	0.61	-12.56
44.00	449.76	625.24	-2.46	-11.59
41.00	497.65	659.40	-1.01	-10.79
-	499.99	661.11	-	-

Table 2. Multipath characterization (324-MHz link above desert).

Surface dielectric constant = 3
Surface conductivity = 10^{-5} mhos m^{-1}
Frequency = 324 MHz
Height of both spacecraft = 221 km
Radius of earth = 6370 km
Maximum separation of spacecraft = 500 km

Grazing angle	Direct path length (km)	Indirect path length (km)	$\frac{\lvert E_{tot}\rvert}{\lvert E_0\rvert}$ (db)	$\frac{\lvert E_r\rvert}{\lvert E_0\rvert}$ (db)
83.50	50.35	444.76	0.25	-30.60
77.00	101.95	453.22	0.50	-24.45
71.00	151.89	466.54	-0.75	-20.96
65.50	200.73	484.06	0.08	-18.51
60.50	248.74	505.14	-1.35	-16.63
55.50	301.41	532.14	-1.65	-14.95
51.50	347.93	558.91	-1.49	-13.72
47.50	399.47	591.29	1.73	-12.56
44.00	449.76	625.24	-1.94	-11.59
41.00	497.65	659.40	1.25	-10.79
-	499.99	661.11	-	-

Table 3. Multipath characterization (162-MHz link above sea water).

Surface dielectric constant = 80
Surface conductivity = 4 mhos m^{-1}
Frequency = 162 MHz
Height of both spacecraft = 221 km
Radius of earth = 6370 km
Maximum separation of spacecraft = 500 km

Grazing angle	Direct path length (km)	Indirect path length (km)	$\frlvert E_{tot} \frrvert / \frlvert E_0 \frrvert$ (db)	$\frlvert E_r \frrvert / \frlvert E_0 \frrvert$ (db)
83:50	50.35	444.76	-0.08	-19.84
77.00	101.95	453.22	0.43	-13.88
71.00	151.89	466.54	-2.86	-10.66
65.50	200.73	484.06	-2.32	-8.56
60.50	248.74	505.14	3.17	-7.06
55.50	301.41	532.14	3.55	-5.85
51.50	347.93	558.91	-5.74	-5.03
47.50	399.47	591.29	1.93	-4.33
44.00	449.76	625.24	-7.67	-3.80
41.00	497.65	659.40	-1.60	-3.41
-	499.99	661.11	-	-

Table 4. Multipath characterization (324-MHz link above sea water).

Surface dielectric constant = 80
Surface conductivity = 4 mhos m^{-1}
Frequency = 324 MHz
Height of both spacecraft = 221 km
Radius of earth = 6370 km
Maximum separation of spacecraft = 500 km

Grazing angle	Direct path length (km)	Indirect path length (km)	$\frac{\lvert E_{tot} \rvert}{\lvert E_0 \rvert}$ (db).	$\frac{\lvert E_r \rvert}{\lvert E_0 \rvert}$ (db)
83°50	50.35	444.76	0.80	-20.14
77.00	101.95	453.22	1.51	-14.17
71.00	151.89	466.54	-2.44	-10.94
65.50	200.73	484.06	2.56	-9.17
60.50	248.74	505.14	-4.48	-7.32
55.50	301.41	532.14	-5.27	-6.09
51.50	347.93	558.91	-3.40	-5.26
47.50	399.47	591.29	3.92	-4.55
44.00	449.76	625.24	-4.80	-4.01
41.00	497.65	659.40	2.90	-3.60
-	499.99	661.11	-	-

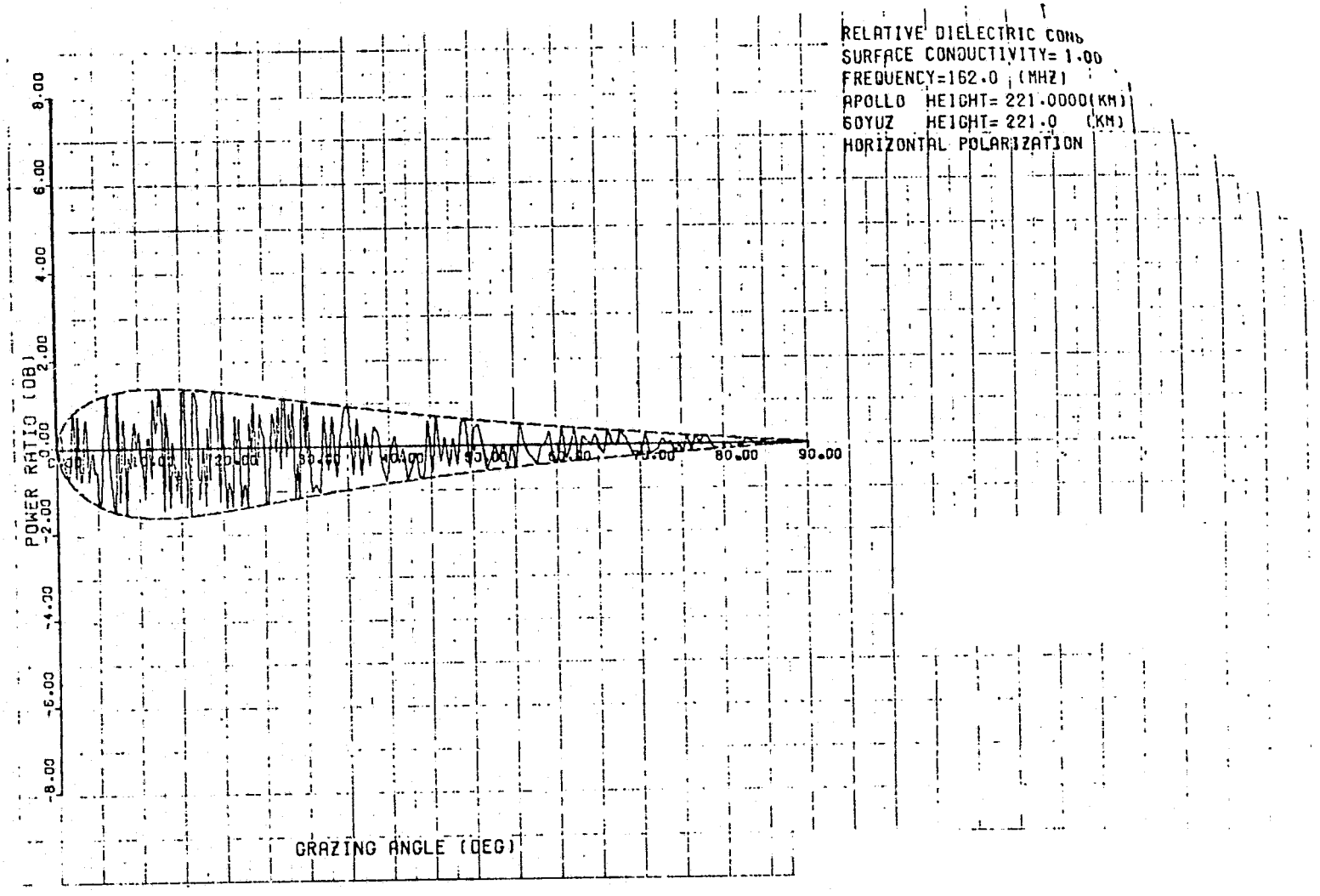

Figure 9. Signal fluctuations at the receiver terminal (162 MHz, DM-to-CSM link above desert, 10-db attenuation in the direction of the reflected path).

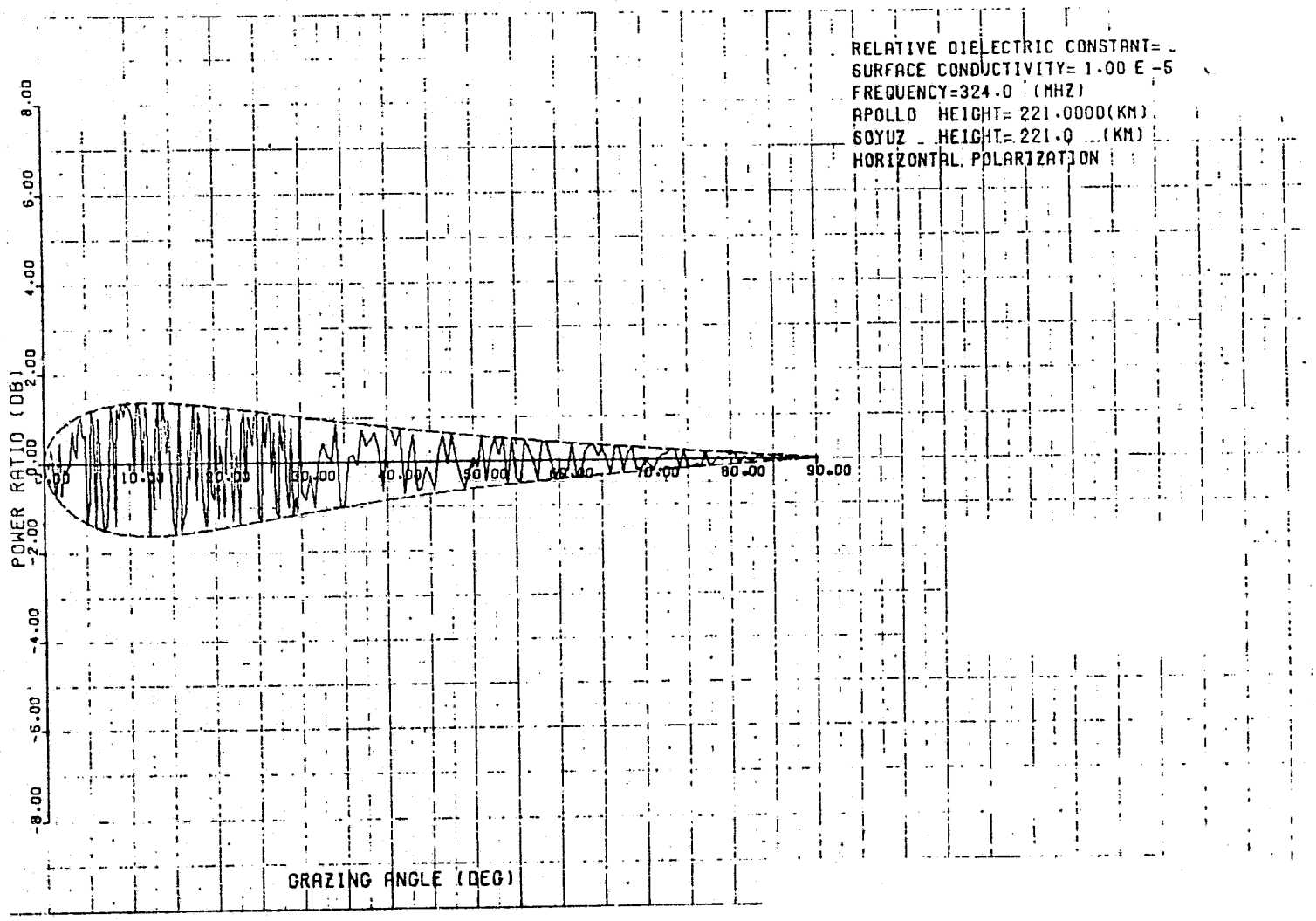

Figure 10. Signal fluctuations at the receiver terminal (324 MHz, DM-to-CSM link above desert, 10-db attenuation in the direction of the reflected path).

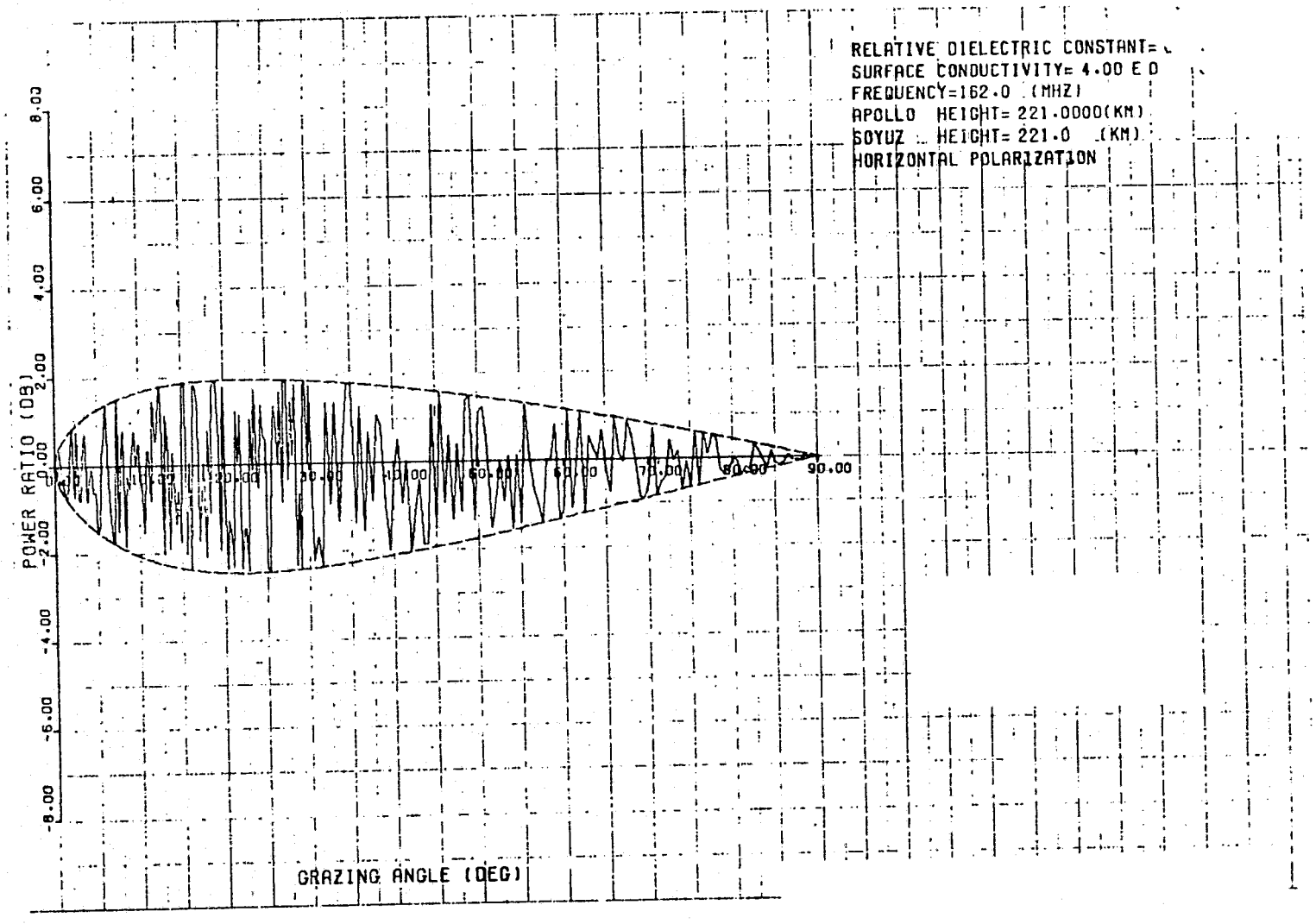

Figure 11. Signal fluctuations at the receiver terminal (162 MHz, DM-to-CSM link above sea water, 10-db attenuation in the direction of the reflected path).

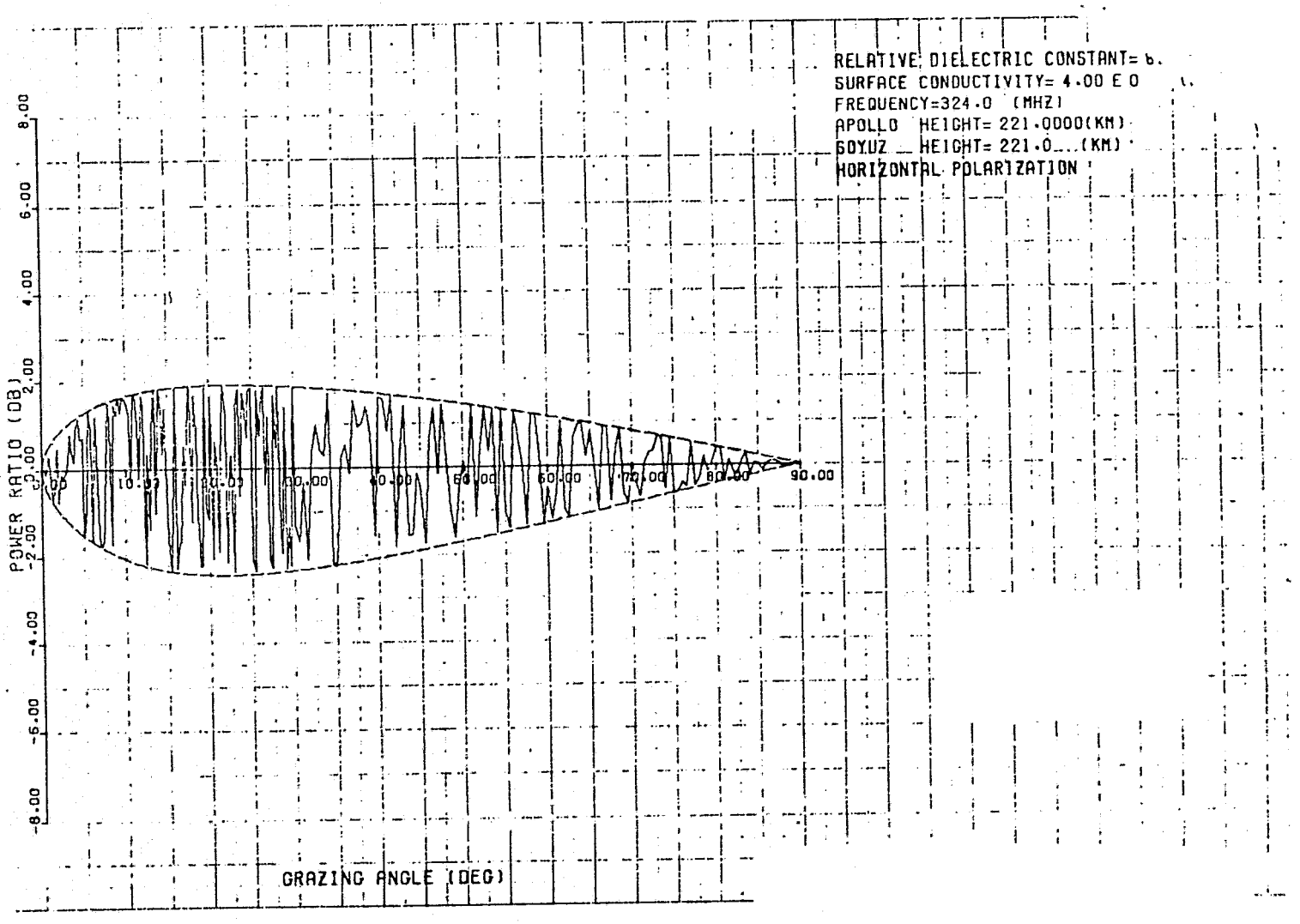

Figure 12. Signal fluctuations at the receiver terminal (324 MHz, DM-to-CSM link above sea water, 10-db attenuation in the direction of the reflected path).

when the difference in antenna gain between the direction of the direct path and that of the reflected path is 10 db, and 1.35 mHz when the gain difference is 15 db.

3.2.3 Overall expected error

From the above discussion, we conclude that the overall expected error in measuring both the doppler shift at a single frequency and the differential doppler shift is between 2 and 3 mHz. We shall adopt 3 mHz as the error in the raw data.

The estimate of the overall measurement error in the complete MA-089 experiment must include the contribution to the error budget of data processing and data inversion. This estimate will be performed in Part II of this report.

4. DOPPLER-TRACKING INSTRUMENTATION

Figures 13, 14, and 15 show block diagrams (Stiffler et al., 1975) of the beacon transmitter installed on the DM (0.1-watt output power at each of the two unmodulated carriers) and of the two-frequency receiver, doppler processor, and recorder, all installed on board the CSM. The antenna on the DM is a linear monopole oriented along the axis of maximum moment of inertia of the DM, perpendicular to the orbital plane. As initially suggested by Colombo (1974), a maneuver of the CSM/DM (before separation) will impose on the DM a rotation of approximately 3° sec^{-1} around that axis. It is expected that this orientation will be maintained by the monopole antenna during the lifetime of the experiment. The receiving antenna on the CSM is a circularly polarized microstrip panel structure.

On board the CSM, the 10-sec doppler samples are encoded in digital words organized in 73-word frames, each of which contains a frame-number word. Each frame contains a total of 5063 bits and represents approximately 12 min of data. There will be, therefore, 120 frames in 24 hours of data collection. The frames will be stored in a redundant pair of on-board, single-channel, start-stop tape recorders, where the elementary bits are written in with a speed of approximately 1 kbit sec^{-1}. Every frame will utilize approximately 5 sec of tape plus a guard band of some 7 sec. Thus, a full 24 hours of data collection will be compressed into approximately 25 min of actual tape recordings. Some similar arrangement is foreseen for the ground recordings.

Because the doppler processor is the heart of the doppler-tracking system, it will be described hereunder in more detail. The concept of the processor has been worked out by Weiffenbach (1973).

The processor consists of five counters: a 10-sec interval counter, two up-down counters, and two zero-crossing counters, with one up-down counter and one zero-crossing counter associated with each of the two channels. The operation of the processor can be explained by referring to Figure 16. The 10-sec counter identifies the time instants t_0, $t_2 = t_0 + 9.996$ sec, $t_0' = t_0 + 10$ sec, $t_2' = t_2 + 10$ sec, etc. The points

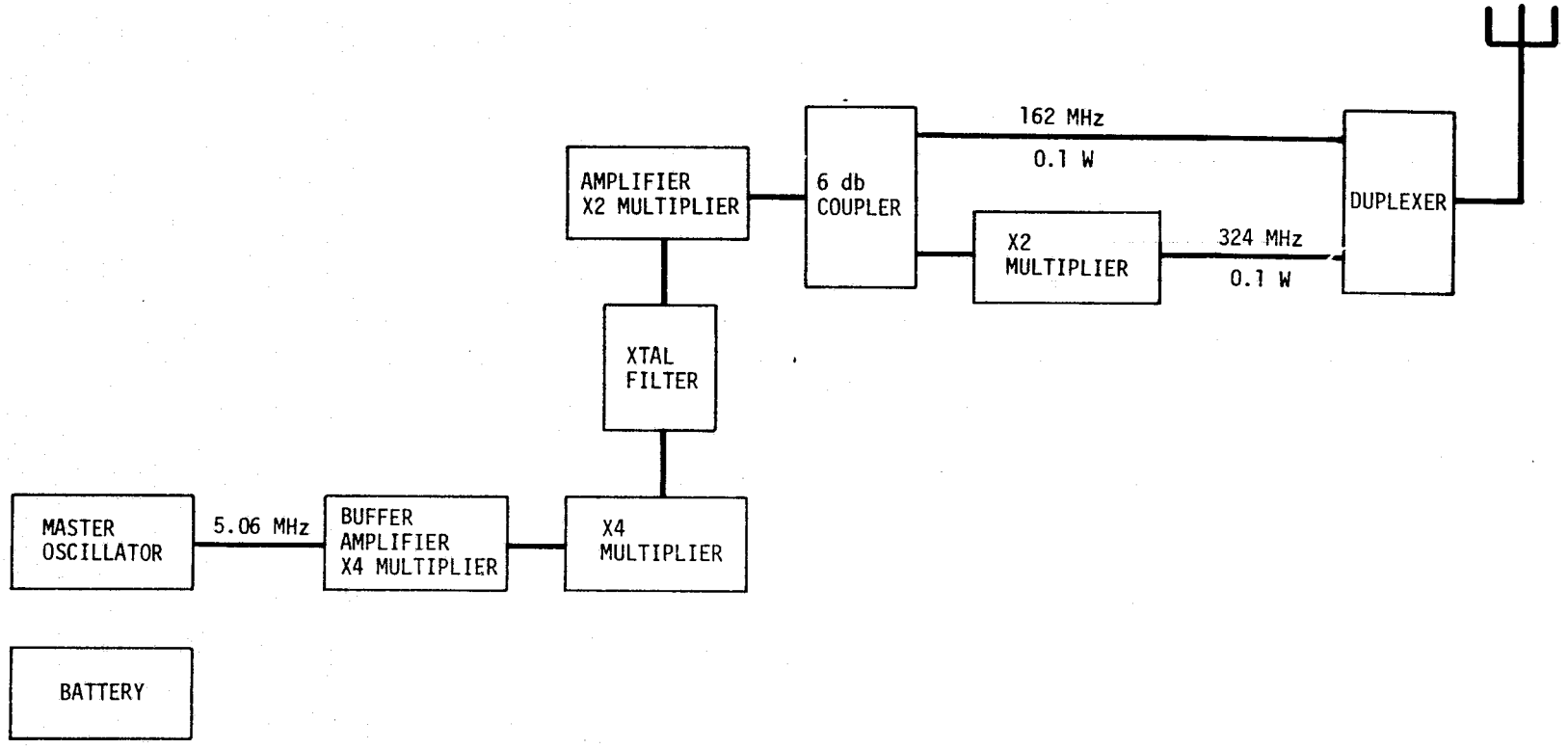

Figure 13. Block diagram of the transmitter.

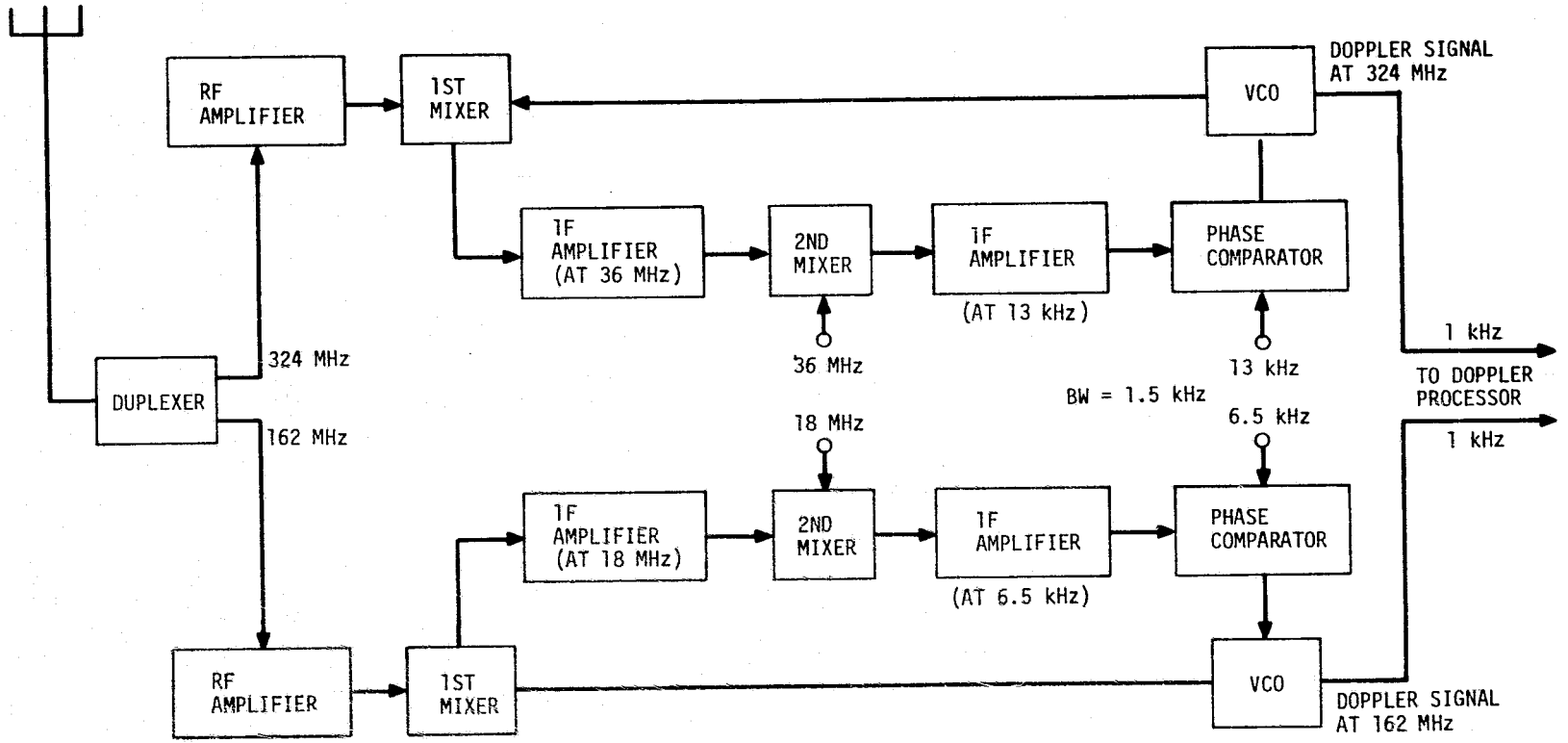

Figure 14. Block diagram of the receiver.

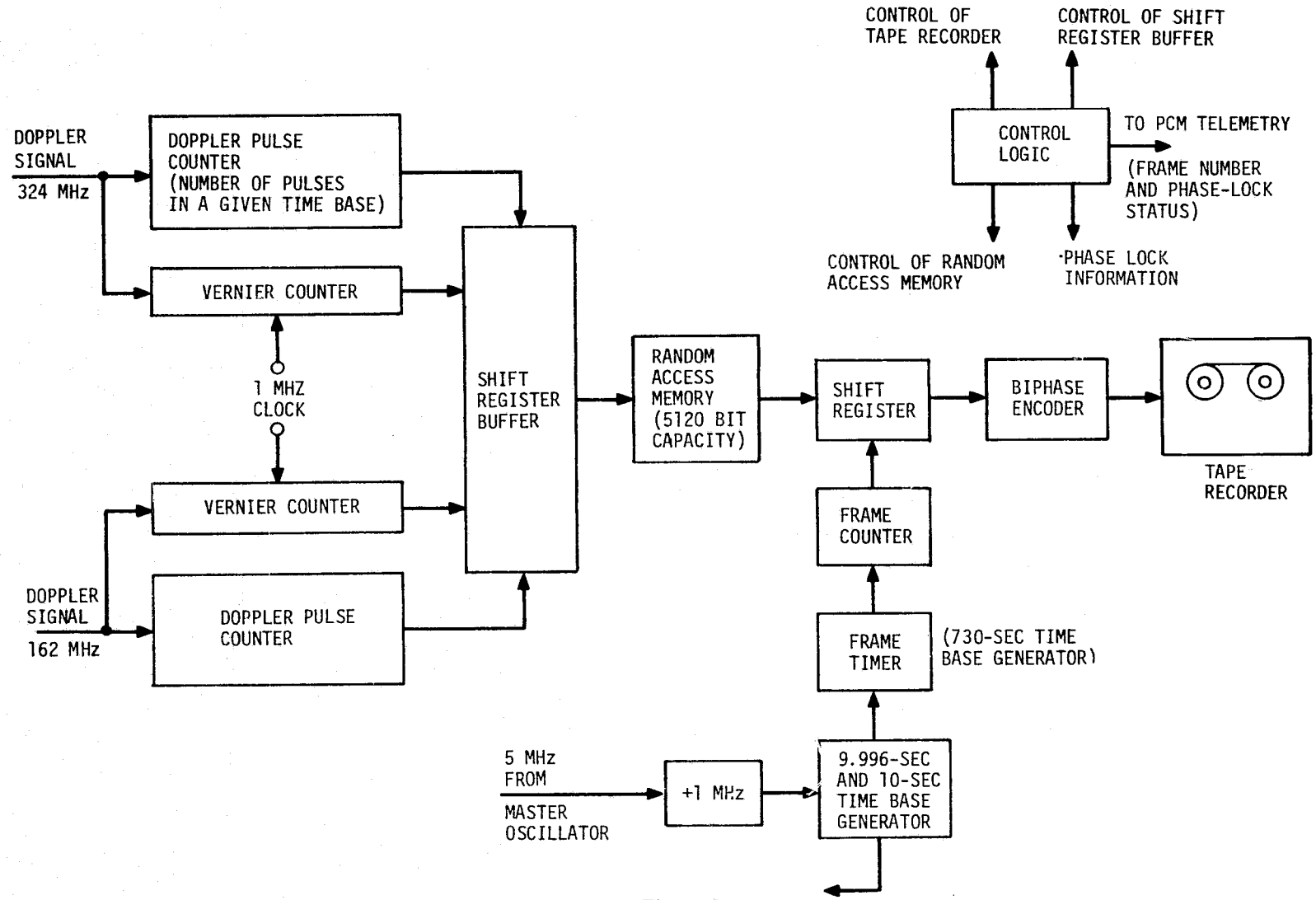

Figure 15

Figure 15. Block diagram of the doppler processor.

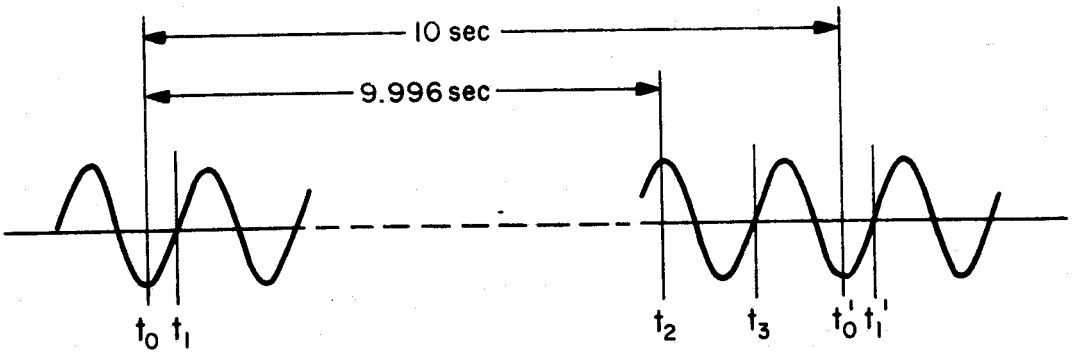

Figure 16. Averaging interval of the doppler processor.

of t_1 and t_3 are determined by the first positive-going zero crossing in the heterodyned signal occurring after times t_0 and t_2, respectively. (Note that while t_0 and t_2 are common to both channels, there are two t_1's and two t_3's, one of each associated with each of the two channels.) For each channel, the associated up-down counter is enabled at time t_0 and counts the number of microsecond clock pulses observed before it is disabled at time t_1. When it is enabled again at t_2, this time in the down-count mode, it down-counts the number of clock pulses in the interval (t_2, t_3). Simultaneously, the zero-crossing counters count the number of positive-going zero crossings in the interval (t_0, t_2) for each channel. These time and zero-crossing counts constitute the raw data associated with the observation interval in question. The counters are reset and the whole process begins anew at time t_0'.

Four quantities, namely, $T_i = [t_1(i) - t_0] - [t_3(i) - t_2]$ and Z_i, the number of positive-going zero crossings in the interval (t_0, t_2), are thus generated during each 10-sec observation period. (Here, $i = 1, 2$ is an index used to distinguish between the two channels.) The average frequencies observed during this interval are estimated by $\hat{f}_i = Z_i/(9.996 - T_i)$; we discuss the error in this estimate below. Although it would be possible to design the processor itself to determine $\hat{f}_i$, it was found to be more efficient to record the data as follows: The first word in each frame contains the quantities Z_2, Z_1, T_2, and T_1; all remaining words contain ΔZ_2, ΔZ_1, T_2, and T_1, with ΔZ defined as the difference between the current value of Z and its immediate predecessor.

Thirteen bits each (12 bits plus sign) are used to record T_1 and T_2, 15 bits each for Z_1 and Z_2, and six bits each for ΔZ_1 and ΔZ_2. This allows unambiguous measurements of all frequencies in the range 250 to 1750 Hz (+750-Hz deviation from the 1000-Hz center frequency), with frequency variations as large as ±3.2 Hz between observation intervals and up to ±1.6 Hz from channel to channel. These ranges are all well in excess of the maximum anticipated for these quantities.

Because the integrity of these data is vital to the success of the MA-089 experiment, various encoding techniques for protecting against random substitution and insertion and deletion errors were examined. The use of two tape recorders, of

course, provides considerable error protection, but not against errors induced before recording, nor does it offer any protection should one of the two recorders fail. We decided that a modified, shortened Hamming code would provide significant error protection at the cost of a negligible increase in the complexity of the processor and a modest increase in its memory requirements. Adjoining seven parity-check bits to each word as it is read into the processor's buffer memory allows any single substitution errors to be corrected, any double (and most multiple) substitution errors to be detected, and insertions or deletions of up to three bits in any word to be found and confined to those words directly affected.

The first word in each frame (after the eight-bit frame number) is then 87 bits long (80 information bits plus seven parity-check bits), with the remaining words requiring 69 bits. As already mentioned, a frame contains 73 words, resulting in a grand total of 5063 bits. Figures 17 and 18 illustrate the frame and word formats.

In addition to the doppler information, each data word contains rate-gyro information obtained from the roll, pitch, and yaw spacecraft channels (each with eight-bit accuracy). This makes it possible to remove from the data the doppler shift due to CSM rotational motions, or at least to identify the times when its attitude jets are fired.

In order to mark in the record the data invalidated by a loss-of-lock condition in either of the two tracking loops, the first affected word is recorded with an 01111 prefix and is followed by the appropriate number of "0's" rather than "1's." The next word is shortened, and any subsequent invalidated data are recorded in the same manner as the first until lock is regained. Data from the first valid observation following this event are then recorded in the 46-bit format, and the normal format is again resumed for the remainder of the frame.

It is tentatively planned to turn on the DM-borne dual-frequency transmitter on July 23, 1975, at the time of the DM/CSM separation. Its battery-limited emissions are expected to last approximately 24 hours. Ground receptions will be attempted at a few sites, one of which is possibly contained in the orbital plane, for at least one pass in the 24 hours.

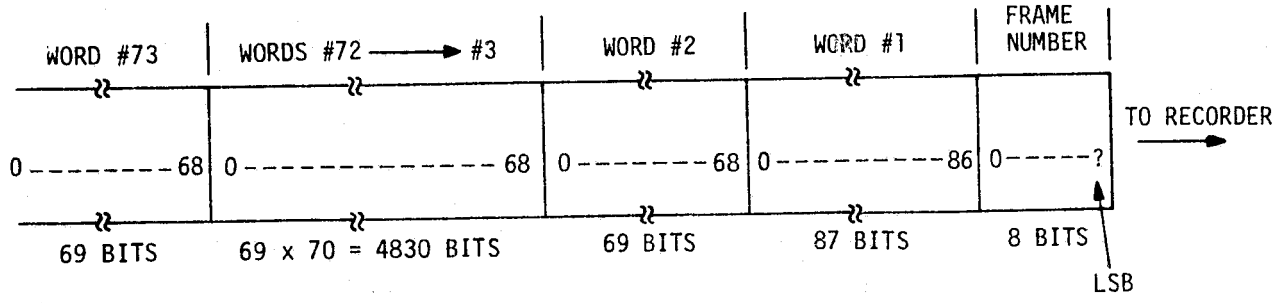

Figure 17. Data-frame format.

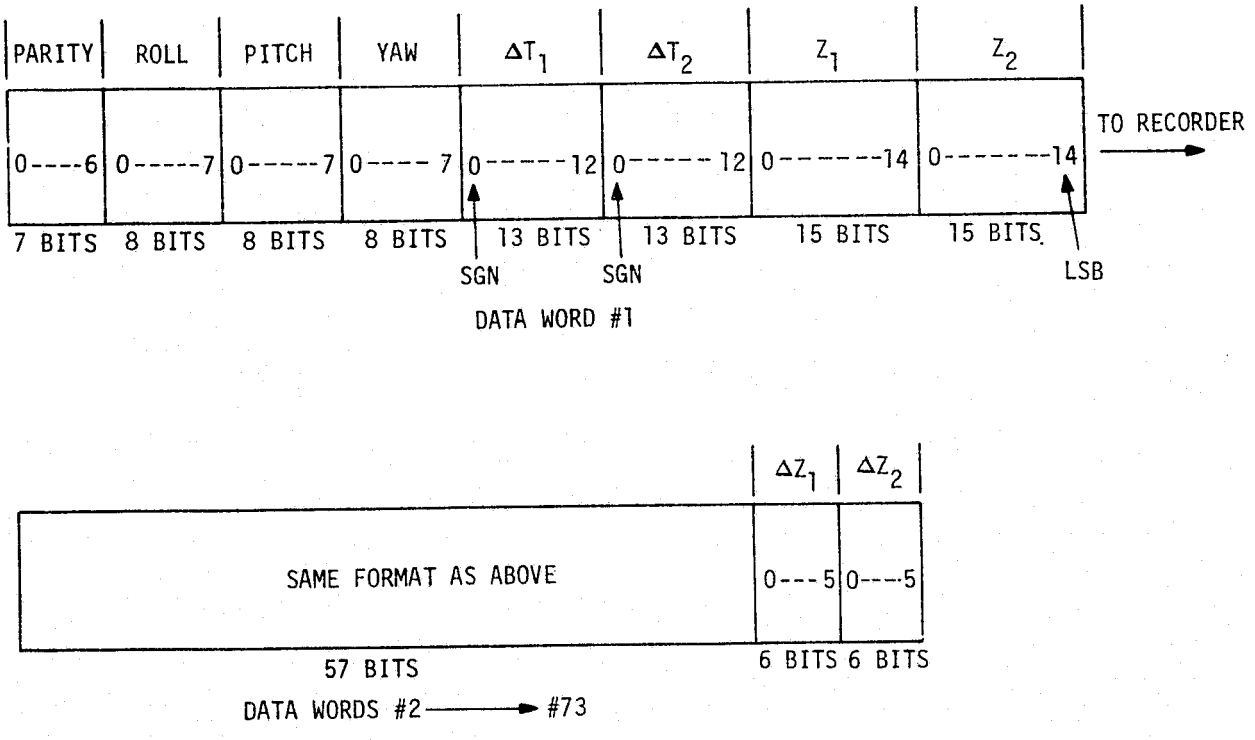

Figure 18. Data-word format.

5. COMPUTER SIMULATION OF IONOSPHERIC-INDUCED DOPPLER SHIFTS

5.1 Background

In order to check the functioning of the software being developed for the reduction and processing of the MA-089 experiment data, we have performed a computer simulation of the expected doppler measurements, anticipating as closely as possible the results of the experiment.

This simulation has been accomplished by using both a model of the 1975 summer ionosphere (Odom, 1974) and a ray-tracing computer program (Sforza, 1970). The ray-tracing program neglects the effect of the earth's magnetic field but otherwise traces rays in a model nonhomogeneous ionosphere, whose structural detail is reasonably realistic. With these tools, we have computed the differential doppler shift expected between the DM and the CSM (relative separation = 300 km) while the pair moves in a complete orbit around the earth. The orbital plane, inclined ~52° with respect to the equator, has been chosen to cross the equator at noon and midnight local time (LT) and to reach the highest northern latitude at 0600 LT and the highest southern latitude at 1800 LT. In the direct motion of the pair, the CSM has been assumed always to be East of the DM, and two ground stations have been assumed to be contained in this orbital plane and located at 0430 and 0930 LT. These times correspond to the lowest and highest ionospheric density as well as to extremes in horizontal gradients. The simulated data we generated will be inverted into the ionospheric parameters of the model (see Part II). How close the original and the reconstructed data come to each other will indicate the accuracies of the ray-tracing simulation and the inversion. Once the actual experiment data become available in late summer 1975, we will invert them by means of the same software used to invert the simulated data.

5.2 Model of the Summer 1975 Ionosphere

Appendix A (Odom, 1974) gives a detailed description of the ionospheric model we have adopted. The following quantities appear in the tabulation:

H_t = height (km),

NL = North Latitude (deg),

WL = West Longitude (deg),

N = electron density (el cm^{-3})

DNDR = vertical gradient of the electron density (el cm^{-3} km^{-1}),

DNDNL = latitudinal gradient of the electron density (el cm^{-3} rad^{-1}),

DNDWL = longitudinal gradient of the electron density (el cm^{-3} rad^{-1}).

The model is fully three-dimensional and includes day–night and night–day transitions. The highest electron content is along the vertical of ~1000 LT, with a secondary relative maximum at 1600 LT. Electron-density minima are along the verticals of ~0300 and 2300 LT.

5.3 Differential Doppler Shift in Spacecraft-to-Spacecraft Paths

From the ionospheric model described above and in Appendix A, we have used ray tracing to compute the differential phase-path length expected at 162 and 324 MHz between the DM and the CSM, which are assumed to orbit at the common height of 221 km and to be separated by 300 km. We define the differential phase-path length as the function (in meters)

$$\Phi = \int_0^S (\mu - 1)\, ds \quad ,$$

or the difference between the electrical length of the DM/CSM separation and its geometric equivalent. Because $\mu < 1$ in the ionosphere at the ASTP frequency, the electrical length ($= \int \mu\, ds$) is smaller than the geometric length and Φ is therefore

negative. Figure 19 provides a plot of this function, with the longitude of the DM as the independent variable. Longitude 0 hours is taken to be at local midnight, and the adopted position of the orbital plane was given in Section 5.1. Figure 20 shows the computed values of the differential doppler shift in the DM-to-CSM path:

$$\delta\dot{\Phi} = \dot{\Phi}_1 - 2\dot{\Phi}_2 \quad ,$$

where $\dot{\Phi}_1$ and $\dot{\Phi}_2$ are the doppler shifts measured at 324 and 162 MHz, respectively. The quantity $\delta\dot{\Phi}$ can be inverted into horizontal gradients of electron content (see Part II).

5.4 Differential Doppler Shift in Spacecraft-to-Ground Paths

Similar calculations have been done for DM-to-ground paths. To cover a variety of ionospheric conditions, we have assumed the ground stations to be located in the orbital plane and situated at various local times. Figure 21 gives the differential phase-path length at 162 and 324 MHz for ground stations at 0430, 0930, and 1230 LT. Because the first and third cases represent widely different ionospheric conditions, we have computed the differential doppler shifts for each and present the results in Figures 22 and 23.

The space-to-ground differential doppler data will be inverted into columnar electron content and electron density at the DM height, as will be done with the actual data collected in the summer of 1975 by the MA-089 experiment (see Part II, Sections 3 and 4).

5.5 Modeling Approach for the Rotating Doppler Shift in Spacecraft-to-Ground Paths

As already mentioned, we expect at least some of the ground stations available for the MA-089 experiment to be equipped with linearly polarized antennas. It will therefore be possible, by recording the signal's amplitude, to measure the Faraday rotation in DM-to-ground paths.

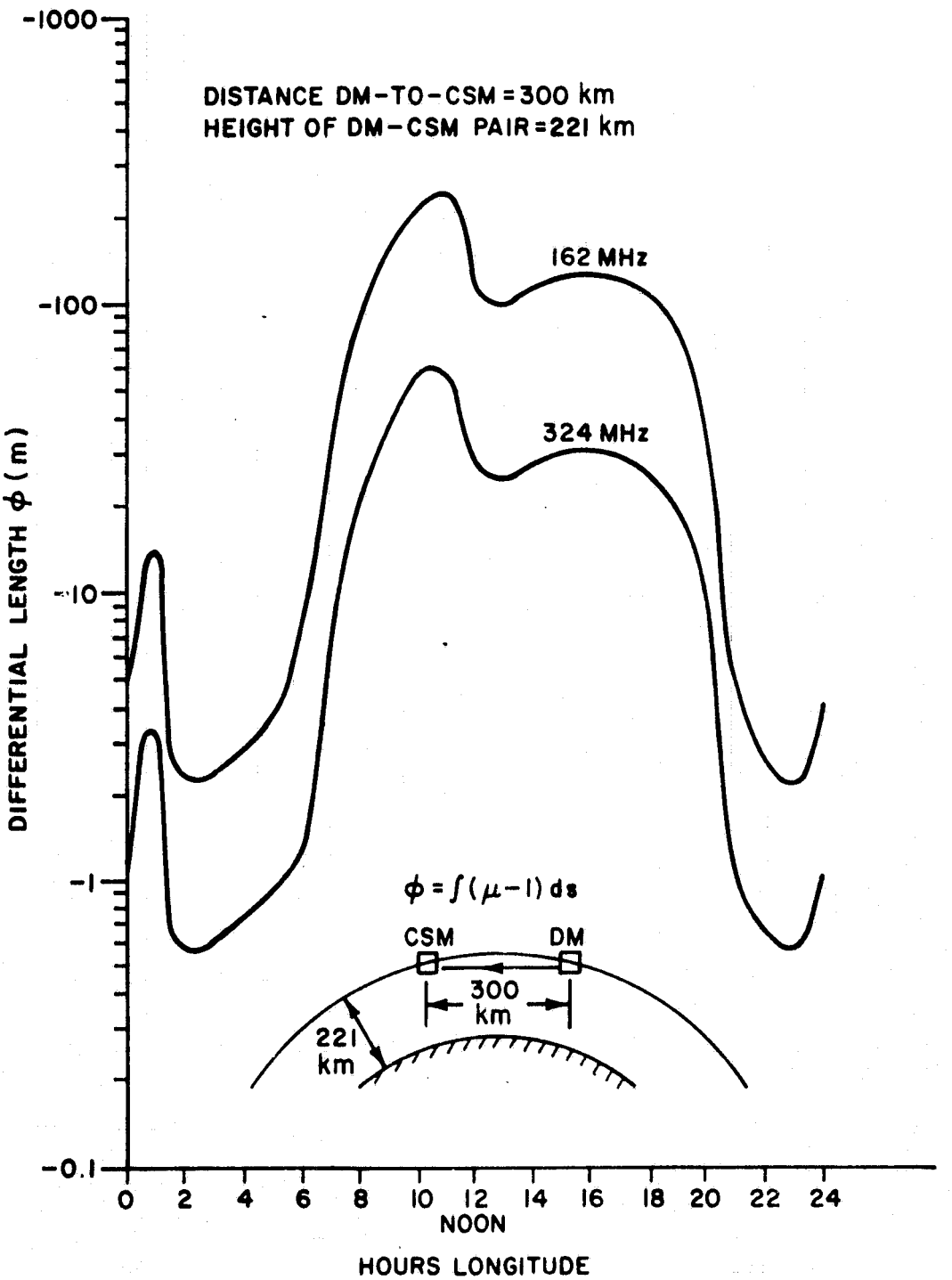

Figure 19. Differential DM-to-CSM phase-path length.

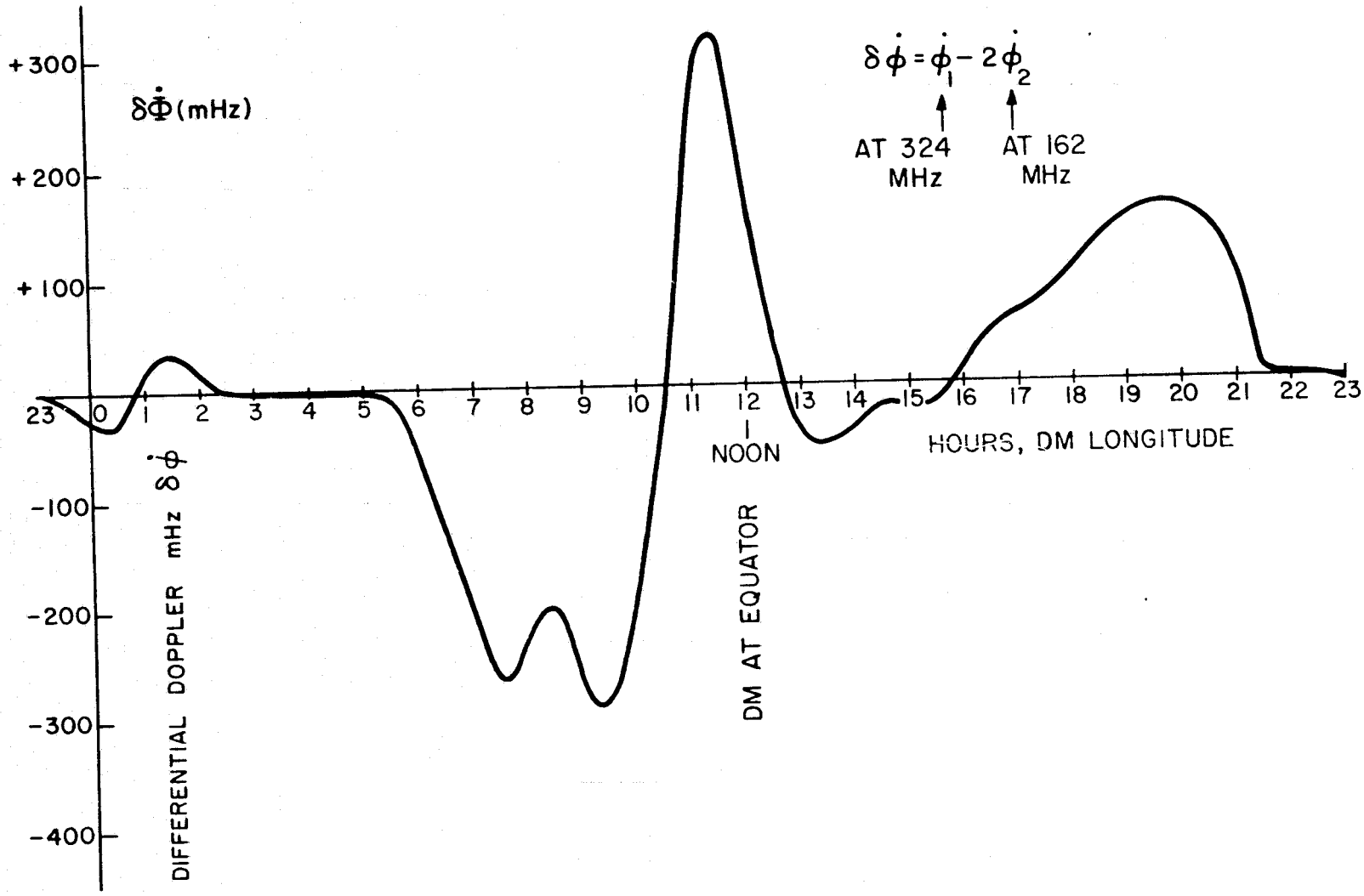

Figure 20. Expected differential doppler shift in the DM-to-CSM path.

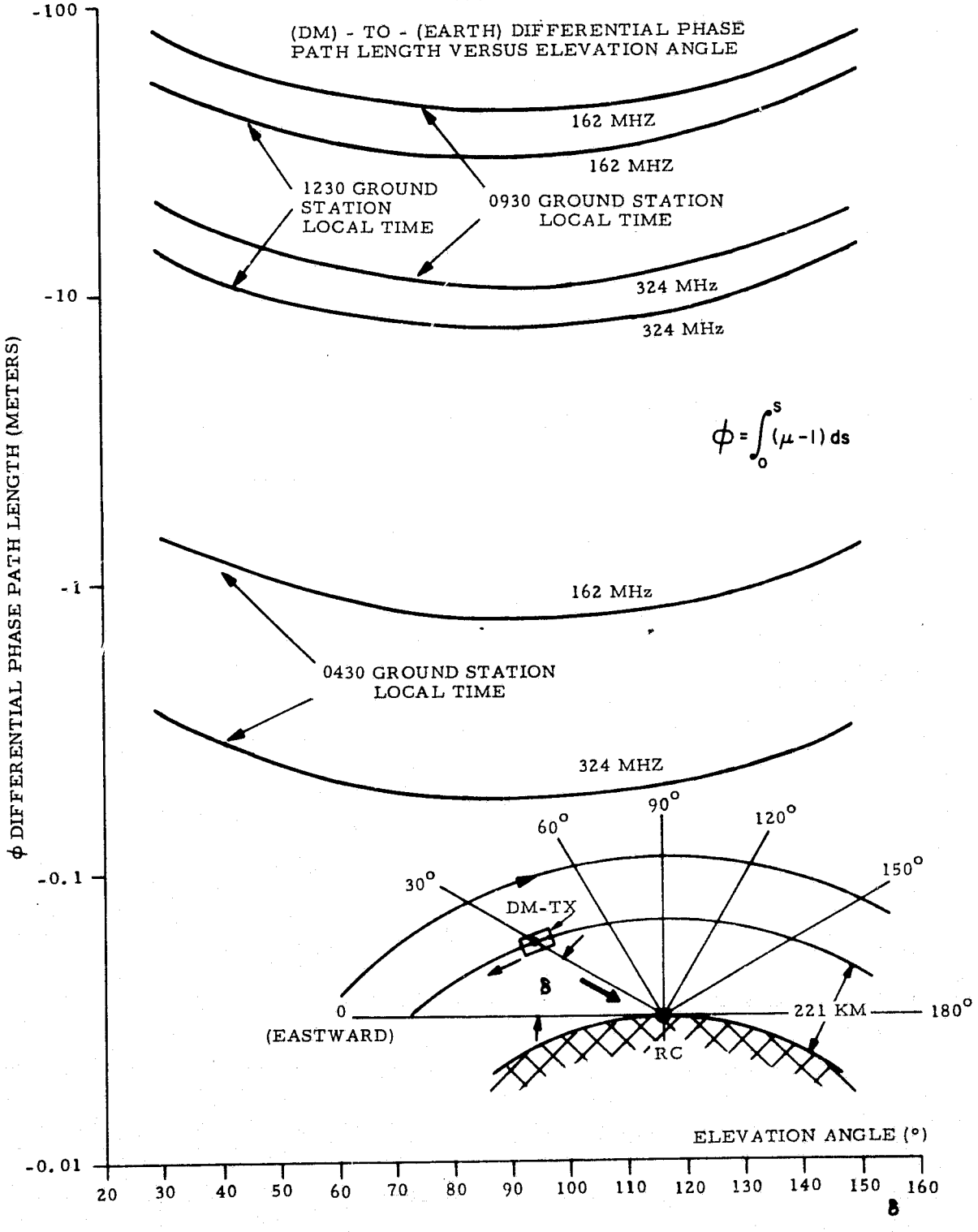

Figure 21. Path length versus elevation angle.

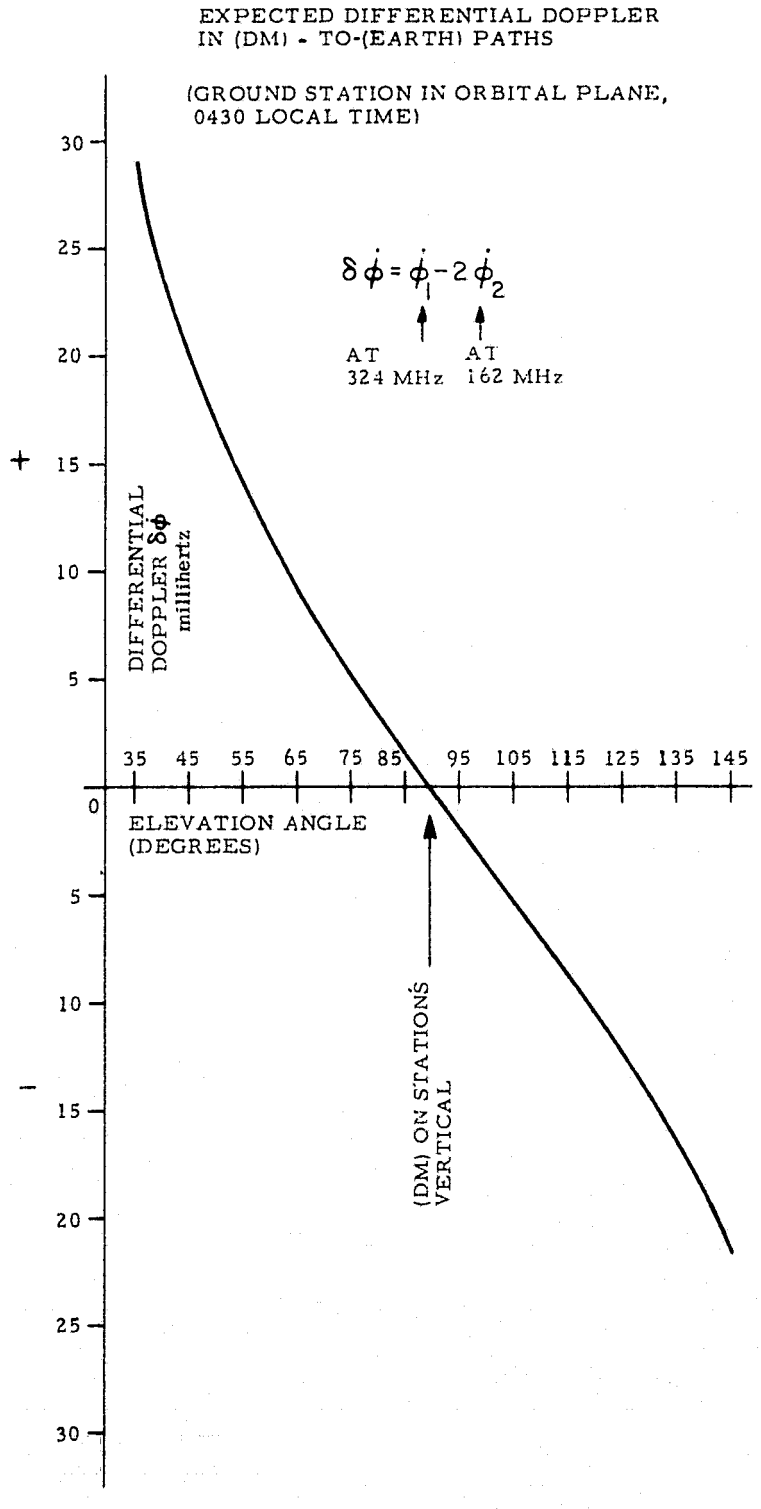

Figure 22. Expected differential doppler shift in DM-to-earth paths, with the ground station in the orbital plane at 0430 LT.

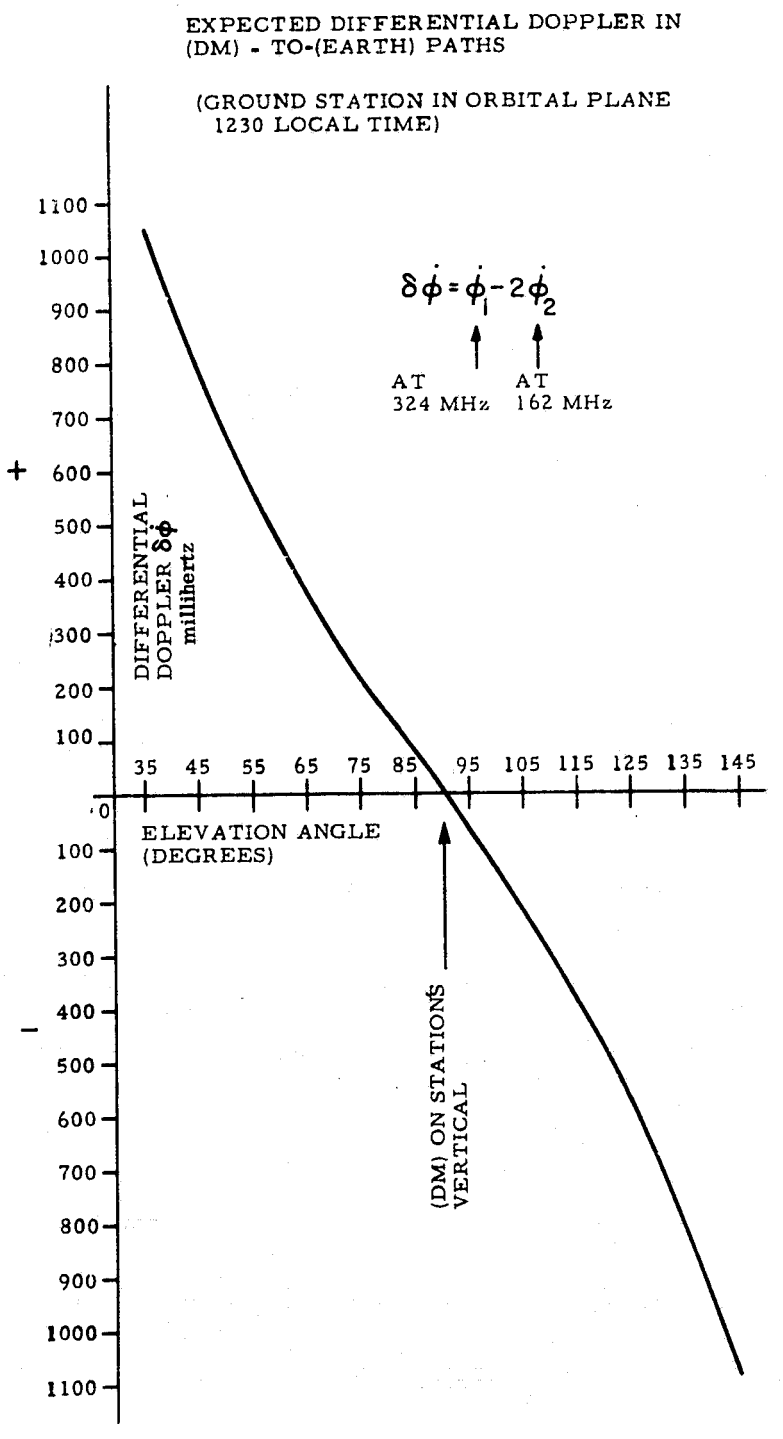

Figure 23. Expected differential doppler shift in DM-to-earth paths, with the ground station in the orbital plane at 1230 LT.

We plan to perform a computer simulation of this phenomenon in the future by choosing one of the available ray-tracing programs (Grossi and Langworthy, 1966; Jones, 1968) that includes the effect of the earth's magnetic field on the index of refraction. The simulation will trace ordinary and extraordinary rays, together with their pertinent properties (e.g., phase-path length and geometric distances). By means of this program, we intend to generate simulated values of $\delta\dot{\Phi}_H$ according to expressions (19) and (20) of Section 3.1.

5.6 Modeling Approach for Traveling Ionospheric Disturbances and Ionospheric Turbulence

Methods for detecting ionospheric disturbances from reception of satellite emissions have recently been proposed (Bratteng and Forsyth, 1974; Forsyth, 1974). The MA-089 experiment offers the opportunity of adding the performance of spacecraft-to-spacecraft sounding of the disturbance along roughly horizontal paths.

A traveling ionospheric disturbance (Thome, 1968; Francis, 1974) could be sampled repeatedly at successive passes of the DM/CSM pair. The electron-density distribution inside the TID could be measured and some rough tracking of the TID position performed. In order to simulate the effect of a TID on the DM-to-CSM doppler tracking link, we are planning to add, to our present ionospheric density model, a three-dimensional, static, localized perturbation of electron density characterized by a few-thousand-kilometer extension in the horizontal plane and a wave-like density structure in its interior. This localized perturbation will be cut through, in the computer simulation, by the DM-to-CSM baseline in successive orbits. We will attempt to reconstruct the TID position and structure by inverting the DM-to-CSM differential doppler data obtained with the computer simulation.

Similarly, we will determine by computer simulation the effect on the DM-to-CSM link of turbulent ionospheric regions, such as the aurora oval (to which the radio path becomes periodically tangent) and the sporadic E belt (which is periodically cut through by the DM-to-CSM path). In this way, we expect to be able to derive the position of the boundaries of these turbulent regions from the MA-089 data.

6. CONCLUSIONS

Our computer simulation of the ionospheric measurements to be performed by the MA-089 doppler-tracking experiment has shown that at all times the expected value of the ionospheric-induced doppler shift in the DM-to-CSM path vastly exceeds the doppler noise of the instrumentation system (multipath effects included). For the space-to-ground paths, this is also generally true, with some rare exceptions occurring at times when the radio path crosses regions of minimum ionospheric density.

We therefore conclude that this analysis confirms the validity of the MA-089 ionospheric measurements and encourages the formulation of optimistic expectations for the outcome of the experiment.

7. ACKNOWLEDGMENTS

We acknowledge the support given by Dr. G. C. Weiffenbach, who provided technical guidance throughout the effort. The encouragement given by Dr. Erwin R. Schmerling was instrumental in starting this project. Helpful discussions with Prof. Ya. L. Al'pert at Izmiran are also acknowledged.

The authors wish to thank Mr. Thomas I. S. Boak III for his programing effort and for the numerical computations that he performed.

8. REFERENCES

Al'pert, Ya. L. (1958). A method for investigating the ionosphere with artificial satellites, Uspekhi Fiz. Nauk, vol. 64, p. 3.

Al'pert, Ya. L. (1965). On the results of ionosphere investigations with the help of coherent radio waves emitted by satellites, in Space Research V, ed. by D. S. King-Hele, P. Muller, and G. Righini, North-Holland Publ. Co., Amsterdam, pp. 652-686.

Al'pert, Ya. L. (1973). Radio Wave Propagation in the Ionosphere, Vol. 1, The Ionosphere, 2nd ed., Consultants Bureau, New York, pp. 61-77.

Al'pert, Ya. L. (1974). On radio methods of ionospheric investigations by means of coherent radio waves emitted by satellites, presented at the COSPAR/URSI Symposium on Beacon Satellite Investigations of the Ionosphere Structure and ATS-6 Data, Moscow, November.

Bratteng, O. M., and P. A. Forsyth (1974). The possible detection of ion-acoustic waves in the polar ionosphere using satellite beacons, Journ. Atmos. Terr. Phys., vol. 36, pp. 929-941.

Colombo, G. (1974). ASTP/MA-089 experiment – On the motion about the center of gravity of the docking module after separation from the command service module, SAO Memoranda, part 1, January 28; part 2, January 28; part 3, January 29.

Comfort, G. C. (1973). Direct mapping of gravity anomalies by using doppler tracking between a satellite pair, Journ. Geophys. Res., vol. 78, pp. 6845-6851.

de Mendoza, F. (1963). Ionospheric studies with the differential doppler technique, in Radio Astronomical and Satellite Studies of the Atmosphere, ed. by J. Aarons, North-Holland Publ. Co., Amsterdam, pp. 289-312.

Forsyth, P. A. (1974). On the possibility of detecting ion-acoustic waves in the polar ionosphere using satellite radio beacons, Journ. Atmos. Terr. Phys., vol. 36, pp. 915-928.

Francis, S. H. (1974). Theory and models of atmospheric acoustic-gravity waves and travelling ionospheric disturbances, Bell Lab. Rep. on Contract DAHC 60-71-C-0005, October 1.

Garriott, O. K. (1960a). The determination of ionospheric electron content and distribution from satellite observations, Part 1, Theory of the analysis, Journ. Geophys. Res., vol. 65, pp. 1139-1150.

Garriott, O. K. (1960b). The determination of ionospheric electron content and distribution from satellite observations, Part 2, Results of the analysis, Journ. Geophys. Res., vol. 65, pp. 1151-1157.

Grossi, M. D. (1972). Proposed PPEPL experiments for IRDM (International Rendezvous Docking Mission), SAO Memorandum, June 16.

Grossi, M. D. (1974). Spacecraft-to-spacecraft ionospheric sounding on occasion of the Apollo-Soyuz Test Project, presented at the COSPAR/URSI Symposium on Beacon Satellite Investigations of the Ionosphere Structure and ATS-6 Data, Moscow, November.

Grossi, M. D., and B. M. Langworthy (1966). Geometric optics investigation of HF and VHF guided propagation in the ionospheric whispering gallery, Radio Sci., vol. 1 (new series), pp. 877-886.

Guier, W. H., and G. C. Weiffenbach (1960). A satellite doppler navigation system, Proc. IRE, vol. 48, pp. 507-516.

Jackson, J. E., and J. C. Seddon (1958). Ionosphere electron density measurements with the Navy Aerobee Hi rocket, Journ. Geophys. Res., vol. 63, pp. 197-208.

Jones, R. M. (1968). A three-dimensional ray tracing computer program, Radio Sci., vol. 3 (new series), pp. 93-94.

Misyura, V. A., G. K. Solodovnikov, and V. M. Migunov (1964). Gradients of the integral electron content in the ionosphere, Geomagn. i Aeronomiya, vol. 4, pp. 1124-1126; transl. in Geomagn. and Aeron., vol. 4, pp. 872-874.

Odom, D. B. (1974). Private communication.

Schwartz, C. R. (1970). Gravity field refinement by satellite-to-satellite doppler tracking, Dept. Geodetic Sci., Ohio State Univ. Res. Found. Rep. No. 147, December.

Seddon, J. C. (1953). Propagation measurements in the ionosphere with the aid of rockets, Journ. Geophys. Res., vol. 58, pp. 323-335.

Sforza, P. F. (1970). An ionospheric ray trace program utilizing a piecewise inverse square electron density profile, Raytheon Co., Sudbury, Mass., April.

Stiffler, J. J., A. C. Berg, and D. G. Young (1975). Phase coherent dual frequency link for high-precision doppler tracking between spacecraft (in preparation).

Thome, G. D. (1968). Long-period waves generated in the polar ionosphere during the onset of magnetic storms, Journ. Geophys. Res., vol. 73, pp. 6319-6336.

Tyagy, T. R. (1974). Determination of total electron content from differential doppler records, Journ. Atmos. Terr. Phys., vol. 36, pp. 1157-1164.

Tzedilina, E. E. (1962). The doppler effect in a magneto-active ionosphere, Geomagn. i Aeronomiya, vol. 2, pp. 865-871; transl. in Geomagn. and Aeron., vol. 2, pp. 717-723.

Von Bun, F. O. (1972). The ATS-F/Nimbus-E Tracking Experiment, in Rotation of the Earth, Proc. IAU Symp. No. 48, ed. by P. Melchior and S. Yumi, Sasaki Printing and Publ. Co., Sendai, Japan, pp. 112-120.

Weiffenbach, G. C. (1973). Private communication.

Wolf, M. (1969). Direct measurements of the earth's gravitational potential using a satellite pair, Journ. Geophys. Res., vol. 74, pp. 5295-5300.

APPENDIX A

THE MODEL OF THE SUMMER 1975 IONOSPHERE

NL= -13.407, WL= 165.000

IPT	NL	WL	N	DNDR	DNDNL	DNDWL
40	-13.41	165.00	0.	0.	0.	0.
45	-13.41	165.00	0.	0.	0.	0.
50	-13.41	165.00	4.070E-13	3.625E-13	5.530E-13	-1.394E-12
55	-13.41	165.00	1.628E-12	4.582E-12	8.295E-12	-2.091E-11
60	-13.41	165.00	1.274E-08	2.026E-08	4.654E-08	-1.173E-07
65	-13.41	165.00	5.569E-06	5.980E-06	1.767E-05	-4.453E-05
70	-13.41	165.00	4.564E-04	3.528E-04	1.350E-03	-3.402E-03
75	-13.41	165.00	1.193E-02	6.765E-03	3.394E-02	-8.554E-02
80	-13.41	165.00	1.337E-01	5.551E-02	3.722E-01	-9.381E-01
85	-13.41	165.00	7.818E-01	2.335E-01	2.149E+00	-5.416E+00
90	-13.41	165.00	2.749E+00	5.739E-01	7.506E+00	-1.892E+01
95	-13.41	165.00	6.547E+00	9.295E-01	1.782E+01	-4.491E+01
100	-13.41	165.00	1.181E+01	1.153E+00	3.211E+01	-8.093E+01
105	-13.41	165.00	1.800E+01	1.333E+00	4.895E+01	-1.234E+02
110	-13.41	165.00	2.503E+01	1.331E+00	6.795E+01	-1.713E+02
115	-13.41	165.00	2.851E+01	2.589E+01	8.108E+01	-1.722E+02
120	-13.41	165.00	3.916E+02	7.430E+01	4.042E+02	-4.870E+02
125	-13.41	165.00	7.545E+02	7.078E+01	7.340E+02	-8.577E+02
130	-13.41	165.00	1.099E+03	6.698E+01	1.031E+03	-1.206E+03
135	-13.41	165.00	1.424E+03	6.308E+01	1.295E+03	-1.528E+03
140	-13.41	165.00	1.730E+03	5.913E+01	1.527E+03	-1.824E+03
145	-13.41	165.00	2.015E+03	5.514E+01	1.725E+03	-2.092E+03
150	-13.41	165.00	2.281E+03	5.114E+01	1.890E+03	-2.332E+03
155	-13.41	165.00	2.527E+03	4.713E+01	2.023E+03	-2.544E+03
160	-13.41	165.00	2.752E+03	4.310E+01	2.122E+03	-2.728E+03
165	-13.41	165.00	2.958E+03	3.906E+01	2.189E+03	-2.882E+03
170	-13.41	165.00	3.143E+03	3.501E+01	2.222E+03	-3.008E+03
175	-13.41	165.00	3.308E+03	3.096E+01	2.223E+03	-3.105E+03
180	-13.41	165.00	3.452E+03	2.690E+01	2.190E+03	-3.173E+03
185	-13.41	165.00	3.577E+03	2.283E+01	2.124E+03	-3.212E+03
190	-13.41	165.00	3.681E+03	1.876E+01	2.025E+03	-3.221E+03
195	-13.41	165.00	3.764E+03	1.468E+01	1.893E+03	-3.200E+03
200	-13.41	165.00	3.828E+03	1.060E+01	1.728E+03	-3.151E+03
205	-13.41	165.00	3.870E+03	6.521E+00	1.529E+03	-3.071E+03
210	-13.41	165.00	3.893E+03	2.433E+00	1.297E+03	-2.962E+03
215	-13.41	165.00	1.328E+04	4.594E+03	3.323E+05	-1.056E+05
220	-13.41	165.00	3.553E+04	4.291E+03	3.835E+05	-1.632E+05
225	-13.41	165.00	5.614E+04	3.952E+03	4.269E+05	-1.591E+05
230	-13.41	165.00	7.503E+04	3.605E+03	4.640E+05	-1.540E+05
235	-13.41	165.00	9.218E+04	3.253E+03	4.953E+05	-1.481E+05
240	-13.41	165.00	1.076E+05	2.899E+03	5.208E+05	-1.415E+05
245	-13.41	165.00	1.212E+05	2.543E+03	5.406E+05	-1.342E+05
250	-13.41	165.00	1.330E+05	2.187E+03	5.546E+05	-1.262E+05

LT 0100

NL= -25.900, WL= 150.000

HT	NL	WL	N	DF DR	DNDNL	DNDWL
40	-25.90	150.00	0.	0.	0.	0.
45	-25.90	150.00	0.	0.	0.	0.
50	-25.90	150.00	1.228E-12	1.063E-12	8.476E-13	-3.046E-12
55	-25.90	150.00	4.914E-12	1.383E-11	1.271E-11	-4.568E-11
60	-25.90	150.00	3.845E-08	6.112E-08	7.133E-08	-2.563E-07
65	-25.90	150.00	1.680E-05	1.804E-05	2.708E-05	-9.730E-05
70	-25.90	150.00	1.377E-03	1.065E-03	2.069E-03	-7.434E-03
75	-25.90	150.00	3.600E-02	2.041E-02	5.202E-02	-1.869E-01
80	-25.90	150.00	4.035E-01	1.675E-01	5.705E-01	-2.050E+00
85	-25.90	150.00	2.359E+00	7.044E-01	3.293E+00	-1.183E+01
90	-25.90	150.00	8.295E+00	1.732E+00	1.150E+01	-4.134E+01
95	-25.90	150.00	1.975E+01	2.805E+00	2.731E+01	-9.813E+01
100	-25.90	150.00	3.563E+01	3.480E+00	4.921E+01	-1.768E+02
105	-25.90	150.00	5.432E+01	4.021E+00	7.502E+01	-2.696E+02
110	-25.90	150.00	7.551E+01	4.016E+00	1.041E+02	-3.742E+02
115	-25.90	150.00	8.602E+01	4.592E+00	1.175E+02	-3.544E+02
120	-25.90	150.00	4.353E+02	7.733E+01	4.971E+02	-6.304E+02
125	-25.90	150.00	8.152E+02	7.448E+01	9.082E+02	-1.026E+03
130	-25.90	150.00	1.179E+03	7.113E+01	1.287E+03	-1.408E+03
135	-25.90	150.00	1.526E+03	6.759E+01	1.629E+03	-1.771E+03
140	-25.90	150.00	1.855E+03	6.395E+01	1.933E+03	-2.111E+03
145	-25.90	150.00	2.166E+03	6.025E+01	2.199E+03	-2.427E+03
150	-25.90	150.00	2.457E+03	5.652E+01	2.426E+03	-2.719E+03
155	-25.90	150.00	2.731E+03	5.275E+01	2.613E+03	-2.986E+03
160	-25.90	150.00	2.985E+03	4.896E+01	2.760E+03	-3.227E+03
165	-25.90	150.00	3.220E+03	4.515E+01	2.867E+03	-3.441E+03
170	-25.90	150.00	3.436E+03	4.133E+01	2.934E+03	-3.629E+03
175	-25.90	150.00	3.633E+03	3.749E+01	2.960E+03	-3.790E+03
180	-25.90	150.00	3.811E+03	3.365E+01	2.945E+03	-3.924E+03
185	-25.90	150.00	3.970E+03	2.979E+01	2.889E+03	-4.030E+03
190	-25.90	150.00	4.109E+03	2.592E+01	2.792E+03	-4.109E+03
195	-25.90	150.00	4.229E+03	2.205E+01	2.654E+03	-4.160E+03
200	-25.90	150.00	4.330E+03	1.817E+01	2.474E+03	-4.183E+03
205	-25.90	150.00	4.411E+03	1.428E+01	2.253E+03	-4.177E+03
210	-25.90	150.00	4.472E+03	1.038E+01	1.990E+03	-4.144E+03
215	-25.90	150.00	4.515E+03	6.478E+00	1.686E+03	-4.081E+03
220	-25.90	150.00	4.537E+03	2.567E+00	1.339E+03	-3.990E+03
225	-25.90	150.00	1.450E+04	3.446E+03	3.470E+05	-1.096E+05
230	-25.90	150.00	2.725E+04	3.237E+03	3.220E+05	-9.339E+04
235	-25.90	150.00	4.282E+04	2.989E+03	2.933E+05	-7.669E+04
240	-25.90	150.00	5.716E+04	2.731E+03	2.638E+05	-6.046E+04
245	-25.90	150.00	7.012E+04	2.468E+03	2.341E+05	-4.485E+04
250	-25.90	150.00	8.180E+04	2.202E+03	2.045E+05	-2.991E+04

LT 0200

NL= -36.628. WL= 135.000

HT	NL	WL	N	DNDR	DNDNL	DNDWL
40	-36.63	135.00	0.	0.	0.	0.
45	-36.63	135.00	0.	0.	0.	0.
50	-36.63	135.00	3.045E-12	2.437E-12	1.367E-12	-5.525E-12
55	-36.63	135.00	1.218E-11	3.428E-11	2.050E-11	-8.288E-11
60	-36.63	135.00	9.533E-08	1.515E-07	1.150E-07	-4.650E-07
65	-36.63	135.00	4.766E-05	4.473E-05	4.366E-05	-1.765E-04
70	-36.63	135.00	3.414E-03	2.639E-03	3.336E-03	-1.349E-02
75	-36.63	135.00	8.925E-02	5.061E-02	8.388E-02	-3.391E-01
80	-36.63	135.00	1.001E+00	4.152E-01	9.199E-01	-3.719E+00
85	-36.63	135.00	5.848E+00	1.747E+00	5.310E+00	-2.147E+01
90	-36.63	135.00	2.057E+01	4.293E+00	1.855E+01	-7.499E+01
95	-36.63	135.00	4.897E+01	6.953E+00	4.403E+01	-1.780E+02
100	-36.63	135.00	8.835E+01	8.628E+00	7.935E+01	-3.208E+02
105	-36.63	135.00	1.347E+02	9.969E+00	1.210E+02	-4.890E+02
110	-36.63	135.00	1.872E+02	9.958E+00	1.679E+02	-6.789E+02
115	-36.63	135.00	2.133E+02	1.023E+00	1.918E+02	-7.755E+02
120	-36.63	135.00	5.279E+02	8.197E+01	4.375E+02	-7.669E+02
125	-36.63	135.00	9.333E+02	7.997E+01	7.550E+02	-1.099E+03
130	-36.63	135.00	1.326E+03	7.715E+01	1.052E+03	-1.432E+03
135	-36.63	135.00	1.704E+03	7.401E+01	1.326E+03	-1.758E+03
140	-36.63	135.00	2.066E+03	7.069E+01	1.575E+03	-2.074E+03
145	-36.63	135.00	2.411E+03	6.726E+01	1.800E+03	-2.377E+03
150	-36.63	135.00	2.739E+03	6.376E+01	1.999E+03	-2.667E+03
155	-36.63	135.00	3.049E+03	6.021E+01	2.172E+03	-2.943E+03
160	-36.63	135.00	3.341E+03	5.661E+01	2.318E+03	-3.203E+03
165	-36.63	135.00	3.615E+03	5.298E+01	2.438E+03	-3.447E+03
170	-36.63	135.00	3.870E+03	4.932E+01	2.531E+03	-3.674E+03
175	-36.63	135.00	4.108E+03	4.564E+01	2.598E+03	-3.884E+03
180	-36.63	135.00	4.327E+03	4.193E+01	2.637E+03	-4.077E+03
185	-36.63	135.00	4.527E+03	3.821E+01	2.649E+03	-4.252E+03
190	-36.63	135.00	4.709E+03	3.447E+01	2.634E+03	-4.408E+03
195	-36.63	135.00	4.872E+03	3.072E+01	2.591E+03	-4.547E+03
200	-36.63	135.00	5.016E+03	2.695E+01	2.521E+03	-4.666E+03
205	-36.63	135.00	5.141E+03	2.318E+01	2.423E+03	-4.767E+03
210	-36.63	135.00	5.248E+03	1.938E+01	2.297E+03	-4.849E+03
215	-36.63	135.00	5.335E+03	1.558E+01	2.143E+03	-4.911E+03
220	-36.63	135.00	5.404E+03	1.176E+01	1.961E+03	-4.954E+03
225	-36.63	135.00	5.453E+03	7.939E+00	1.751E+03	-4.977E+03
230	-36.63	135.00	5.483E+03	4.103E+00	1.513E+03	-4.980E+03
235	-36.63	135.00	5.494E+03	5.810E+02	1.022E+05	-1.482E+04
240	-36.63	135.00	1.811E+04	2.642E+03	2.076E+05	-1.374E+04
245	-36.63	135.00	3.088E+04	2.461E+03	2.068E+05	-1.715E+03
250	-36.63	135.00	4.269E+04	2.262E+03	2.036E+05	9.500E+03

LT 0300

NL= -44.860, WL= 120.000

IFT	NL	WL	N	DNDR	DNDNL	DNDWL
40	-44.86	120.00	0.	0.	0.	0.
45	-44.86	120.00	0.	0.	0.	0.
50	-44.86	120.00	6.145E-12	5.321E-12	2.528E-12	-8.340E-12
55	-44.86	120.00	2.458E-11	6.918E-11	3.791E-11	-1.251E-10
60	-44.86	120.00	1.924E-07	3.058E-07	2.127E-07	-7.019E-07
65	-44.86	120.00	8.408E-05	9.028E-05	8.075E-05	-2.665E-04
70	-44.86	120.00	6.891E-03	5.327E-03	6.169E-03	-2.036E-02
75	-44.86	120.00	1.801E-01	1.021E-01	1.551E-01	-5.119E-01
80	-44.86	120.00	2.919E+00	8.380E-01	1.701E+00	-5.614E+00
85	-44.86	120.00	1.180E+01	3.525E+00	9.821E+00	-3.241E+01
90	-44.86	120.00	4.151E+01	8.665E+00	3.431E+01	-1.132E+02
95	-44.86	120.00	9.884E+01	1.403E+01	8.144E+01	-2.687E+02
100	-44.86	120.00	1.783E+02	1.741E+01	1.468E+02	-4.843E+02
105	-44.86	120.00	2.718E+02	2.012E+01	2.237E+02	-7.382E+02
110	-44.86	120.00	3.778E+02	2.010E+01	3.106E+02	-1.025E+03
115	-44.86	120.00	4.304E+02	2.065E+00	3.547E+02	-1.171E+03
120	-44.86	120.00	7.030E+02	9.148E+01	4.077E+02	-1.056E+03
125	-44.86	120.00	1.158E+03	9.034E+01	6.115E+02	-1.415E+03
130	-44.86	120.00	1.604E+03	8.795E+01	8.025E+02	-1.778E+03
135	-44.86	120.00	2.037E+03	8.500E+01	9.808E+02	-2.137E+03
140	-44.86	120.00	2.454E+03	8.173E+01	1.147E+03	-2.489E+03
145	-44.86	120.00	2.854E+03	7.825E+01	1.300E+03	-2.829E+03
150	-44.86	120.00	3.236E+03	7.463E+01	1.440E+03	-3.157E+03
155	-44.86	120.00	3.600E+03	7.090E+01	1.568E+03	-3.471E+03
160	-44.86	120.00	3.945E+03	6.708E+01	1.683E+03	-3.768E+03
165	-44.86	120.00	4.271E+03	6.320E+01	1.786E+03	-4.049E+03
170	-44.86	120.00	4.577E+03	5.926E+01	1.875E+03	-4.312E+03
175	-44.86	120.00	4.863E+03	5.527E+01	1.952E+03	-4.556E+03
180	-44.86	120.00	5.129E+03	5.124E+01	2.017E+03	-4.782E+03
185	-44.86	120.00	5.375E+03	4.717E+01	2.068E+03	-4.988E+03
190	-44.86	120.00	5.601E+03	4.307E+01	2.107E+03	-5.174E+03
195	-44.86	120.00	5.806E+03	3.894E+01	2.132E+03	-5.339E+03
200	-44.86	120.00	5.990E+03	3.478E+01	2.145E+03	-5.483E+03
205	-44.86	120.00	6.154E+03	3.059E+01	2.145E+03	-5.605E+03
210	-44.86	120.00	6.296E+03	2.638E+01	2.132E+03	-5.706E+03
215	-44.86	120.00	6.418E+03	2.215E+01	2.106E+03	-5.785E+03
220	-44.86	120.00	6.518E+03	1.789E+01	2.067E+03	-5.841E+03
225	-44.86	120.00	6.597E+03	1.361E+01	2.014E+03	-5.873E+03
230	-44.86	120.00	6.654E+03	9.312E+00	1.949E+03	-5.883E+03
235	-44.86	120.00	6.690E+03	4.990E+00	1.871E+03	-5.869E+03
240	-44.86	120.00	6.704E+03	6.471E-01	1.779E+03	-5.831E+03
245	-44.86	120.00	1.400E+04	1.684E+03	5.679E+04	-2.135E+04
250	-44.86	120.00	2.217E+04	1.582E+03	7.262E+04	-1.437E+04

LT 0400

NL= -50.035, WL= 105.000

HT	NL	WL	N	DNDR	DNDNL	DNDWL
40	-50.03	105.00	0.	0.	0.	0.
45	-50.03	105.00	0.	0.	0.	0.
50	-50.03	105.00	1.060E-11	9.182E-12	4.781E-12	-1.101E-11
55	-50.03	105.00	4.241E-11	1.194E-10	7.171E-11	-1.652E-10
60	-50.03	105.00	3.320E-07	5.277E-07	4.024E-07	-9.268E-07
65	-50.03	105.00	1.451E-04	1.558E-04	1.527E-04	-3.518E-04
70	-50.03	105.00	1.189E-02	9.191E-03	1.167E-02	-2.688E-02
75	-50.03	105.00	3.108E-01	1.762E-01	2.934E-01	-6.759E-01
80	-50.03	105.00	3.484E+00	1.446E+00	3.218E+00	-7.412E+00
85	-50.03	105.00	2.037E+01	6.082E+00	1.858E+01	-4.279E+01
90	-50.03	105.00	7.162E+01	1.495E+01	6.489E+01	-1.495E+02
95	-50.03	105.00	1.705E+02	2.421E+01	1.540E+02	-3.548E+02
100	-50.03	105.00	3.077E+02	3.005E+01	2.776E+02	-6.394E+02
105	-50.03	105.00	4.690E+02	3.472E+01	4.231E+02	-9.746E+02
110	-50.03	105.00	6.519E+02	3.468E+01	5.874E+02	-1.353E+03
115	-50.03	105.00	7.427E+02	3.562E+00	6.710E+02	-1.545E+03
120	-50.03	105.00	9.018E+02	1.102E+02	5.756E+02	-1.481E+03
125	-50.03	105.00	1.542E+03	1.096E+02	7.718E+02	-1.998E+03
130	-50.03	105.00	2.085E+03	1.073E+02	9.539E+02	-2.510E+03
135	-50.03	105.00	2.614E+03	1.040E+02	1.124E+03	-3.010E+03
140	-50.03	105.00	3.124E+03	1.002E+02	1.284E+03	-3.491E+03
145	-50.03	105.00	3.615E+03	9.598E+01	1.435E+03	-3.949E+03
150	-50.03	105.00	4.083E+03	9.153E+01	1.576E+03	-4.381E+03
155	-50.03	105.00	4.530E+03	8.688E+01	1.709E+03	-4.786E+03
160	-50.03	105.00	4.952E+03	8.206E+01	1.833E+03	-5.160E+03
165	-50.03	105.00	5.350E+03	7.711E+01	1.949E+03	-5.504E+03
170	-50.03	105.00	5.723E+03	7.206E+01	2.057E+03	-5.814E+03
175	-50.03	105.00	6.070E+03	6.690E+01	2.158E+03	-6.091E+03
180	-50.03	105.00	6.392E+03	6.166E+01	2.250E+03	-6.333E+03
185	-50.03	105.00	6.687E+03	5.635E+01	2.336E+03	-6.538E+03
190	-50.03	105.00	6.955E+03	5.096E+01	2.413E+03	-6.707E+03
195	-50.03	105.00	7.196E+03	4.551E+01	2.484E+03	-6.838E+03
200	-50.03	105.00	7.410E+03	4.000E+01	2.547E+03	-6.931E+03
205	-50.03	105.00	7.596E+03	3.444E+01	2.603E+03	-6.984E+03
210	-50.03	105.00	7.754E+03	2.882E+01	2.652E+03	-6.998E+03
215	-50.03	105.00	7.884E+03	2.315E+01	2.694E+03	-6.970E+03
220	-50.03	105.00	7.986E+03	1.743E+01	2.730E+03	-6.902E+03
225	-50.03	105.00	8.059E+03	1.166E+01	2.759E+03	-6.791E+03
230	-50.03	105.00	8.102E+03	5.839E+00	2.781E+03	-6.637E+03
235	-50.03	105.00	8.149E+03	6.771E+02	2.440E+03	-3.072E+04
240	-50.03	105.00	1.456E+04	1.756E+03	1.676E+04	-5.554E+04
245	-50.03	105.00	2.066E+04	1.182E+03	3.254E+04	-5.508E+04
250	-50.03	105.00	2.635E+04	1.095E+03	4.717E+04	-5.398E+04

LT 0500

NL= -51.800, WL= 90.000

HT	NL	WL	N	DNDR	DNDNL	DNDWL
40	-51.80	90.00	0.	0.	0.	0.
45	-51.80	90.00	0.	0.	0.	0.
50	-51.80	90.00	1.666E-11	1.442E-11	8.320E-12	-1.346E-11
55	-51.80	90.00	6.662E-11	1.875E-10	1.248E-10	-2.020E-10
60	-51.80	90.00	5.215E-07	8.290E-07	7.002E-07	-1.133E-06
65	-51.80	90.00	2.279E-04	2.447E-04	2.658E-04	-4.301E-04
70	-51.80	90.00	1.868E-02	1.444E-02	2.031E-02	-3.286E-02
75	-51.80	90.00	4.882E-01	2.768E-01	5.106E-01	-8.264E-01
80	-51.80	90.00	5.474E+00	2.272E+00	5.600E+00	-9.063E+00
85	-51.80	90.00	3.194E+01	9.555E+00	3.233E+01	-5.232E+01
90	-51.80	90.00	1.125E+02	2.349E+01	1.129E+02	-1.827E+02
95	-51.80	90.00	2.679E+02	3.804E+01	2.681E+02	-4.338E+02
100	-51.80	90.00	4.833E+02	4.720E+01	4.831E+02	-7.818E+02
105	-51.80	90.00	7.368E+02	5.454E+01	7.364E+02	-1.192E+03
110	-51.80	90.00	1.024E+03	5.448E+01	1.022E+03	-1.654E+03
115	-51.80	90.00	1.167E+03	5.597E+00	1.168E+03	-1.890E+03
120	-51.80	90.00	1.426E+03	1.427E+02	1.152E+03	-1.996E+03
125	-51.80	90.00	2.135E+03	1.418E+02	1.611E+03	-2.804E+03
130	-51.80	90.00	2.836E+03	1.385E+02	2.044E+03	-3.583E+03
135	-51.80	90.00	3.517E+03	1.338E+02	2.450E+03	-4.323E+03
140	-51.80	90.00	4.173E+03	1.283E+02	2.827E+03	-5.016E+03
145	-51.80	90.00	4.799E+03	1.222E+02	3.174E+03	-5.656E+03
150	-51.80	90.00	5.394E+03	1.157E+02	3.490E+03	-6.239E+03
155	-51.80	90.00	5.956E+03	1.089E+02	3.775E+03	-6.762E+03
160	-51.80	90.00	6.483E+03	1.018E+02	4.027E+03	-7.221E+03
165	-51.80	90.00	6.974E+03	9.449E+01	4.245E+03	-7.616E+03
170	-51.80	90.00	7.427E+03	8.697E+01	4.431E+03	-7.943E+03
175	-51.80	90.00	7.843E+03	7.928E+01	4.582E+03	-8.200E+03
180	-51.80	90.00	8.220E+03	7.144E+01	4.699E+03	-8.386E+03
185	-51.80	90.00	8.557E+03	6.346E+01	4.782E+03	-8.500E+03
190	-51.80	90.00	8.854E+03	5.535E+01	4.829E+03	-8.539E+03
195	-51.80	90.00	9.111E+03	4.712E+01	4.841E+03	-8.503E+03
200	-51.80	90.00	9.325E+03	3.877E+01	4.817E+03	-8.390E+03
205	-51.80	90.00	9.498E+03	3.032E+01	4.757E+03	-8.197E+03
210	-51.80	90.00	9.628E+03	2.175E+01	4.660E+03	-7.925E+03
215	-51.80	90.00	9.715E+03	1.308E+01	4.526E+03	-7.571E+03
220	-51.80	90.00	9.759E+03	4.303E+00	4.355E+03	-7.134E+03
225	-51.80	90.00	1.379E+04	1.555E+03	5.028E+04	-1.044E+05
230	-51.80	90.00	2.139E+04	1.479E+03	6.642E+04	-1.119E+05
235	-51.80	90.00	2.855E+04	1.380E+03	8.079E+04	-1.172E+05
240	-51.80	90.00	3.518E+04	1.269E+03	9.353E+04	-1.210E+05
245	-51.80	90.00	4.123E+04	1.150E+03	1.047E+05	-1.234E+05
250	-51.80	90.00	4.667E+04	1.027E+03	1.143E+05	-1.245E+05

LT 0600

NL= -50.035, wL= 75.000

IHT	NL	wL	N	DNDR	DNDNL	DNDWL
40	-50.03	75.00	8.247E-02	1.321E-02	1.999E-01	-2.417E-01
45	-50.03	75.00	2.009E-01	4.018E-02	4.885E-01	-5.905E-01
50	-50.03	75.00	6.296E-01	1.670E-01	1.540E+00	-1.862E+00
55	-50.03	75.00	3.037E+00	1.158E+00	7.534E+00	-9.107E+00
60	-50.03	75.00	2.581E+01	1.019E+01	6.304E+01	-7.621E+01
65	-50.03	75.00	5.163E+01	3.677E-04	1.245E+02	-1.505E+02
70	-50.03	75.00	2.584E+01	-1.017E+01	6.308E+01	-7.625E+01
75	-50.03	75.00	3.770E+00	-7.421E-01	8.336E+00	-1.008E+01
80	-50.03	75.00	8.854E+00	3.246E+00	1.035E+01	-1.251E+01
85	-50.03	75.00	4.828E+01	1.432E+01	5.132E+01	-6.204E+01
90	-50.03	75.00	1.691E+02	3.528E+01	1.778E+02	-2.149E+02
95	-50.03	75.00	4.026E+02	5.715E+01	4.216E+02	-5.096E+02
100	-50.03	75.00	7.263E+02	7.092E+01	7.596E+02	-9.183E+02
105	-50.03	75.00	1.107E+03	8.195E+01	1.158E+03	-1.400E+03
110	-50.03	75.00	1.539E+03	8.186E+01	1.607E+03	-1.943E+03
115	-50.03	75.00	1.753E+03	8.409E+00	1.836E+03	-2.220E+03
120	-50.03	75.00	2.094E+03	2.033E+02	2.446E+03	-2.724E+03
125	-50.03	75.00	3.105E+03	2.003E+02	3.696E+03	-4.014E+03
130	-50.03	75.00	4.091E+03	1.936E+02	4.869E+03	-5.229E+03
135	-50.03	75.00	5.037E+03	1.848E+02	5.942E+03	-6.347E+03
140	-50.03	75.00	5.936E+03	1.746E+02	6.899E+03	-7.351E+03
145	-50.03	75.00	6.786E+03	1.635E+02	7.729E+03	-8.230E+03
150	-50.03	75.00	7.570E+03	1.516E+02	8.423E+03	-8.977E+03
155	-50.03	75.00	8.297E+03	1.392E+02	8.976E+03	-9.584E+03
160	-50.03	75.00	8.961E+03	1.263E+02	9.381E+03	-1.005E+04
165	-50.03	75.00	9.559E+03	1.129E+02	9.633E+03	-1.036E+04
170	-50.03	75.00	1.009E+04	9.925E+01	9.728E+03	-1.051E+04
175	-50.03	75.00	1.055E+04	8.523E+01	9.662E+03	-1.051E+04
180	-50.03	75.00	1.094E+04	7.090E+01	9.429E+03	-1.034E+04
185	-50.03	75.00	1.126E+04	5.629E+01	9.027E+03	-1.001E+04
190	-50.03	75.00	1.150E+04	4.140E+01	8.450E+03	-9.504E+03
195	-50.03	75.00	1.167E+04	2.624E+01	7.695E+03	-8.821E+03
200	-50.03	75.00	1.177E+04	1.081E+01	6.757E+03	-7.957E+03
205	-50.03	75.00	1.583E+04	2.612E+03	2.049E+05	-1.943E+05
210	-50.03	75.00	2.863E+04	2.492E+03	2.153E+05	-2.084E+05
215	-50.03	75.00	4.068E+04	2.324E+03	2.209E+05	-2.179E+05
220	-50.03	75.00	5.184E+04	2.138E+03	2.237E+05	-2.243E+05
225	-50.03	75.00	6.204E+04	1.940E+03	2.242E+05	-2.282E+05
230	-50.03	75.00	7.123E+04	1.735E+03	2.226E+05	-2.299E+05
235	-50.03	75.00	7.938E+04	1.525E+03	2.191E+05	-2.294E+05
240	-50.03	75.00	8.647E+04	1.311E+03	2.138E+05	-2.269E+05
245	-50.03	75.00	9.249E+04	1.094E+03	2.066E+05	-2.223E+05
250	-50.03	75.00	9.741E+04	8.741E+02	1.977E+05	-2.156E+05

LT 0700

NL= -44.860, WL= 60.000

HT	NL	WL	N	DNDR	DNDNL	DNDWL
40	-44.86	60.00	1.226E-01	1.964E-02	7.045E-02	-6.739E-02
45	-44.86	60.00	2.987E-01	5.974E-02	1.721E-01	-1.646E-01
50	-44.86	60.00	9.760E-01	2.483E-01	5.427E-01	-5.191E-01
55	-44.86	60.00	4.515E+00	1.722E+00	2.654E+00	-2.539E+00
60	-44.86	60.00	3.838E+01	1.515E+01	2.221E+01	-2.125E+01
65	-44.86	60.00	7.677E+01	1.147E-02	4.388E+01	-4.198E+01
70	-44.86	60.00	3.025E+01	-1.447E+01	2.400E+01	-2.295E+01
75	-44.86	60.00	2.739E+01	1.125E+01	4.748E+01	-4.542E+01
80	-44.86	60.00	2.574E+02	1.062E+02	4.921E+02	-4.707E+02
85	-44.86	60.00	1.499E+03	4.476E+02	2.838E+03	-2.715E+03
90	-44.86	60.00	5.272E+03	1.100E+03	9.912E+03	-9.482E+03
95	-44.86	60.00	1.255E+04	1.782E+03	2.353E+04	-2.251E+04
100	-44.86	60.00	2.265E+04	2.212E+03	4.240E+04	-4.056E+04
105	-44.86	60.00	3.452E+04	2.555E+03	6.464E+04	-6.183E+04
110	-44.86	60.00	4.799E+04	2.552E+03	8.973E+04	-8.584E+04
115	-44.86	60.00	5.467E+04	2.622E+02	1.025E+05	-9.805E+04
120	-44.86	60.00	5.581E+04	1.675E+03	1.147E+05	-1.031E+05
125	-44.86	60.00	6.490E+04	1.835E+03	1.464E+05	-1.227E+05
130	-44.86	60.00	7.412E+04	1.845E+03	1.693E+05	-1.397E+05
135	-44.86	60.00	8.330E+04	1.822E+03	1.922E+05	-1.565E+05
140	-44.86	60.00	9.228E+04	1.760E+03	2.142E+05	-1.726E+05
145	-44.86	60.00	1.008E+05	1.650E+03	2.339E+05	-1.874E+05
150	-44.86	60.00	1.087E+05	1.476E+03	2.490E+05	-1.995E+05
155	-44.86	60.00	1.154E+05	1.214E+03	2.559E+05	-2.072E+05
160	-44.86	60.00	1.206E+05	8.096E+02	2.470E+05	-2.069E+05
165	-44.86	60.00	1.231E+05	1.373E+02	2.048E+05	-1.902E+05
170	-44.86	60.00	1.293E+05	1.419E+03	3.128E+05	-2.454E+05
175	-44.86	60.00	1.363E+05	1.370E+03	3.075E+05	-2.525E+05
180	-44.86	60.00	1.430E+05	1.308E+03	3.012E+05	-2.588E+05
185	-44.86	60.00	1.493E+05	1.231E+03	2.938E+05	-2.641E+05
190	-44.86	60.00	1.553E+05	1.137E+03	2.851E+05	-2.682E+05
195	-44.86	60.00	1.607E+05	1.021E+03	2.748E+05	-2.709E+05
200	-44.86	60.00	1.654E+05	8.796E+02	2.625E+05	-2.718E+05
205	-44.86	60.00	1.694E+05	7.056E+02	2.472E+05	-2.705E+05
210	-44.86	60.00	1.724E+05	4.885E+02	2.279E+05	-2.663E+05
215	-44.86	60.00	1.742E+05	2.110E+02	2.025E+05	-2.582E+05
220	-44.86	60.00	1.743E+05	-2.386E+02	1.594E+05	-2.411E+05
225	-44.86	60.00	1.715E+05	-8.906E+02	9.359E+04	-2.118E+05
230	-44.86	60.00	1.657E+05	-1.405E+03	3.794E+04	-1.836E+05
235	-44.86	60.00	1.576E+05	-1.782E+03	-6.839E+03	-1.574E+05
240	-44.86	60.00	1.480E+05	-2.033E+03	-4.108E+04	-1.339E+05
245	-44.86	60.00	1.375E+05	-2.174E+03	-6.577E+04	-1.132E+05
250	-44.86	60.00	1.264E+05	-2.225E+03	-8.227E+04	-9.525E+04

LT 0800

NL= -36.628, ML= 45.000

FT	NL	ML	N	DNDR	DNDNL	DNDML
40	-36.63	45.00	1.435E-01	2.298E-02	4.630E-02	-3.606E-02
45	-36.63	45.00	3.495E-01	6.992E-02	1.131E-01	-8.810E-02
50	-36.63	45.00	1.095E+00	2.506E-01	3.567E-01	-2.778E-01
55	-36.63	45.00	5.284E+00	2.015E+00	1.745E+00	-1.359E+00
60	-36.63	45.00	4.491E+01	1.773E+01	1.460E+01	-1.137E+01
65	-36.63	45.00	8.984E+01	1.812E-02	2.884E+01	-2.247E+01
70	-36.63	45.00	4.630E+01	-1.666E+01	1.589E+01	-1.238E+01
75	-36.63	45.00	4.144E+01	1.849E+01	3.416E+01	-2.661E+01
80	-36.63	45.00	4.164E+02	1.679E+02	3.558E+02	-2.772E+02
85	-36.63	45.00	2.376E+03	7.075E+02	2.052E+03	-1.598E+03
90	-36.63	45.00	8.331E+03	1.739E+03	7.168E+03	-5.583E+03
95	-36.63	45.00	1.984E+04	2.817E+03	1.702E+04	-1.325E+04
100	-36.63	45.00	3.579E+04	3.495E+03	3.066E+04	-2.388E+04
105	-36.63	45.00	5.456E+04	4.039E+03	4.674E+04	-3.641E+04
110	-36.63	45.00	7.584E+04	4.034E+03	6.489E+04	-5.054E+04
115	-36.63	45.00	9.641E+04	4.144E+02	7.412E+04	-5.773E+04
120	-36.63	45.00	9.006E+04	3.078E+03	7.932E+04	-5.452E+04
125	-36.63	45.00	1.056E+05	3.134E+03	1.000E+05	-6.305E+04
130	-36.63	45.00	1.213E+05	3.121E+03	1.200E+05	-7.130E+04
135	-36.63	45.00	1.367E+05	3.022E+03	1.383E+05	-7.907E+04
140	-36.63	45.00	1.513E+05	2.811E+03	1.534E+05	-8.617E+04
145	-36.63	45.00	1.645E+05	2.439E+03	1.632E+05	-9.243E+04
150	-36.63	45.00	1.753E+05	1.802E+03	1.640E+05	-9.788E+04
155	-36.63	45.00	1.817E+05	6.218E+02	1.476E+05	-1.034E+05
160	-36.63	45.00	1.925E+05	3.018E+03	2.289E+05	-1.089E+05
165	-36.63	45.00	2.074E+05	2.913E+03	2.718E+05	-1.304E+05
170	-36.63	45.00	2.216E+05	2.777E+03	3.121E+05	-1.510E+05
175	-36.63	45.00	2.351E+05	2.610E+03	3.491E+05	-1.705E+05
180	-36.63	45.00	2.477E+05	2.408E+03	3.822E+05	-1.888E+05
185	-36.63	45.00	2.591E+05	2.169E+03	4.111E+05	-2.056E+05
190	-36.63	45.00	2.693E+05	1.887E+03	4.352E+05	-2.207E+05
195	-36.63	45.00	2.779E+05	1.557E+03	4.540E+05	-2.339E+05
200	-36.63	45.00	2.848E+05	1.169E+03	4.673E+05	-2.452E+05
205	-36.63	45.00	2.895E+05	7.105E+02	4.746E+05	-2.545E+05
210	-36.63	45.00	2.917E+05	1.626E+02	4.759E+05	-2.619E+05
215	-36.63	45.00	2.904E+05	-8.256E+02	4.684E+05	-2.698E+05
220	-36.63	45.00	2.836E+05	-1.836E+03	4.518E+05	-2.729E+05
225	-36.63	45.00	2.724E+05	-2.614E+03	4.292E+05	-2.699E+05
230	-36.63	45.00	2.578E+05	-3.167E+03	4.024E+05	-2.618E+05
235	-36.63	45.00	2.411E+05	-3.518E+03	3.730E+05	-2.498E+05
240	-36.63	45.00	2.230E+05	-3.696E+03	3.424E+05	-2.350E+05
245	-36.63	45.00	2.043E+05	-3.734E+03	3.117E+05	-2.185E+05
250	-36.63	45.00	1.858E+05	-3.666E+03	2.817E+05	-2.010E+05

LT 0900

NL= -25.900, WL= 30.000

HT	NL	WL	N	DNDR	DNDNL	DNDWL
40	-25.90	30.00	1.579E-01	2.529E-02	3.259E-02	-2.011E-02
45	-25.90	30.00	3.846E-01	7.693E-02	7.963E-02	-4.914E-02
50	-25.90	30.00	1.205E+00	3.197E-01	2.511E-01	-1.549E-01
55	-25.90	30.00	5.814E+00	2.217E+00	1.228E+00	-7.578E-01
60	-25.90	30.00	4.941E+01	1.950E+01	1.028E+01	-6.342E+00
65	-25.90	30.00	9.885E+01	2.321E-02	2.031E+01	-1.253E+01
70	-25.90	30.00	5.119E+01	-1.813E+01	1.128E+01	-6.961E+00
75	-25.90	30.00	5.213E+01	2.405E+01	2.647E+01	-1.633E+01
80	-25.90	30.00	5.204E+02	2.152E+02	2.770E+02	-1.710E+02
85	-25.90	30.00	3.036E+03	9.063E+02	1.598E+03	-9.860E+02
90	-25.90	30.00	1.067E+04	2.228E+03	5.581E+03	-3.444E+03
95	-25.90	30.00	2.542E+04	3.609E+03	1.325E+04	-8.175E+03
100	-25.90	30.00	4.585E+04	4.478E+03	2.388E+04	-1.473E+04
105	-25.90	30.00	6.990E+04	5.174E+03	3.639E+04	-2.246E+04
110	-25.90	30.00	9.716E+04	5.168E+03	5.052E+04	-3.118E+04
115	-25.90	30.00	1.307E+05	5.309E+02	5.771E+04	-3.561E+04
120	-25.90	30.00	1.112E+05	1.106E+03	4.801E+04	-2.453E+04
125	-25.90	30.00	1.289E+05	3.729E+03	4.508E+04	-4.785E+03
130	-25.90	30.00	1.475E+05	3.671E+03	5.194E+04	4.471E+03
135	-25.90	30.00	1.655E+05	3.525E+03	5.774E+04	1.231E+04
140	-25.90	30.00	1.826E+05	3.275E+03	6.263E+04	1.741E+04
145	-25.90	30.00	1.980E+05	2.897E+03	6.711E+04	1.793E+04
150	-25.90	30.00	2.113E+05	2.351E+03	7.226E+04	1.103E+04
155	-25.90	30.00	2.212E+05	1.560E+03	8.053E+04	-8.217E+03
160	-25.90	30.00	2.262E+05	3.608E+02	9.777E+04	-4.991E+04
165	-25.90	30.00	2.518E+05	6.487E+03	6.682E+04	2.058E+05
170	-25.90	30.00	2.836E+05	6.230E+03	1.756E+05	1.976E+05
175	-25.90	30.00	3.140E+05	5.899E+03	2.801E+05	1.862E+05
180	-25.90	30.00	3.425E+05	5.499E+03	3.791E+05	1.716E+05
185	-25.90	30.00	3.688E+05	5.034E+03	4.715E+05	1.541E+05
190	-25.90	30.00	3.927E+05	4.504E+03	5.567E+05	1.337E+05
195	-25.90	30.00	4.138E+05	3.911E+03	6.340E+05	1.105E+05
200	-25.90	30.00	4.317E+05	3.252E+03	7.033E+05	8.448E+04
205	-25.90	30.00	4.462E+05	2.525E+03	7.643E+05	5.556E+04
210	-25.90	30.00	4.566E+05	1.724E+03	8.173E+05	2.370E+04
215	-25.90	30.00	4.633E+05	8.415E+02	8.625E+05	-1.125E+04
220	-25.90	30.00	4.651E+05	-1.942E+02	9.034E+05	-5.264E+04
225	-25.90	30.00	4.594E+05	-2.019E+03	9.560E+05	-1.227E+05
230	-25.90	30.00	4.455E+05	-3.482E+03	9.807E+05	-1.786E+05
235	-25.90	30.00	4.252E+05	-4.576E+03	9.800E+05	-2.194E+05
240	-25.90	30.00	4.003E+05	-5.323E+03	9.583E+05	-2.463E+05
245	-25.90	30.00	3.725E+05	-5.766E+03	9.201E+05	-2.609E+05
250	-25.90	30.00	3.431E+05	-5.955E+03	8.698E+05	-2.655E+05

LT 1000

NL= -13.407. WL= 15.000

HT	NL	WL	N	DNDR	DNDNL	DNDWL
40	-13.41	15.00	1.675E-01	2.682E-02	2.200E+02	-8.929E-03
45	-13.41	15.00	4.079E-01	8.159E-02	5.374E+02	-2.181E-02
50	-13.41	15.00	1.278E+00	3.391E-01	1.695E+01	-6.878E-02
55	-13.41	15.00	6.166E+00	2.352E+00	8.288E+01	-3.364E-01
60	-13.41	15.00	5.241E+01	2.069E+01	6.936E+00	-2.815E+00
65	-13.41	15.00	1.049E+02	2.692E-02	1.370E+01	-5.563E+00
70	-13.41	15.00	5.447E+01	-1.910E+01	7.666E+00	-3.112E+00
75	-13.41	15.00	5.987E+01	2.810E+01	1.918E+01	-7.785E+00
80	-13.41	15.00	6.034E+02	2.496E+02	2.014E+02	-8.175E+01
85	-13.41	15.00	3.520E+03	1.051E+03	1.162E+03	-4.716E+02
90	-13.41	15.00	1.238E+04	2.584E+03	4.058E+03	-1.647E+03
95	-13.41	15.00	2.947E+04	4.185E+03	9.632E+03	-3.910E+03
100	-13.41	15.00	5.317E+04	5.192E+03	1.736E+04	-7.046E+03
105	-13.41	15.00	8.105E+04	5.999E+03	2.646E+04	-1.074E+04
110	-13.41	15.00	1.127E+05	5.993E+03	3.673E+04	-1.491E+04
115	-13.41	15.00	1.284E+05	6.157E+02	4.196E+04	-1.703E+04
120	-13.41	15.00	1.289E+05	-5.209E-04	4.208E+04	-1.708E+04
125	-13.41	15.00	1.289E+05	-3.371E-04	4.208E+04	-1.708E+04
130	-13.41	15.00	1.408E+05	2.714E+03	-3.475E+04	3.410E+04
135	-13.41	15.00	1.542E+05	2.670E+03	-4.872E+04	4.820E+04
140	-13.41	15.00	1.674E+05	2.604E+03	-6.180E+04	6.114E+04
145	-13.41	15.00	1.803E+05	2.515E+03	-7.347E+04	7.252E+04
150	-13.41	15.00	1.926E+05	2.404E+03	-8.315E+04	8.189E+04
155	-13.41	15.00	2.042E+05	2.268E+03	-9.022E+04	8.880E+04
160	-13.41	15.00	2.152E+05	2.107E+03	-9.396E+04	9.272E+04
165	-13.41	15.00	2.253E+05	1.919E+03	-9.352E+04	9.307E+04
170	-13.41	15.00	2.343E+05	1.701E+03	-8.790E+04	8.919E+04
175	-13.41	15.00	2.422E+05	1.451E+03	-7.589E+04	8.026E+04
180	-13.41	15.00	2.488E+05	1.163E+03	-5.594E+04	6.530E+04
185	-13.41	15.00	2.538E+05	8.320E+02	-2.608E+04	4.307E+04
190	-13.41	15.00	2.570E+05	4.487E+02	1.634E+04	1.191E+04
195	-13.41	15.00	2.582E+05	5.825E+03	-7.442E+05	5.678E+05
200	-13.41	15.00	3.762E+05	1.142E+04	-1.324E+06	1.184E+06
205	-13.41	15.00	3.721E+05	1.090E+04	-1.049E+06	1.192E+06
210	-13.41	15.00	4.249E+05	1.023E+04	-7.669E+05	1.182E+06
215	-13.41	15.00	4.742E+05	9.456E+03	-4.838E+05	1.156E+06
220	-13.41	15.00	5.193E+05	8.581E+03	-2.030E+05	1.116E+06
225	-13.41	15.00	5.599E+05	7.618E+03	7.328E+04	1.061E+06
230	-13.41	15.00	5.954E+05	6.574E+03	3.435E+05	9.929E+05
235	-13.41	15.00	6.255E+05	5.453E+03	6.069E+05	9.119E+05
240	-13.41	15.00	6.498E+05	4.257E+03	8.631E+05	8.180E+05
245	-13.41	15.00	6.679E+05	2.985E+03	1.112E+06	7.114E+05
250	-13.41	15.00	6.795E+05	1.635E+03	1.355E+06	5.921E+05

LT 1100

NL= .000, WL= 360.000

PT	NL	WL	N	DN/DR	DN/DNL	DN/DWL
40	.00	360.00	1.726E-01	2.765E-02	1.309E-02	-1.065E-05
45	.00	360.00	4.205E-01	8.411E-02	3.198E-02	-2.603E-05
50	.00	360.00	1.318E+00	3.496E-01	1.008E-01	-8.206E-05
55	.00	360.00	6.357E+00	2.424E+00	4.932E-01	-4.014E-04
60	.00	360.00	5.403E+01	2.133E+01	4.127E+00	-3.359E-03
65	.00	360.00	1.081E+02	2.904E+02	8.155E+00	-6.637E-03
70	.00	360.00	5.625E+01	-1.961E+01	4.580E+00	-3.728E-03
75	.00	360.00	6.430E+01	3.043E+01	1.188E+01	-9.670E-03
80	.00	360.00	6.509E+02	2.692E+02	1.250E+02	-1.017E-01
85	.00	360.00	3.797E+03	1.134E+03	7.210E+02	-5.868E-01
90	.00	360.00	1.335E+04	2.787E+03	2.518E+03	-2.050E+00
95	.00	360.00	3.179E+04	4.514E+03	5.978E+03	-4.865E+00
100	.00	360.00	5.736E+04	5.601E+03	1.077E+04	-8.768E+00
105	.00	360.00	8.744E+04	6.472E+03	1.642E+04	-1.337E+01
110	.00	360.00	1.215E+05	6.465E+03	2.280E+04	-1.855E+01
115	.00	360.00	1.385E+05	6.642E+02	2.604E+04	-2.119E+01
120	.00	360.00	1.391E+05	-5.370E-04	2.611E+04	-2.125E+01
125	.00	360.00	1.391E+05	-3.476E-04	2.611E+04	-2.125E+01
130	.00	360.00	1.391E+05	-2.329E-04	2.611E+04	-2.125E+01
135	.00	360.00	1.391E+05	-1.608E-04	2.611E+04	-2.125E+01
140	.00	360.00	1.411E+05	1.490E+03	-6.982E+04	6.865E+03
145	.00	360.00	1.485E+05	1.478E+03	-8.625E+04	7.835E+03
150	.00	360.00	1.559E+05	1.463E+03	-1.022E+05	8.782E+03
155	.00	360.00	1.632E+05	1.445E+03	-1.174E+05	9.700E+03
160	.00	360.00	1.703E+05	1.425E+03	-1.320E+05	1.058E+04
165	.00	360.00	1.774E+05	1.401E+03	-1.457E+05	1.143E+04
170	.00	360.00	1.844E+05	1.375E+03	-1.585E+05	1.222E+04
175	.00	360.00	1.912E+05	1.346E+03	-1.702E+05	1.296E+04
180	.00	360.00	1.978E+05	1.314E+03	-1.808E+05	1.364E+04
185	.00	360.00	2.043E+05	1.280E+03	-1.902E+05	1.424E+04
190	.00	360.00	2.106E+05	1.243E+03	-1.982E+05	1.478E+04
195	.00	360.00	2.167E+05	1.203E+03	-2.048E+05	1.523E+04
200	.00	360.00	2.226E+05	1.160E+03	-2.098E+05	1.559E+04
205	.00	360.00	2.283E+05	1.114E+03	-2.131E+05	1.585E+04
210	.00	360.00	2.338E+05	1.066E+03	-2.147E+05	1.601E+04
215	.00	360.00	2.390E+05	1.014E+03	-2.144E+05	1.605E+04
220	.00	360.00	2.439E+05	9.596E+02	-2.120E+05	1.596E+04
225	.00	360.00	2.486E+05	9.020E+02	-2.074E+05	1.574E+04
230	.00	360.00	2.529E+05	8.412E+02	-2.006E+05	1.537E+04
235	.00	360.00	2.570E+05	7.771E+02	-1.912E+05	1.485E+04
240	.00	360.00	2.607E+05	7.095E+02	-1.792E+05	1.415E+04
245	.00	360.00	2.640E+05	6.383E+02	-1.644E+05	1.328E+04
250	.00	360.00	2.671E+05	5.634E+02	-1.465E+05	1.220E+04

LT 1200 Noon

NL= 13.407, WL= 345.000

HT	NL	WL	N	DNDR	DNDNL	DNDWL
40	13.41	345.00	1.738E-01	2.784E-02	5.849E-03	7.263E-03
45	13.41	345.00	4.234E-01	8.470E-02	1.429E-02	1.774E-02
50	13.41	345.00	1.327E+00	3.520E-01	4.506E-02	5.595E-02
55	13.41	345.00	6.401E+00	2.441E+00	2.204E-01	2.737E-01
60	13.41	345.00	5.441E+01	2.147E+01	1.844E+00	2.290E+00
65	13.41	345.00	1.688E+02	2.554E-02	3.644E+00	4.525E+00
70	13.41	345.00	5.666E+01	-1.573E+01	2.049E+00	2.544E+00
75	13.41	345.00	6.534E+01	3.098E+01	5.360E+00	6.656E+00
80	13.41	345.00	6.621E+02	2.739E+02	5.641E+01	7.005E+01
85	13.41	345.00	3.863E+03	1.153E+03	3.254E+02	4.041E+02
90	13.41	345.00	1.358E+04	2.836E+03	1.136E+03	1.411E+03
95	13.41	345.00	3.234E+04	4.592E+03	2.698E+03	3.350E+03
100	13.41	345.00	5.835E+04	5.698E+03	4.862E+03	6.038E+03
105	13.41	345.00	8.895E+04	6.584E+03	7.411E+03	9.203E+03
110	13.41	345.00	1.236E+05	6.577E+03	1.029E+04	1.278E+04
115	13.41	345.00	1.409E+05	6.757E+02	1.175E+04	1.459E+04
120	13.41	345.00	1.415E+05	-5.407E-04	1.178E+04	1.463E+04
125	13.41	345.00	1.415E+05	-3.500E-04	1.178E+04	1.463E+04
130	13.41	345.00	1.415E+05	-2.345E-04	1.178E+04	1.463E+04
135	13.41	345.00	1.415E+05	-1.619E-04	1.178E+04	1.463E+04
140	13.41	345.00	1.415E+05	-1.147E-04	1.178E+04	1.463E+04
145	13.41	345.00	1.415E+05	-8.304E-05	1.178E+04	1.463E+04
150	13.41	345.00	1.415E+05	-6.132E-05	1.178E+04	1.463E+04
155	13.41	345.00	1.458E+05	9.967E+02	-3.504E+04	1.803E+01
160	13.41	345.00	1.508E+05	9.913E+02	-3.883E+04	-1.361E+03
165	13.41	345.00	1.557E+05	9.851E+02	-4.257E+04	-2.704E+03
170	13.41	345.00	1.606E+05	9.780E+02	-4.623E+04	-4.007E+03
175	13.41	345.00	1.655E+05	9.701E+02	-4.981E+04	-5.265E+03
180	13.41	345.00	1.703E+05	9.613E+02	-5.329E+04	-6.475E+03
185	13.41	345.00	1.751E+05	9.517E+02	-5.667E+04	-7.632E+03
190	13.41	345.00	1.798E+05	9.412E+02	-5.993E+04	-8.733E+03
195	13.41	345.00	1.845E+05	9.300E+02	-6.306E+04	-9.772E+03
200	13.41	345.00	1.891E+05	9.179E+02	-6.605E+04	-1.075E+04
205	13.41	345.00	1.937E+05	9.050E+02	-6.889E+04	-1.165E+04
210	13.41	345.00	1.982E+05	8.913E+02	-7.155E+04	-1.248E+04
215	13.41	345.00	2.026E+05	8.767E+02	-7.404E+04	-1.324E+04
220	13.41	345.00	2.069E+05	8.614E+02	-7.634E+04	-1.391E+04
225	13.41	345.00	2.112E+05	8.452E+02	-7.843E+04	-1.450E+04
230	13.41	345.00	2.154E+05	8.283E+02	-8.031E+04	-1.499E+04
235	13.41	345.00	2.195E+05	8.105E+02	-8.195E+04	-1.540E+04
240	13.41	345.00	2.235E+05	7.919E+02	-8.334E+04	-1.570E+04
245	13.41	345.00	2.274E+05	7.724E+02	-8.447E+04	-1.590E+04
250	13.41	345.00	2.312E+05	7.521E+02	-8.532E+04	-1.599E+04

LT 1300

NL= 25.900, WL= 330.000

HT	NL	WL	N	DNDR	DNDNL	DNDWL
40	25.90	330.00	1.718E-01	2.752E-02	6.367E-04	1.308E-02
45	25.90	330.00	4.185E-01	8.372E-02	1.555E-03	3.195E-02
50	25.90	330.00	1.312E+00	3.480E-01	4.904E-03	1.007E-01
55	25.90	330.00	6.327E+00	2.413E+00	2.399E-02	4.927E-01
60	25.90	330.00	5.378E+01	2.123E+01	2.007E-01	4.123E+00
65	25.90	330.00	1.076E+02	2.870E-02	3.967E-01	8.148E+00
70	25.90	330.00	5.597E+01	-1.953E+01	2.226E-01	4.573E+00
75	25.90	330.00	6.359E+01	3.006E+01	5.742E-01	1.179E+01
80	25.90	330.00	6.433E+02	2.661E+02	6.039E+00	1.240E+02
85	25.90	330.00	3.753E+03	1.121E+03	3.484E+01	7.156E+02
90	25.90	330.00	1.320E+04	2.755E+03	1.217E+02	2.499E+03
95	25.90	330.00	3.142E+04	4.462E+03	2.888E+02	5.933E+03
100	25.90	330.00	5.669E+04	5.536E+03	5.205E+02	1.069E+04
105	25.90	330.00	8.642E+04	6.297E+03	7.934E+02	1.630E+04
110	25.90	330.00	1.201E+05	6.390E+03	1.102E+03	2.263E+04
115	25.90	330.00	1.369E+05	6.564E+02	1.258E+03	2.584E+04
120	25.90	330.00	1.375E+05	-5.345E-04	1.262E+03	2.592E+04
125	25.90	330.00	1.375E+05	-3.459E-04	1.262E+03	2.592E+04
130	25.90	330.00	1.375E+05	-2.319E-04	1.262E+03	2.592E+04
135	25.90	330.00	1.375E+05	-1.600E-04	1.262E+03	2.592E+04
140	25.90	330.00	1.391E+05	1.472E+03	1.110E+05	1.318E+04
145	25.90	330.00	1.465E+05	1.460E+03	1.292E+05	1.200E+04
150	25.90	330.00	1.537E+05	1.445E+03	1.468E+05	1.087E+04
155	25.90	330.00	1.609E+05	1.428E+03	1.639E+05	9.819E+03
160	25.90	330.00	1.680E+05	1.407E+03	1.802E+05	8.855E+03
165	25.90	330.00	1.750E+05	1.384E+03	1.957E+05	7.987E+03
170	25.90	330.00	1.818E+05	1.358E+03	2.102E+05	7.229E+03
175	25.90	330.00	1.886E+05	1.329E+03	2.237E+05	6.589E+03
180	25.90	330.00	1.951E+05	1.298E+03	2.360E+05	6.079E+03
185	25.90	330.00	2.015E+05	1.264E+03	2.470E+05	5.711E+03
190	25.90	330.00	2.076E+05	1.228E+03	2.566E+05	5.495E+03
195	25.90	330.00	2.138E+05	1.188E+03	2.647E+05	5.442E+03
200	25.90	330.00	2.196E+05	1.146E+03	2.712E+05	5.565E+03
205	25.90	330.00	2.253E+05	1.102E+03	2.759E+05	5.875E+03
210	25.90	330.00	2.307E+05	1.054E+03	2.788E+05	6.384E+03
215	25.90	330.00	2.358E+05	1.004E+03	2.796E+05	7.106E+03
220	25.90	330.00	2.407E+05	9.509E+02	2.782E+05	8.055E+03
225	25.90	330.00	2.453E+05	8.948E+02	2.745E+05	9.244E+03
230	25.90	330.00	2.496E+05	8.357E+02	2.684E+05	1.069E+04
235	25.90	330.00	2.537E+05	7.735E+02	2.595E+05	1.241E+04
240	25.90	330.00	2.574E+05	7.080E+02	2.478E+05	1.441E+04
245	25.90	330.00	2.607E+05	6.391E+02	2.331E+05	1.673E+04
250	25.90	330.00	2.638E+05	5.666E+02	2.151E+05	1.937E+04

LT 1400

NL= 36.628, WL= 315.000

IFT	NL	WL	N	DNDR	DNDNL	DNDWL
40	36.63	315.00	1.676E-01	2.685E-02	-2.152E-03	1.775E-02
45	36.63	315.00	4.083E-01	8.167E-02	-5.258E-03	4.337E-02
50	36.63	315.00	1.240E+00	3.394E-01	-1.658E-02	1.367E-01
55	36.63	315.00	6.172E+00	2.354E+00	-8.110E-02	6.689E-01
60	36.63	315.00	5.246E+01	2.071E+01	-6.786E-01	5.597E+00
65	36.63	315.00	1.050E+02	2.698E-02	-1.341E+00	1.106E+01
70	36.63	315.00	5.452E+01	-1.511E+01	-7.501E-01	6.187E+00
75	36.63	315.00	6.001E+01	2.817E+01	-1.879E+00	1.550E+01
80	36.63	315.00	6.048E+02	2.501E+02	-1.973E+01	1.627E+02
85	36.63	315.00	3.528E+03	1.053E+03	-1.138E+02	9.387E+02
90	36.63	315.00	1.241E+04	2.590E+03	-3.975E+02	3.279E+03
95	36.63	315.00	2.954E+04	4.194E+03	-9.436E+02	7.783E+03
100	36.63	315.00	5.329E+04	5.205E+03	-1.701E+03	1.403E+04
105	36.63	315.00	8.124E+04	6.014E+03	-2.592E+03	2.138E+04
110	36.63	315.00	1.129E+05	6.007E+03	-3.599E+03	2.968E+04
115	36.63	315.00	1.287E+05	6.171E+02	-4.111E+03	3.390E+04
120	36.63	315.00	1.292E+05	-5.214E-04	-4.122E+03	3.400E+04
125	36.63	315.00	1.292E+05	-3.375E-04	-4.122E+03	3.400E+04
130	36.63	315.00	1.301E+05	1.698E+03	1.744E+04	3.078E+04
135	36.63	315.00	1.399E+05	1.955E+03	4.302E+04	2.814E+04
140	36.63	315.00	1.496E+05	1.936E+03	4.766E+04	2.880E+04
145	36.63	315.00	1.592E+05	1.909E+03	5.234E+04	2.949E+04
150	36.63	315.00	1.687E+05	1.874E+03	5.695E+04	3.023E+04
155	36.63	315.00	1.779E+05	1.830E+03	6.140E+04	3.102E+04
160	36.63	315.00	1.870E+05	1.778E+03	6.558E+04	3.188E+04
165	36.63	315.00	1.957E+05	1.717E+03	6.936E+04	3.282E+04
170	36.63	315.00	2.041E+05	1.646E+03	7.260E+04	3.386E+04
175	36.63	315.00	2.122E+05	1.566E+03	7.511E+04	3.503E+04
180	36.63	315.00	2.198E+05	1.475E+03	7.673E+04	3.633E+04
185	36.63	315.00	2.269E+05	1.374E+03	7.722E+04	3.780E+04
190	36.63	315.00	2.335E+05	1.261E+03	7.633E+04	3.946E+04
195	36.63	315.00	2.395E+05	1.136E+03	7.376E+04	4.134E+04
200	36.63	315.00	2.448E+05	9.969E+02	6.913E+04	4.347E+04
205	36.63	315.00	2.494E+05	8.425E+02	6.200E+04	4.592E+04
210	36.63	315.00	2.532E+05	6.709E+02	5.184E+04	4.873E+04
215	36.63	315.00	2.561E+05	4.795E+02	3.794E+04	5.197E+04
220	36.63	315.00	2.580E+05	2.652E+02	1.943E+04	5.575E+04
225	36.63	315.00	2.587E+05	7.039E+02	3.339E+05	1.526E+03
230	36.63	315.00	2.869E+05	6.107E+03	4.873E+05	-4.452E+04
235	36.63	315.00	3.168E+05	5.862E+03	2.812E+05	-3.004E+04
240	36.63	315.00	3.454E+05	5.550E+03	7.774E+04	-1.480E+04
245	36.63	315.00	3.722E+05	5.174E+03	-1.208E+05	1.070E+03
250	36.63	315.00	3.970E+05	4.732E+03	-3.127E+05	1.746E+04

LT 1500

NL= 44.860, WL= 300.000

PT	NL	WL	N	DNDR	DNDNL	DNDWL
40	44.86	300.00	1.621E-01	2.596E-02	-2.069E-03	2.197E-02
45	44.86	300.00	3.948E-01	7.899E-02	-5.053E-03	5.367E-02
50	44.86	300.00	1.236E+00	3.293E-01	-1.593E-02	1.692E-01
55	44.86	300.00	5.969E+00	2.276E+00	-7.793E-02	8.278E-01
60	44.86	300.00	5.074E+01	2.002E+01	-6.521E-01	6.928E+00
65	44.86	300.00	1.115E+02	2.482E-02	-1.289E+00	1.369E+01
70	44.86	300.00	5.263E+01	-1.856E+01	-7.179E-01	7.626E+00
75	44.86	300.00	5.548E+01	2.580E+01	-1.732E+00	1.840E+01
80	44.86	300.00	5.563E+02	2.300E+02	-1.815E+01	1.928E+02
85	44.86	300.00	3.245E+03	9.688E+02	-1.047E+02	1.112E+03
90	44.86	300.00	1.141E+04	2.382E+03	-3.657E+02	3.885E+03
95	44.86	300.00	2.717E+04	3.857E+03	-8.682E+02	9.223E+03
100	44.86	300.00	4.901E+04	4.786E+03	-1.565E+03	1.662E+04
105	44.86	300.00	7.472E+04	5.530E+03	-2.385E+03	2.534E+04
110	44.86	300.00	1.039E+05	5.524E+03	-3.311E+03	3.517E+04
115	44.86	300.00	1.183E+05	5.675E+02	-3.782E+03	4.018E+04
120	44.86	300.00	1.189E+05	-5.043E-04	-3.793E+03	4.029E+04
125	44.86	300.00	1.189E+05	-3.264E-04	-3.793E+03	4.029E+04
130	44.86	300.00	1.254E+05	1.985E+03	1.493E+04	4.125E+04
135	44.86	300.00	1.353E+05	1.979E+03	1.531E+04	4.280E+04
140	44.86	300.00	1.451E+05	1.963E+03	1.588E+04	4.442E+04
145	44.86	300.00	1.549E+05	1.935E+03	1.661E+04	4.611E+04
150	44.86	300.00	1.645E+05	1.897E+03	1.748E+04	4.786E+04
155	44.86	300.00	1.738E+05	1.847E+03	1.844E+04	4.970E+04
160	44.86	300.00	1.829E+05	1.784E+03	1.944E+04	5.160E+04
165	44.86	300.00	1.916E+05	1.709E+03	2.040E+04	5.357E+04
170	44.86	300.00	2.000E+05	1.618E+03	2.123E+04	5.561E+04
175	44.86	300.00	2.078E+05	1.512E+03	2.181E+04	5.770E+04
180	44.86	300.00	2.151E+05	1.389E+03	2.198E+04	5.983E+04
185	44.86	300.00	2.217E+05	1.245E+03	2.153E+04	6.198E+04
190	44.86	300.00	2.275E+05	1.079E+03	2.019E+04	6.414E+04
195	44.86	300.00	2.324E+05	8.855E+02	1.760E+04	6.626E+04
200	44.86	300.00	2.363E+05	6.596E+02	1.324E+04	6.830E+04
205	44.86	300.00	2.389E+05	3.931E+02	6.388E+03	7.020E+04
210	44.86	300.00	2.401E+05	7.424E+01	-4.063E+03	7.185E+04
215	44.86	300.00	2.522E+05	3.001E+03	5.912E+04	5.068E+04
220	44.86	300.00	2.669E+05	2.898E+03	-3.414E+03	3.896E+04
225	44.86	300.00	2.811E+05	2.767E+03	-6.421E+04	2.797E+04
230	44.86	300.00	2.946E+05	2.604E+03	-1.227E+05	1.787E+04
235	44.86	300.00	3.071E+05	2.405E+03	-1.785E+05	8.801E+03
240	44.86	300.00	3.185E+05	2.163E+03	-2.312E+05	8.944E+02
245	44.86	300.00	3.286E+05	1.870E+03	-2.806E+05	-5.758E+03
250	44.86	300.00	3.371E+05	1.514E+03	-3.270E+05	-1.111E+04

LT 1600

NL= 50.035, WL= 285.000

HT	NL	WL	N	DNDR	DNDAL	DNDWL
40	50.03	285.00	1.557E-01	2.494E-02	1.631E-03	2.691E-02
45	50.03	285.00	3.793E-01	7.587E-02	3.984E-03	6.573E-02
50	50.03	285.00	1.189E+00	3.153E-01	1.256E-02	2.073E-01
55	50.03	285.00	5.733E+00	2.187E+00	6.145E-02	1.014E+00
60	50.03	285.00	4.873E+01	1.923E+01	5.142E-01	8.484E+00
65	50.03	285.00	9.749E+01	2.241E-02	1.016E+00	1.676E+01
70	50.03	285.00	5.045E+01	-1.791E+01	5.636E-01	9.299E+00
75	50.03	285.00	5.045E+01	2.317E+01	1.304E+00	2.151E+01
80	50.03	285.00	5.025E+02	2.077E+02	1.364E+01	2.250E+02
85	50.03	285.00	2.930E+03	8.749E+02	7.866E+01	1.298E+03
90	50.03	285.00	1.030E+04	2.151E+03	2.748E+02	4.533E+03
95	50.03	285.00	2.454E+04	3.484E+03	6.522E+02	1.076E+04
100	50.03	285.00	4.426E+04	4.323E+03	1.175E+03	1.939E+04
105	50.03	285.00	6.748E+04	4.995E+03	1.792E+03	2.956E+04
110	50.03	285.00	9.380E+04	4.989E+03	2.487E+03	4.104E+04
115	50.03	285.00	1.069E+05	5.125E+02	2.841E+03	4.688E+04
120	50.03	285.00	1.073E+05	-4.844E-04	2.849E+03	4.701E+04
125	50.03	285.00	1.073E+05	-3.135E-04	2.849E+03	4.701E+04
130	50.03	285.00	1.132E+05	1.847E+03	-5.961E+02	5.378E+04
135	50.03	285.00	1.224E+05	1.839E+03	-3.577E+03	5.642E+04
140	50.03	285.00	1.316E+05	1.822E+03	-6.367E+03	5.915E+04
145	50.03	285.00	1.406E+05	1.794E+03	-8.919E+03	6.197E+04
150	50.03	285.00	1.495E+05	1.756E+03	-1.119E+04	6.485E+04
155	50.03	285.00	1.582E+05	1.707E+03	-1.312E+04	6.778E+04
160	50.03	285.00	1.665E+05	1.647E+03	-1.468E+04	7.072E+04
165	50.03	285.00	1.746E+05	1.574E+03	-1.580E+04	7.364E+04
170	50.03	285.00	1.823E+05	1.489E+03	-1.646E+04	7.650E+04
175	50.03	285.00	1.895E+05	1.390E+03	-1.658E+04	7.924E+04
180	50.03	285.00	1.961E+05	1.275E+03	-1.612E+04	8.179E+04
185	50.03	285.00	2.022E+05	1.143E+03	-1.502E+04	8.406E+04
190	50.03	285.00	2.075E+05	9.908E+02	-1.321E+04	8.594E+04
195	50.03	285.00	2.121E+05	8.163E+02	-1.061E+04	8.728E+04
200	50.03	285.00	2.157E+05	6.148E+02	-7.129E+03	8.788E+04
205	50.03	285.00	2.182E+05	3.804E+02	-2.657E+03	8.748E+04
210	50.03	285.00	2.194E+05	1.047E+02	2.952E+03	8.569E+04
215	50.03	285.00	2.305E+05	3.302E+03	-8.990E+04	1.000E+05
220	50.03	285.00	2.467E+05	3.190E+03	-1.253E+05	7.058E+04
225	50.03	285.00	2.623E+05	3.045E+03	-1.582E+05	4.218E+04
230	50.03	285.00	2.771E+05	2.865E+03	-1.881E+05	1.517E+04
235	50.03	285.00	2.909E+05	2.648E+03	-2.146E+05	-1.020E+04
240	50.03	285.00	3.035E+05	2.388E+03	-2.371E+05	-3.375E+04
245	50.03	285.00	3.147E+05	2.078E+03	-2.554E+05	-5.538E+04
250	50.03	285.00	3.242E+05	1.711E+03	-2.691E+05	-7.512E+04

LT 1700

NL= 51.800, WL= 270.000

HT	NL	WL	N	DNDR	DNDNL	DNDWL
40	51.80	270.00	1.479E-01	2.369E-02	1.040E-02	3.461E-02
45	51.80	270.00	3.603E-01	7.207E-02	2.541E-02	8.455E-02
50	51.80	270.00	1.129E+00	2.495E-01	8.013E-02	2.666E-01
55	51.80	270.00	5.447E+00	2.077E+00	3.919E-01	1.304E+00
60	51.80	270.00	4.630E+01	1.827E+01	3.280E+00	1.091E+01
65	51.80	270.00	9.261E+01	1.963E-02	6.480E+00	2.156E+01
70	51.80	270.00	4.779E+01	-1.711E+01	3.578E+00	1.190E+01
75	51.80	270.00	4.462E+01	2.013E+01	7.890E+00	2.625E+01
80	51.80	270.00	4.403E+02	1.819E+02	8.231E+01	2.739E+02
85	51.80	270.00	2.567E+03	7.665E+02	4.747E+02	1.579E+03
90	51.80	270.00	9.026E+03	1.884E+03	1.658E+03	5.517E+03
95	51.80	270.00	2.149E+04	3.052E+03	3.936E+03	1.310E+04
100	51.80	270.00	3.878E+04	3.787E+03	7.093E+03	2.360E+04
105	51.80	270.00	5.911E+04	4.375E+03	1.081E+04	3.598E+04
110	51.80	270.00	8.217E+04	4.370E+03	1.501E+04	4.994E+04
115	51.80	270.00	9.361E+04	4.490E+02	1.715E+04	5.705E+04
120	51.80	270.00	9.403E+04	-4.601E-04	1.719E+04	5.720E+04
125	51.80	270.00	9.403E+04	-2.578E-04	1.719E+04	5.720E+04
130	51.80	270.00	9.812E+04	1.672E+03	8.010E+03	6.215E+04
135	51.80	270.00	1.065E+05	1.661E+03	4.577E+03	6.555E+04
140	51.80	270.00	1.147E+05	1.641E+03	1.389E+03	6.903E+04
145	51.80	270.00	1.229E+05	1.612E+03	-1.489E+03	7.255E+04
150	51.80	270.00	1.308E+05	1.574E+03	-3.995E+03	7.611E+04
155	51.80	270.00	1.386E+05	1.526E+03	-6.066E+03	7.968E+04
160	51.80	270.00	1.461E+05	1.470E+03	-7.638E+03	8.322E+04
165	51.80	270.00	1.533E+05	1.403E+03	-8.648E+03	8.672E+04
170	51.80	270.00	1.601E+05	1.327E+03	-9.031E+03	9.011E+04
175	51.80	270.00	1.665E+05	1.240E+03	-8.715E+03	9.336E+04
180	51.80	270.00	1.725E+05	1.142E+03	-7.625E+03	9.641E+04
185	51.80	270.00	1.779E+05	1.031E+03	-5.678E+03	9.919E+04
190	51.80	270.00	1.828E+05	9.070E+02	-2.782E+03	1.016E+05
195	51.80	270.00	1.870E+05	7.681E+02	1.172E+03	1.036E+05
200	51.80	270.00	1.904E+05	6.124E+02	6.308E+03	1.050E+05
205	51.80	270.00	1.930E+05	4.375E+02	1.278E+04	1.057E+05
210	51.80	270.00	1.948E+05	2.400E+02	2.078E+04	1.055E+05
215	51.80	270.00	1.954E+05	1.130E+03	-8.154E+04	1.256E+05
220	51.80	270.00	2.181E+05	4.781E+03	-2.371E+05	1.118E+05
225	51.80	270.00	2.416E+05	4.587E+03	-2.832E+05	7.319E+04
230	51.80	270.00	2.639E+05	4.339E+03	-3.238E+05	3.028E+04
235	51.80	270.00	2.849E+05	4.041E+03	-3.583E+05	1.510E+03
240	51.80	270.00	3.044E+05	3.693E+03	-3.864E+05	-3.080E+04
245	51.80	270.00	3.217E+05	3.293E+03	-4.075E+05	-6.047E+04
250	51.80	270.00	3.371E+05	2.839E+03	-4.215E+05	-8.744E+04

LT 1800

NL= 50.035, WL= 255.000

IPT	NL	WL	N	DNDR	DNDNL	DNDWL
40	50.03	255.00	1.365E-01	2.187E-02	2.799E-02	4.598E-02
45	50.03	255.00	3.325E-01	6.652E-02	6.838E-02	1.221E-01
50	50.03	255.00	1.042E+00	2.765E-01	2.156E-01	3.850E-01
55	50.03	255.00	5.027E+00	1.917E+00	1.055E+00	1.883E+00
60	50.03	255.00	4.273E+01	1.686E+01	8.825E+00	1.576E+01
65	50.03	255.00	8.548E+01	1.582E-02	1.744E+01	3.113E+01
70	50.03	255.00	4.394E+01	-1.593E+01	9.573E+00	1.709E+01
75	50.03	255.00	3.659E+01	1.598E+01	1.985E+01	3.545E+01
80	50.03	255.00	3.549E+02	1.466E+02	2.063E+02	3.685E+02
85	50.03	255.00	2.065E+03	6.177E+02	1.190E+03	2.125E+03
90	50.03	255.00	7.275E+03	1.519E+03	4.156E+03	7.422E+03
95	50.03	255.00	1.732E+04	2.460E+03	9.867E+03	1.762E+04
100	50.03	255.00	3.125E+04	3.052E+03	1.778E+04	3.175E+04
105	50.03	255.00	4.764E+04	3.526E+03	2.710E+04	4.840E+04
110	50.03	255.00	6.622E+04	3.522E+03	3.763E+04	6.719E+04
115	50.03	255.00	7.544E+04	3.619E+02	4.298E+04	7.675E+04
120	50.03	255.00	7.578E+04	-4.247E-04	4.310E+04	7.696E+04
125	50.03	255.00	7.578E+04	-2.749E-04	4.310E+04	7.696E+04
130	50.03	255.00	7.867E+04	1.439E+03	3.700E+04	8.325E+04
135	50.03	255.00	8.593E+04	1.425E+03	3.673E+04	8.954E+04
140	50.03	255.00	9.291E+04	1.403E+03	3.666E+04	9.580E+04
145	50.03	255.00	9.985E+04	1.373E+03	3.682E+04	1.020E+05
150	50.03	255.00	1.066E+05	1.335E+03	3.724E+04	1.080E+05
155	50.03	255.00	1.132E+05	1.291E+03	3.794E+04	1.139E+05
160	50.03	255.00	1.195E+05	1.239E+03	3.894E+04	1.195E+05
165	50.03	255.00	1.256E+05	1.179E+03	4.026E+04	1.249E+05
170	50.03	255.00	1.313E+05	1.113E+03	4.193E+04	1.298E+05
175	50.03	255.00	1.367E+05	1.038E+03	4.397E+04	1.344E+05
180	50.03	255.00	1.417E+05	9.558E+02	4.638E+04	1.385E+05
185	50.03	255.00	1.462E+05	8.652E+02	4.919E+04	1.420E+05
190	50.03	255.00	1.503E+05	7.658E+02	5.241E+04	1.448E+05
195	50.03	255.00	1.539E+05	6.570E+02	5.607E+04	1.468E+05
200	50.03	255.00	1.569E+05	5.381E+02	6.018E+04	1.479E+05
205	50.03	255.00	1.592E+05	4.080E+02	6.477E+04	1.480E+05
210	50.03	255.00	1.609E+05	2.655E+02	6.986E+04	1.469E+05
215	50.03	255.00	1.619E+05	1.089E+02	7.550E+04	1.443E+05
220	50.03	255.00	1.754E+05	7.433E+03	-2.189E+05	3.181E+05
225	50.03	255.00	2.120E+05	7.163E+03	-2.952E+05	2.730E+05
230	50.03	255.00	2.469E+05	6.792E+03	-3.633E+05	2.275E+05
235	50.03	255.00	2.798E+05	6.341E+03	-4.226E+05	1.828E+05
240	50.03	255.00	3.102E+05	5.823E+03	-4.730E+05	1.394E+05
245	50.03	255.00	3.379E+05	5.245E+03	-5.143E+05	9.770E+04
250	50.03	255.00	3.625E+05	4.613E+03	-5.466E+05	5.779E+04

LT 1900

NL= 44.860, WL= 240.000

FT	NL	WL	N	DNDR	DNDNL	DNDWL
40	44.86	240.00	1.144E-01	1.833E-02	7.433E-02	9.732E-02
45	44.86	240.00	2.788E-01	5.577E-02	1.816E-01	2.377E-01
50	44.86	240.00	8.737E-01	2.318E-01	5.726E-01	7.496E-01
55	44.86	240.00	4.214E+00	1.607E+00	2.801E+00	3.667E+00
60	44.86	240.00	3.582E+01	1.414E+01	2.344E+01	3.068E+01
65	44.86	240.00	7.165E+01	8.967E-03	4.630E+01	6.062E+01
70	44.86	240.00	3.651E+01	-1.361E+01	2.533E+01	3.316E+01
75	44.86	240.00	2.210E+01	8.537E+00	5.044E+01	6.603E+01
80	44.86	240.00	2.014E+02	8.201E+01	5.230E+02	6.847E+02
85	44.86	240.00	1.173E+03	3.500E+02	3.016E+03	3.949E+03
90	44.86	240.00	4.123E+03	8.606E+02	1.053E+04	1.379E+04
95	44.86	240.00	9.817E+03	1.394E+03	2.501E+04	3.274E+04
100	44.86	240.00	1.771E+04	1.730E+03	4.507E+04	5.900E+04
105	44.86	240.00	2.700E+04	1.998E+03	6.870E+04	8.994E+04
110	44.86	240.00	3.753E+04	1.996E+03	9.537E+04	1.249E+05
115	44.86	240.00	4.275E+04	2.051E+02	1.089E+05	1.426E+05
120	44.86	240.00	4.295E+04	-3.560E-04	1.092E+05	1.430E+05
125	44.86	240.00	4.295E+04	-2.304E-04	1.092E+05	1.430E+05
130	44.86	240.00	4.478E+04	9.300E+02	1.060E+05	1.470E+05
135	44.86	240.00	4.940E+04	9.176E+02	1.134E+05	1.594E+05
140	44.86	240.00	5.395E+04	9.002E+02	1.207E+05	1.716E+05
145	44.86	240.00	5.840E+04	8.782E+02	1.280E+05	1.836E+05
150	44.86	240.00	6.273E+04	8.520E+02	1.353E+05	1.953E+05
155	44.86	240.00	6.691E+04	8.218E+02	1.424E+05	2.066E+05
160	44.86	240.00	7.094E+04	7.877E+02	1.495E+05	2.174E+05
165	44.86	240.00	7.478E+04	7.499E+02	1.563E+05	2.276E+05
170	44.86	240.00	7.843E+04	7.085E+02	1.630E+05	2.373E+05
175	44.86	240.00	8.186E+04	6.636E+02	1.694E+05	2.462E+05
180	44.86	240.00	8.506E+04	6.152E+02	1.755E+05	2.543E+05
185	44.86	240.00	8.801E+04	5.633E+02	1.813E+05	2.615E+05
190	44.86	240.00	9.069E+04	5.079E+02	1.868E+05	2.678E+05
195	44.86	240.00	9.308E+04	4.489E+02	1.918E+05	2.730E+05
200	44.86	240.00	9.517E+04	3.861E+02	1.964E+05	2.771E+05
205	44.86	240.00	9.694E+04	3.196E+02	2.004E+05	2.799E+05
210	44.86	240.00	9.836E+04	2.489E+02	2.039E+05	2.814E+05
215	44.86	240.00	9.942E+04	1.741E+02	2.068E+05	2.813E+05
220	44.86	240.00	1.001E+05	9.462E+01	2.089E+05	2.795E+05
225	44.86	240.00	1.004E+05	1.565E+01	1.841E+05	3.015E+05
230	44.86	240.00	1.482E+05	1.066E+04	2.695E+04	8.302E+05
235	44.86	240.00	2.402E+05	1.010E+04	-5.525E+04	7.751E+05
240	44.86	240.00	2.490E+05	9.410E+03	-1.288E+05	7.161E+05
245	44.86	240.00	2.941E+05	8.635E+03	-1.938E+05	6.556E+05
250	44.86	240.00	3.352E+05	7.801E+03	-2.505E+05	5.946E+05

LT 2000

NL= 36.628, WL= 225.000

HT	NL	WL	N	DNDR	DNDNL	DNDWL
40	36.63	225.00	0.	0.	0.	0.
45	36.63	225.00	0.	0.	0.	0.
50	36.63	225.00	1.90BE-11	1.653E-11	1.408E-11	1.628E-11
55	36.63	225.00	7.633E-11	2.148E-10	2.113E-10	2.443E-10
60	36.63	225.00	5.975E-07	9.498E-07	1.185E-06	1.371E-06
65	36.63	225.00	2.611E-04	2.804E-04	4.499E-04	5.202E-04
70	36.63	225.00	2.140E-02	1.654E-02	3.438E-02	3.975E-02
75	36.63	225.00	5.594E-01	3.172E-01	8.644E-01	9.995E-01
80	36.63	225.00	6.271E+00	2.603E+00	9.480E+00	1.096E+01
85	36.63	225.00	3.666E+01	1.095E+01	5.473E+01	6.328E+01
90	36.63	225.00	1.289E+02	2.691E+01	1.912E+02	2.210E+02
95	36.63	225.00	3.969E+02	4.358E+01	4.538E+02	5.247E+02
100	36.63	225.00	5.537E+02	5.408E+01	8.178E+02	9.455E+02
105	36.63	225.00	8.442E+02	6.248E+01	1.247E+03	1.441E+03
110	36.63	225.00	1.173E+03	6.241E+01	1.731E+03	2.001E+03
115	36.63	225.00	1.337E+03	6.412E+00	1.977E+03	2.285E+03
120	36.63	225.00	1.423E+03	1.290E+02	1.744E+03	2.121E+03
125	36.63	225.00	2.065E+03	1.275E+02	2.280E+03	2.842E+03
130	36.63	225.00	2.696E+03	1.246E+02	2.806E+03	3.545E+03
135	36.63	225.00	3.310E+03	1.209E+02	3.315E+03	4.223E+03
140	36.63	225.00	3.904E+03	1.168E+02	3.805E+03	4.870E+03
145	36.63	225.00	4.477E+03	1.123E+02	4.272E+03	5.483E+03
150	36.63	225.00	5.027E+03	1.076E+02	4.714E+03	6.058E+03
155	36.63	225.00	5.553E+03	1.027E+02	5.129E+03	6.593E+03
160	36.63	225.00	6.054E+03	9.772E+01	5.516E+03	7.087E+03
165	36.63	225.00	6.530E+03	9.257E+01	5.873E+03	7.537E+03
170	36.63	225.00	6.980E+03	8.732E+01	6.200E+03	7.944E+03
175	36.63	225.00	7.403E+03	8.198E+01	6.496E+03	8.304E+03
180	36.63	225.00	7.799E+03	7.656E+01	6.760E+03	8.618E+03
185	36.63	225.00	8.168E+03	7.108E+01	6.991E+03	8.885E+03
190	36.63	225.00	8.510E+03	6.553E+01	7.188E+03	9.104E+03
195	36.63	225.00	8.824E+03	5.992E+01	7.351E+03	9.273E+03
200	36.63	225.00	9.109E+03	5.426E+01	7.480E+03	9.392E+03
205	36.63	225.00	9.366E+03	4.855E+01	7.573E+03	9.461E+03
210	36.63	225.00	9.595E+03	4.280E+01	7.631E+03	9.479E+03
215	36.63	225.00	9.794E+03	3.700E+01	7.652E+03	9.444E+03
220	36.63	225.00	9.965E+03	3.115E+01	7.637E+03	9.358E+03
225	36.63	225.00	1.011E+04	2.527E+01	7.584E+03	9.217E+03
230	36.63	225.00	1.024E+04	1.934E+01	7.494E+03	9.023E+03
235	36.63	225.00	1.030E+04	1.338E+01	7.365E+03	8.775E+03
240	36.63	225.00	1.035E+04	7.373E+00	7.198E+03	8.471E+03
245	36.63	225.00	1.037E+04	1.328E+00	6.992E+03	8.112E+03
250	36.63	225.00	5.784E+04	1.189E+04	4.988E+05	8.343E+05

LT 2100

NL= 25.900, WL= 210.000

PT	NL	WL	N	DNDR	DNDNL	DNDWL
40	25.90	210.00	0.	0.	0.	0.
45	25.90	210.00	0.	0.	0.	0.
50	25.90	210.00	7.782E-12	6.739E-12	8.656E-12	1.010E-11
55	25.90	210.00	3.113E-11	8.761E-11	1.298E-10	1.515E-10
60	25.90	210.00	2.437E-07	3.873E-07	7.285E-07	8.500E-07
65	25.90	210.00	1.065E-04	1.143E-04	2.765E-04	3.227E-04
70	25.90	210.00	8.727E-03	6.746E-03	2.113E-02	2.465E-02
75	25.90	210.00	2.291E-01	1.294E-01	5.313E-01	6.199E-01
80	25.90	210.00	2.557E+00	1.061E+00	5.827E+00	6.798E+00
85	25.90	210.00	1.495E+01	4.464E+00	3.364E+01	3.925E+01
90	25.90	210.00	5.257E+01	1.097E+01	1.175E+02	1.371E+02
95	25.90	210.00	1.252E+02	1.777E+01	2.789E+02	3.254E+02
100	25.90	210.00	2.258E+02	2.205E+01	5.026E+02	5.865E+02
105	25.90	210.00	3.443E+02	2.548E+01	7.662E+02	8.939E+02
110	25.90	210.00	4.785E+02	2.645E+01	1.064E+03	1.241E+03
115	25.90	210.00	5.452E+02	2.615E+00	1.215E+03	1.418E+03
120	25.90	210.00	7.041E+02	7.581E+01	1.076E+03	1.224E+03
125	25.90	210.00	1.101E+03	7.887E+01	1.448E+03	1.625E+03
130	25.90	210.00	1.492E+03	7.721E+01	1.815E+03	2.022E+03
135	25.90	210.00	1.873E+03	7.520E+01	2.173E+03	2.411E+03
140	25.90	210.00	2.243E+03	7.299E+01	2.520E+03	2.790E+03
145	25.90	210.00	2.603E+03	7.065E+01	2.854E+03	3.156E+03
150	25.90	210.00	2.950E+03	6.822E+01	3.174E+03	3.509E+03
155	25.90	210.00	3.285E+03	6.573E+01	3.479E+03	3.846E+03
160	25.90	210.00	3.607E+03	6.318E+01	3.769E+03	4.168E+03
165	25.90	210.00	3.916E+03	6.059E+01	4.044E+03	4.474E+03
170	25.90	210.00	4.213E+03	5.796E+01	4.302E+03	4.764E+03
175	25.90	210.00	4.496E+03	5.530E+01	4.543E+03	5.036E+03
180	25.90	210.00	4.766E+03	5.262E+01	4.767E+03	5.290E+03
185	25.90	210.00	5.022E+03	4.992E+01	4.974E+03	5.527E+03
190	25.90	210.00	5.265E+03	4.720E+01	5.164E+03	5.746E+03
195	25.90	210.00	5.494E+03	4.446E+01	5.336E+03	5.946E+03
200	25.90	210.00	5.710E+03	4.171E+01	5.490E+03	6.127E+03
205	25.90	210.00	5.911E+03	3.894E+01	5.626E+03	6.290E+03
210	25.90	210.00	6.099E+03	3.616E+01	5.744E+03	6.433E+03
215	25.90	210.00	6.273E+03	3.336E+01	5.843E+03	6.557E+03
220	25.90	210.00	6.432E+03	3.056E+01	5.923E+03	6.662E+03
225	25.90	210.00	6.578E+03	2.774E+01	5.985E+03	6.747E+03
230	25.90	210.00	6.710E+03	2.491E+01	6.028E+03	6.812E+03
235	25.90	210.00	6.827E+03	2.208E+01	6.052E+03	6.857E+03
240	25.90	210.00	6.931E+03	1.923E+01	6.056E+03	6.881E+03
245	25.90	210.00	7.020E+03	1.638E+01	6.042E+03	6.886E+03
250	25.90	210.00	7.094E+03	1.351E+01	6.008E+03	6.870E+03

LT 2200

NL= 13.407, WL= 195.000

RT	NL	WL	N	DNDR	DNDNL	DNDWL
40	13.41	195.00	0.	0.	0.	0.
45	13.41	195.00	0.	0.	0.	0.
50	13.41	195.00	1.777E-12	1.539E-12	2.941E-12	3.870E-12
55	13.41	195.00	7.110E-12	2.001E-11	4.411E-11	5.806E-11
60	13.41	195.00	5.565E-08	8.847E-08	2.475E-07	3.257E-07
65	13.41	195.00	2.432E-05	2.611E-05	9.394E-05	1.237E-04
70	13.41	195.00	1.993E-03	1.541E-03	7.177E-03	9.447E-03
75	13.41	195.00	5.210E-02	2.954E-02	1.805E-01	2.376E-01
80	13.41	195.00	5.841E-01	2.424E-01	1.979E+00	2.605E+00
85	13.41	195.00	3.414E+00	1.020E+00	1.143E+01	1.504E+01
90	13.41	195.00	1.201E+01	2.506E+00	3.991E+01	5.253E+01
95	13.41	195.00	2.859E+01	4.059E+00	9.474E+01	1.247E+02
100	13.41	195.00	5.158E+01	5.037E+00	1.707E+02	2.247E+02
105	13.41	195.00	7.863E+01	5.820E+00	2.603E+02	3.426E+02
110	13.41	195.00	1.093E+02	5.813E+00	3.613E+02	4.756E+02
115	13.41	195.00	1.245E+02	5.972E-01	4.127E+02	5.432E+02
120	13.41	195.00	3.737E+02	6.121E+01	-1.816E+01	5.611E+02
125	13.41	195.00	6.762E+02	5.669E+01	-2.367E+02	8.298E+02
130	13.41	195.00	9.701E+02	5.784E+01	-4.284E+02	1.095E+03
135	13.41	195.00	1.254E+03	5.586E+01	-5.945E+02	1.354E+03
140	13.41	195.00	1.529E+03	5.382E+01	-7.357E+02	1.605E+03
145	13.41	195.00	1.793E+03	5.174E+01	-8.524E+02	1.846E+03
150	13.41	195.00	2.046E+03	4.963E+01	-9.449E+02	2.078E+03
155	13.41	195.00	2.289E+03	4.750E+01	-1.013E+03	2.300E+03
160	13.41	195.00	2.521E+03	4.536E+01	-1.058E+03	2.511E+03
165	13.41	195.00	2.742E+03	4.320E+01	-1.079E+03	2.711E+03
170	13.41	195.00	2.953E+03	4.104E+01	-1.076E+03	2.900E+03
175	13.41	195.00	3.153E+03	3.886E+01	-1.049E+03	3.078E+03
180	13.41	195.00	3.342E+03	3.668E+01	-9.989E+02	3.245E+03
185	13.41	195.00	3.519E+03	3.450E+01	-9.252E+02	3.400E+03
190	13.41	195.00	3.687E+03	3.231E+01	-8.279E+02	3.544E+03
195	13.41	195.00	3.843E+03	3.011E+01	-7.071E+02	3.677E+03
200	13.41	195.00	3.988E+03	2.791E+01	-5.628E+02	3.797E+03
205	13.41	195.00	4.122E+03	2.571E+01	-3.950E+02	3.906E+03
210	13.41	195.00	4.245E+03	2.351E+01	-2.038E+02	4.002E+03
215	13.41	195.00	4.357E+03	2.130E+01	1.081E+01	4.087E+03
220	13.41	195.00	4.458E+03	1.909E+01	2.489E+02	4.160E+03
225	13.41	195.00	4.548E+03	1.687E+01	5.103E+02	4.221E+03
230	13.41	195.00	4.626E+03	1.465E+01	7.952E+02	4.269E+03
235	13.41	195.00	4.694E+03	1.243E+01	1.104E+03	4.305E+03
240	13.41	195.00	4.751E+03	1.021E+01	1.435E+03	4.329E+03
245	13.41	195.00	4.796E+03	7.984E+00	1.790E+03	4.341E+03
250	13.41	195.00	4.831E+03	5.756E+00	2.169E+03	4.341E+03

LT 2300

NL= -.000, WL= 180.000

HT	NL	WL	N	DNDR	DNDNL	DNDWL
40	-.00	180.00	0.	0.	0.	0.
45	-.00	180.00	0.	0.	0.	0.
50	-.00	180.00	1.276E-13	1.105E-13	3.512E-13	5.872E-13
55	-.00	180.00	5.105E-13	1.437E-12	5.268E-12	8.808E-12
60	-.00	180.00	3.996E-09	6.353E-09	2.956E-08	4.942E-08
65	-.00	180.00	1.746E-06	1.875E-06	1.122E-05	1.876E-05
70	-.00	180.00	1.431E-04	1.106E-04	8.573E-04	1.433E-03
75	-.00	180.00	3.741E-03	2.121E-03	2.156E-02	3.604E-02
80	-.00	180.00	4.194E-02	1.741E-02	2.364E-01	3.952E-01
85	-.00	180.00	2.452E-01	7.322E-02	1.365E+00	2.282E+00
90	-.00	180.00	8.621E-01	1.800E-01	4.767E+00	7.970E+00
95	-.00	180.00	2.053E+00	2.615E-01	1.132E+01	1.892E+01
100	-.00	180.00	3.704E+00	3.617E-01	2.039E+01	3.409E+01
105	-.00	180.00	5.646E+00	4.179E-01	3.109E+01	5.197E+01
110	-.00	180.00	7.848E+00	4.174E-01	4.316E+01	7.215E+01
115	-.00	180.00	8.941E+00	2.838E+01	2.265E+01	7.372E+01
120	-.00	180.00	3.292E+02	6.304E+01	-2.267E+02	2.338E+02
125	-.00	180.00	6.336E+02	6.012E+01	-4.502E+02	4.203E+02
130	-.00	180.00	9.262E+02	5.708E+01	-6.429E+02	5.985E+02
135	-.00	180.00	1.204E+03	5.400E+01	-8.050E+02	7.673E+02
140	-.00	180.00	1.466E+03	5.090E+01	-9.362E+02	9.263E+02
145	-.00	180.00	1.713E+03	4.779E+01	-1.037E+03	1.075E+03
150	-.00	180.00	1.944E+03	4.467E+01	-1.107E+03	1.214E+03
155	-.00	180.00	2.160E+03	4.155E+01	-1.146E+03	1.343E+03
160	-.00	180.00	2.360E+03	3.842E+01	-1.154E+03	1.462E+03
165	-.00	180.00	2.544E+03	3.529E+01	-1.131E+03	1.570E+03
170	-.00	180.00	2.712E+03	3.215E+01	-1.078E+03	1.668E+03
175	-.00	180.00	2.865E+03	2.902E+01	-9.937E+02	1.755E+03
180	-.00	180.00	3.003E+03	2.588E+01	-8.787E+02	1.832E+03
185	-.00	180.00	3.124E+03	2.273E+01	-7.329E+02	1.899E+03
190	-.00	180.00	3.230E+03	1.959E+01	-5.562E+02	1.955E+03
195	-.00	180.00	3.320E+03	1.644E+01	-3.487E+02	2.000E+03
200	-.00	180.00	3.394E+03	1.330E+01	-1.104E+02	2.035E+03
205	-.00	180.00	3.453E+03	1.015E+01	1.589E+02	2.059E+03
210	-.00	180.00	3.496E+03	6.998E+00	4.590E+02	2.073E+03
215	-.00	180.00	3.523E+03	3.847E+00	7.900E+02	2.076E+03
220	-.00	180.00	3.534E+03	6.944E-01	1.152E+03	2.069E+03
225	-.00	180.00	3.208E+04	7.145E+03	-8.616E+05	4.980E+04
230	-.00	180.00	6.649E+04	6.612E+03	-7.874E+05	9.321E+04
235	-.00	180.00	9.817E+04	6.060E+03	-7.117E+05	7.528E+04
240	-.00	180.00	1.271E+05	5.503E+03	-6.360E+05	8.604E+04
245	-.00	180.00	1.532E+05	4.943E+03	-5.607E+05	9.548E+04
250	-.00	180.00	1.765E+05	4.381E+03	-4.859E+05	1.036E+05

LT 2400 Midnight

BIOGRAPHICAL NOTES

RAY H. GAY received a B.S. in astro-science from Pan-American College in 1970, and an M.S. in aerospace engineering from the University of Texas at Austin in 1973.

Before joining Smithsonian Astrophysical Observatory, he was a research assistant at the University of Texas. At Smithsonian Astrophysical Observatory, where he is employed as a mathematician, his interests include mathematical and computational techniques in geodesy; orbit determination; and celestial mechanics.

MARIO D. GROSSI received a Dr. Eng. Degree in 1948 from the University of Pisa, Italy. After 10 years of research and development work in Italy in the fields of radiophysics and radioengineering, he came to the United States in 1958. He has been active since then at the Smithsonian Astrophysical Observatory, and as a Consulting Scientist for the Raytheon Company, in designing and conducting space experiments and space scientific missions. His principal research areas include radiophysics and remote sensing of media by electromagnetic waves.

At present, Dr. Grossi is a member of the Working Group on Wave Phenomena of the NASA Shuttle AMPS Laboratory and is coinvestigator of the Spacecraft-to-Spacecraft Doppler Tracking Experiment of the Apollo-Soyuz Test Project. He is also a member of the Radio Team of NASA's 1975 Viking Mission to Mars.